

# From Thought to Movement - A Brain Physiological Interface for Motor Impairments

Author: Tobias Bendix Nielsen

School: Egaa Gymnasium, Denmark

Year: 2025

Mostratec 2025 - Electronic Engineering

# From Thought to Movement -

## A Brain Physiological Interface for Motor Impairments

Author: Tobias Bendix Nielsen, Denmark

School: Egaa Gymnasium, Denmark

Mentors: Martin Olsen & Sabine Færge

Contacts:

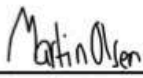
Email: [tobiasbn05@gmail.com](mailto:tobiasbn05@gmail.com)

Phone: +45 30 14 43 13

## Approval page

The undersigned student has written this research paper for Mostratec 2025 under the mentor's guidance. The research paper is written in accordance with Mostratec's structure and specifications.

**Mentor:** Martin Haurballe Olsen

**Signature:** 

**Student:** Tobias Bendix Nielsen

**Signature:** 

# **Dedication**

I hereby dedicate all my work and research to my father Kasper Bendix Nielsen, who inspired this project. My goal has always been to help you, and this remains true until the date it's been achieved. Nothing else will ever satisfy.

# Acknowledgement

A big thank you goes to the researchers Per Borghammer (Clinical Professor, Ph.D., Dr. Med., AU Department of Clinical Medicine, Nuclear Medicine and PET,) and Casper Skjærbæk (Ph.D. candidate, AU Department of Clinical Medicine - Nuclear Medicine and PET), who answered my questions about Parkinson's disease and provided constructive feedback on the project.

Thanks also to Dan Bang (Associate Professor, PhD, AUH Department of Clinical Medicine, Center for Functional Integrative Neuroscience (CFIN)) and Andreas Nørgaard Glud (Clinical Associate Professor, MD, PhD, AUH Department of Clinical Medicine, Neurosurgery), who answered my questions about the brain and Parkinson's disease, and for inviting me to their research group to gain valuable insights and feedback.

Thanks to Thomas Nielsen (Associate Professor, AU Department of Electrical and Computer Engineering, Biomedical Engineering) and Preben Kidmose (Professor, AU Department of Electrical and Computer Engineering - Biomedical Engineering) for discussing my ideas and help finishing off the self-assembled EEG-circuit. Also, for loaning me their equipment.

My mentor and former physics teacher Pia Møller Jensen must also get a enormous thanks, for her unvaluable help and guidance. Without her, the project wouldn't ever had been possible! I owe all my success to her!

My friend and now fellow student Nanna Kalmar for always taking time out of her calendar to discuss my ideas and proofread my unfinished reports.

The biggest thanks of all, goes to my father, who both inspired me to do this project and in the future voluntary will provide his own body biosignals to data collection. He is the reason the project was started and is still the reason that I stay motivated and want to optimise the project even further in the future! So, from the bottom of my heart, thank you father. I really hope my work can help you and other people!

# Abstract

My father has had Parkinson's disease (PD) since he was 37 years old, which has affected every aspect of his life. I therefore dedicate this project to him, aiming to one day make his life, and the lives of others with similar diseases, a little easier through my ideas.

PD is a progressive neurodegenerative disorder where current medical and surgical treatments can only alleviate symptoms and slow progression, not halt or cure it. Over time, their effectiveness diminishes. Degeneration of the substantia nigra disrupts the basal ganglia, causing Motor Impairments (MI) such as stiffness, tremor, and loss of speech. This creates a critical need for new approaches to restore motor function without interfering with medication.

This project presents a Brain Physiological Interface (BPI), a non-invasive system that detects motor intentions from EEG, EMG, and IMU signals and, via AI modelling, translates them in real time into direct muscle activation using Focused Ultrasound (FUS) and Electrical Muscle Stimulation (EMS). Unlike traditional BCIs that control external devices, the BPI aims to re-enable a patient's own muscles, bypassing damaged neural pathways and restoring natural movement.

## **Methods:**

The research followed three phases. First, seven AI architectures were trained on a public EEG/EMG dataset, evaluated using precision, AUC, F1-score, inference time, and a custom efficiency metric. The Transformer model was chosen for its suitability for sequential biosignals and balanced performance.

Second, a 6-axis robotic arm was built and controlled in real time using three IMUs mounted on the forearm, wrist, and upper arm, proving the feasibility of biosignals-driven actuation.

Third, a multimodal dataset was collected from myself using both a custom 3-channel EEG circuit inspired by [1] and an 8-channel OpenBCI system, alongside EMG and IMU signals. The Transformer model was trained using 5-fold cross-validation and tested in real time to control the robotic arm.

## **Results:**

The Transformer model achieved a balanced performance across evaluation metrics (F1-score: 83%, AUC: 94%), demonstrating real-time responsiveness and accurate movement classification.

The robotic arm successfully mirrored intended movements based on biosignals, validating the concept of thought-to-action control.

### **Conclusions & Applications:**

This work demonstrates that AI can accurately decode motor intentions from multimodal biosignals and translate them into real-time movement. The approach could form the basis for next-generation neurorehabilitation tools, wearable assistive devices, and clinical systems that restore movement in individuals with PD and other motor impairments. Future steps include testing with PD patients, refining AI performance, and transitioning from robotic actuation to direct muscle stimulation.

### **Keywords:**

Parkinson's disease, Brain Physiological Interface, EEG, EMG, IMU, BCI, Transformer AI, Robotic Arm, Electrical Muscle Stimulation, Focused Ultrasound, Neurorehabilitation.

# List of illustrations

FIGURE 1: AN OVERVIEW OF THE DIFFERENT FREQUENCY BANDS	18
FIGURE 2: THE INTERNATIONAL 10/20 SYSTEM FOR THE PLACEMENT OF EEG-ELECTRODES	18
FIGURE 3: ELECTROENCEPHALOGRAM BASED ON BASELINE DATA FROM THE PATIENT AQ59D ANALYSED FROM DATA IN (KUEPER, ET AL., 2024)	20
FIGURE 4: SPECTROGRAM OF THE C4 ELECTROENCEPHALOGRAM OF THE PATIENT AQ59D, FROM (KUEPER, ET AL., 2024)	20
FIGURE 5: EXAMPLE OF BP	20
FIGURE 6: EMG-MEASUREMENT, WITH ELECTRODES REGISTERING SIGNALS FROM UNDERARM MUSCLES DURING ACTIVATION	22
FIGURE 7: EXAMPLE OF AN ELECTROMYOGRAM FROM THE PROJECT FOR THE SUBJECT AC17D FROM (KUEPER, ET AL., 2024)	23
FIGURE 8: THE FUNCTIONAL PRINCIPLE OF A CLASSICAL BCI-SYSTEM	32
FIGURE 9: OVERVIEW OF THE DBS SYSTEM PATHWAY	34
FIGURE 10: FLOW DIAGRAM OF THE PROJECT	39
FIGURE 11: GRAPH OF AI-MODELS' EFFICIENCY	42
FIGURE 12: : GRAPH OF AI-MODELS' F1-SCORE VS. INFERENCE TIME. THE X-AXIS IS IN A LOGARITHMIC SCALE WITH BASE 10. EVEN THOUGH THE TRANSFORMER PERFORMED WORSE HERE, I HAVE WORKED EXTENSIVELY WITH THIS MODEL TYPE BEFORE, WHICH ALLOWS ME TO KEEP DEVELOPING AND IMPROVING IT, ESPECIALLY BECAUSE IT FITS WELL WITH COMBINING EEG, EMG, AND IMU SIGNALS IN REAL-TIME. ITS PERFORMANCE IS ALSO LIKELY TO IMPROVE WITH MORE TRAINING DATA AND BETTER HYPERPARAMETER TUNING	43
FIGURE 13: THE ROBOTIC ARM USED IN THIS PROJECT	44
FIGURE 14: THREE IMUS ARE MOUNTED ON THE RIGHT ARM TO TRACK MOTION DYNAMICS. SURFACE EMG IS RECORDED FROM THE BB USING AN ACTIVE ELECTRODE, WITH A NEARBY REFERENCE ELECTRODE AND GROUND PLACED AT THE ELBOW. EEG SIGNALS ARE ACQUIRED USING THE OPENBCI CYTON BOARD AND 8-CHANNEL EEG HEADSET (DONATED BY OPENBCI)	45
FIGURE 15: THE CIRCUIT FOR THE IMU, ROBOTIC ARM TEENSY 4.1 MICROCONTROLLER	45
FIGURE 16: ELECTRODE PLACEMENT WITH EEG-HARDWARE DONATED BY OPENBCI	47
FIGURE 17: SELF-ASSEMBLED EEG-CIRCUIT WITH 3 ACTIVE ELECTRODES	48
FIGURE 18: SELF-ASSEMBLED EEG-CIRCUIT CIRCUIT DIAGRAM	48
FIGURE 19: EMG-SETUP WITH ELECTRODES ON MY ARM	49
FIGURE 20: TARGET MUSCLES FOR EMG ELECTRODE PLACEMENT	50
FIGURE 21: EMG OF MY OWN MUSCLE ACTIVITY DURING FLEXION AND EXTENSION OF MY RIGHT ARM	50
FIGURE 22: IMU-DATA DURING TRAINING SESSION WITH FLEXION AND EXTENSION OF MY RIGHT ARM	51



FIGURE 23: EEG ACTIVITY, ICA AND POWER SPECTRUM OF MY EEG-SIGNALS DURING A TRAINING SESSSION.	52
FIGURE 24: A SCHEMATIC OVERVIEW OF BPI	57
FIGURE 25: FUS CAN INCREASE THE CALCIUM PERMEABILITY, WHICH MAKES IT EASIER FOR CURRENT TO ACTIVATE MUSCLES	58
FIGURE 26: THE INTERPLAY BETWEEN BRAIN ACTIVITY FOR MOTOR CONTROLS AND MOVEMENTS MAY BE MORE INTERTWINED, WHICH FROM MOVEMENT TO THOUGHT WILL EXPLORE IN THE FUTURE	60
FIGURE 27: THE IDEA BEHIND FGPA - SYNCHRONISED WAVES CAN ENHANCE EEG ACTIVUTY, JUST LIKE A RUNNER PACING FOR YOU	61
FIGURE 28: OVERVIEW OF THE BRAIN'S STRUCTURE AND DIFFERENT REGIONS	75
FIGURE 29: THE DIRECT AND INDIRECT PATHWAYS IN THE BASAL GANGLIA	77
FIGURE 30: THE HYPERDIRECT PATHWAY IN THE BASAL GANGLIA	79
FIGURE 31: FFT USED ON A C-MAJOR CHORD	81
FIGURE 32: EXAMPLE ON THE APPLICATION OF SAVITZKY-GOLAY FILTER	83
FIGURE 33: THE ARCHITECTURE OF A NN	84
FIGURE 34: THE DIFFERENCE BETWEEN FEEDWORD NETWORK AND RNN	85
FIGURE 35: THE ARCHITECTURE BEHIND AN LSTM	86
FIGURE 36: THE ARCHITECTURE BEHIND A CNN	87
FIGURE 37: OVERVIEW OF THE DATAFLOW IN A TRANSFORMER-MODEL	90
FIGURE 38: RELU GRAPH	92
FIGURE 39: SIGMOID FUNCTION AND DIFFERENTIATED FUNCTION	93
FIGURE 40: THE EEG-CIRCUIT FROM THE REFERENCE ARTICLE, HERE WITHOUT ELECTRODES, USB-ADAPTER AND BATTERY	98
FIGURE 41: CIRCUIT DIAGRAM FOR THE REFERENCE ARTICLE	99
FIGURE 42: CIRCUIT DIAGRAM FOR OPTOISOLATION CIRCUIT FROM THE REFERENCE ARTICLE	99
FIGURE 43: THE CONFIGURATION OF THE F303K8 NUCLEOSTM32 MICROCONTROLLER	106
FIGURE 44: SETTINGS FOR ADC1	107
FIGURE 45: SETTINGS FOR TIM2	108
FIGURE 46: SETTINGS FOR USART	109
FIGURE 47: SETTINGS FOR DMA	110
FIGURE 48: SETTINGS FOR NVIC	111
FIGURE 49: THE DIFFERENT MUSCLES WHERE EMG-ELECTRODES WERE PLACED	117
FIGURE 50: THE EFFICIENCY OF THE DIFFERENT AI-MODELS	119
FIGURE 51: GRAPH OF AI-MODELS' EFFCIENCY	120
FIGURE 52: GRAPH OF AI-MODELS' F1-SCORE VS. INFERENCE TIME. THE X-AXIS IS IN A LOGARITHMIC SCALE OF 10. EVEN THOUGH THE TRANSFORMER PERFORMED WORSE HERE, I HAVE WORKED EXTENSIVELY WITH THIS MODEL TYPE BEFORE, WHICH ALLOWS ME TO KEEP DEVELOPING AND IMPROVING IT, ESPECIALLY BECAUSE IT FITS WELL WITH COMBINING EEG,	

EMG, AND IMU SIGNALS IN REAL-TIME. ITS PERFORMANCE IS ALSO LIKELY TO IMPROVE WITH MORE TRAINING DATA AND BETTER HYPERPARAMETER TUNING	121
FIGURE 53: THE EMG-SETUP WITH ELECTRODES PLACED ON MY ARM	127
FIGURE 54: PLACEMENT OF IMU'S ON MY ARM	127
FIGURE 55: THE ROBOTIC ARM USED IN THIS PROJECT	132
FIGURE 56: THREE IMUS ARE MOUNTED ON THE RIGHT ARM TO TRACK MOTION DYNAMICS	134
FIGURE 57: THE CIRCUIT FOR THE IMU, ROBOTIC ARM TEENSY 4.1 MICROCONTROLLER	135
FIGURE 58: ROBOTIC ARM CONNECTED TO ARDUINO	140
FIGURE 59: THE FIRST SKETCH OF IDEA: FROM BRAIN ACTIVITY, THROUGH AI-MODEL TO EXECUTION OF MOVEMENT	153
FIGURE 60: MY SKETCH OF A BPI SOLUTION. I PUT MY HAND ON A PIECE OF PAPER AND THEREAFTER I STARTED TO DRAW THE SOLUTION	154
FIGURE 61: FROM INTENTION TO THE REACTIVATION OF THE MUSCLES THROUGH A BPI	155

# List of Tables

TABLE 1: OVERVIEW OF DIFFERENCES AND SIMILARITIES BETWEEN MY PROJECT AND SIMILAR SOLUTIONS	35
TABLE 2: FIRST ITERATION OF AI-MODEL TRAINING, USING K-FOLD CROSS-VALIDATION AND DIFFERENT AMOUNT OF PARAMETERS . THE MODELS MIGHT HAVE OVERFITTED IN THIS ITERATION, BECAUSE OF THE HIGH PRECISIONS ACHIEVED. THE MODELS WERE BUILT TO CLASSIFY BETWEEN NON-MOVEMENT	41
TABLE 3: SECOND ITERATION OF AI-MODEL TRAINING, USING GROUPKFOLD CROSS-VALIDATION AND AROUND THE SAME AMOUNT OF PARAMETERS TO BETTER COMPARE DIFFERENT ARCHITECTURES. THE PRECISIONS HAVE DECREASED AND THE MODELS LIKELY DID NOT OVERFIT THIS TIME. THE MODELS WERE BUILT TO CLASIFY BETWEEN NON-MOVEMENT AND MOVEMENT IN EEG AND EMG SIGNALS	43
TABLE 4: OVERVIEW OF THE EXPERIMENTAL DESIGN AND FUNCTIONS	46
TABLE 5: THE DIFFERENT MOVEMENT TYPES	53
TABLE 6: THE FUNCTIONAL REQUIREMENTS OF THE FUTURE PRODUCT	55
TABLE 7: THE NON-FUNCTIONAL REQUIREMENTS OF THE FUTURE PRODUCT	56
TABLE 8: THE RESULTS FROM THE AI-MODELS	118
TABLE 9: FIRST ITERATION OF AI-MODEL TRAINING, USING K-FOLD CROSS-VALIDATION AND DIFFERENT AMOUNT OF PARAMETERS . THE MODELS MIGHT HAVE OVERFITTED IN THIS ITERATION, BECAUSE OF THE HIGH PRECISIONS ACHIEVED. THE MODELS WERE BUILT TO CLASSIFY BETWEEN NON-MOVEMENT	119
TABLE 10: SECOND ITERATION OF AI-MODEL TRAINING, USING GROUPKFOLD CROSS-VALIDATION AND AROUND THE SAME NUMBER OF PARAMETERS TO BETTER COMPARE DIFFERENT ARCHITECTURES. THE PRECISIONS HAVE DECREASED, AND THE MODELS LIKELY DID NOT OVERFIT THIS TIME. THE MODELS WERE BUILT TO CLASSIFY BETWEEN NON-MOVEMENT AND MOVEMENT IN EEG AND EMG SIGNALS	121
TABLE 11: THE DIFFERENT MOVEMENT TYPES	125

# List of Abbreviations and Acronyms

## Abbreviation Definition

A-SVM	Adaptive Support Vector Machine
ANN	Artificial Neural Network
AUC	Area Under Curve
BCI	Brain-Computer-Interface
BB	Biceps Brachii
BP	Bereitschaftspotential
CNN	Convolutional Neural Network
CNS	Central Nervous System
CSP	Common Spatial Patterns
DBS	Deep Brain Stimulation
EEG	Electroencephalography
EMG	Electromyography
EMS	Electrical Muscle Stimulation
ERD	Event Related Desynchronisation
ERS	Event Related Synchronisation
FDS	Flexor Digitorum Superficialis
FOG	Freezing of Gait
FUS	Focused Ultrasound
FTtM	From Thought to Movement
GDPR	The General Data Protection Regulation
GPI	Globus Pallidus Internus
IMU	Inertial Measurement Unit
KNN	K-Nearest Neighbour
LSTM	Long Short-Term Memory
MCI	Mild Cognitive Impairment
MLP	Multi-Layer Perceptrons
ORICA	Online Recursive Independent Component Analysis
RNN	Recursive Neural Network
STN	Subthalamic Nucleus
SVM	Support Vector Machine
TB	Triceps Brachii
TBLH	Triceps Brachii Long Head
TKEO	Teager-Kaiser Energy Operator

## Table of Contents

<b>Introduction.....</b>	<b>15</b>
<b>Formulation of problem.....</b>	<b>16</b>
<b>Biosignals and Parkinson's Disease .....</b>	<b>17</b>
Parkinson's Disease .....	17
Electroencephalography .....	17
Bereitschaftspotential .....	20
Electromyography .....	22
<b>Literature review .....</b>	<b>23</b>
<b>Current research .....</b>	<b>23</b>
EEG-based movement classification .....	23
EMG-based movement detection and personalisation .....	24
Combination of EEG/EMG and real-time aspects .....	25
EEG/EMG and Parkinson's Disease .....	25
Electrical Muscle Stimulation and Functional Electrical Stimulation.....	29
Focused Ultrasound .....	30
Biochemical Aspects .....	31
<b>Existing solutions related to the project.....</b>	<b>31</b>
Brain Computer Interface .....	31
Neuroprosthetics .....	33
Deep Brain Stimulation .....	33
<b>Overall conclusion of the literature review .....</b>	<b>36</b>
<b>Hypothesis .....</b>	<b>36</b>
<b>Design and methodology.....</b>	<b>37</b>
<b>Methodical considerations.....</b>	<b>39</b>
Test of AI-models on public dataset.....	39
Real-time control of a robotic arm by using IMU's .....	44
Training and application of the Transformer-model on my own EEG/EMG/IMU-data.....	46
<b>Product, future and ethics.....</b>	<b>55</b>
<b>Product.....</b>	<b>55</b>
Functional requirements .....	55
Non-functional requirements .....	56
Product idea: Brain Physiological Interface .....	56
<b>Future perspectives .....</b>	<b>59</b>
<b>Ethical considerations of the project.....</b>	<b>62</b>
<b>Conclusion.....</b>	<b>63</b>
<b>Scientific Articles .....</b>	<b>64</b>
<b>Bibliography.....</b>	<b>67</b>
<b>Appendix A - Background Theory.....</b>	<b>75</b>
<b>The Brain and Basal Ganglia.....</b>	<b>75</b>
<b>Signal Preprocessing Methods .....</b>	<b>80</b>

Fouriertransformation.....	80
<b>Neural Network.....</b>	<b>83</b>
Recurrent Neural Network & Long Short-Term Memory.....	85
Convolutional Neural Network .....	86
<b>Transformer-model.....</b>	<b>88</b>
<b>Some of the Mathematics behind the Project.....</b>	<b>90</b>
<b><i>Appendix B - Self-assembled EEG-hardware.....</i></b>	<b><i>98</i></b>
<b>Circuit diagrams .....</b>	<b>98</b>
Reference article circuit.....	98
My Own Circuits .....	100
<b>Component list .....</b>	<b>100</b>
<b>The Function of the System.....</b>	<b>102</b>
Protection circuit.....	102
Instrumentation amplifier .....	103
AC amplification stage and anti-aliasing filter.....	103
DRL circuit .....	104
Power supply .....	104
Opto-isolation circuit.....	104
Summary.....	105
<b>Code and software.....</b>	<b>105</b>
ADC1 configuration .....	106
TIM2 Configuration .....	108
USART Configuration.....	108
DMA Configuration .....	110
NVIC Configuration.....	111
Summary.....	111
<b><i>Project Data Book .....</i></b>	<b><i>112</i></b>
<b>Timeline .....</b>	<b>114</b>
<b>Experimental observations.....</b>	<b>115</b>
Journal - Choice of AI-model.....	115
<b>Journal: Orthosis arm movement with public data (28<sup>th</sup> of February) .....</b>	<b>115</b>
Method description .....	116
Observation, results and data analysis .....	118
Model descriptions .....	123
Journal 2: Real-time Transformer with Movement Classification, Linked to the Robotic Arm (the 8 <sup>th</sup> of April) .....	124
<b>Robotic arm .....</b>	<b>130</b>
Journal: Testing the Robotic Arm as a Proof-of-Concept (27 <sup>th</sup> of February).....	131
Construction of the Robotic Arm .....	136
2.3) Finished robotic arm.....	139
Photos of the robotic arm in action.....	140
<b>Scientific Articles .....</b>	<b>141</b>
<b>Bibliography .....</b>	<b>144</b>
Interviews & Input.....	152
Photos .....	153

# Introduction

More than 10 million people worldwide are affected by Parkinson's disease (PD), a progressive neurodegenerative disorder caused by the gradual loss of dopamine-producing neurons in the substantia nigra. This disrupts the basal ganglia circuitry and results in motor impairments such as tremor, rigidity, bradykinesia, and reduced speech clarity. While medication and surgical treatments such as deep brain stimulation can temporarily alleviate symptoms, their effectiveness decreases over time, and they do not halt disease progression. This creates an urgent need for innovative approaches to restore motor function<sup>1</sup>.

My father was diagnosed with PD at the age of 37. Witnessing the daily challenges he faces has been my strongest motivation. In December, a conversation with my best friend's father sparked the idea: "Why not combine AI with PD?" This became the starting point for my project.

The aim is to develop a Brain Physiological Interface (BPI): a non-invasive system that detects movement intentions from biosignals, electroencephalography (EEG), electromyography (EMG), and inertial measurement units (IMU<sup>2</sup>), and translates them into real-time movement. Unlike traditional Brain-Computer Interfaces (BCI<sup>3</sup>), which mainly control external devices, the BPI seeks to reactivate a patient's own muscles by bypassing damaged neural pathways through Electrical Muscle Stimulation (EMS) and Focused Ultrasound (FUS).

The project has progressed through many iterations. In the first, I constructed a custom 3-channel EEG circuit with electrodes placed over the motor cortex and developed a 6-axis robotic arm prototype for real-time testing, proving the concept of biosignal-driven control. In the second generation, I integrated professional OpenBCI hardware, expanded EEG electrode coverage to eight positions, and combined data from EEG, EMG, and IMU sensors. I implemented and compared multiple AI architectures, including Long-Short-Term-Memory (LSTM<sup>4</sup>), Convolutional Neural Network

---

<sup>1</sup> Sources: (Parkinson.org, 2025), (Parkinson.dk, u.d.), (Paulson, 2024)

<sup>2</sup> A measurement-instrument, which registers movement by using gyroscopes and accelerometers.

<sup>3</sup> A BCI is a system that allows direct communication between the brain and an external device, by translating brain signals into digital commandos.

<sup>4</sup> LSTM is an AI-model, that remembers patterns over long time in data and is used to analyse sequences.

(CNN<sup>5</sup>), Adaptive-Support Vector Machine (A-SVM<sup>6</sup>), and Transformer models<sup>7</sup>. I selected the Transformer due to its ability to handle sequential multimodal data efficiently. Using 5-fold cross-validation, the model demonstrated strong performance across F1-score, AUC, and inference time, achieving accurate results for movement or no movement.

This report presents the complete workflow: from biosignal acquisition and hardware development to AI modelling and actuation. It discusses the potential of replacing robotic proof-of-concept output with direct muscle activation. A comprehensive literature review was conducted to explore the neurophysiological differences between PD patients and healthy individuals, as well as the challenges in signal processing, AI modelling and EMS/FUS. Ethical aspects are also considered, including privacy, safety, and the implications of technologies that can directly influence motor function.

Ultimately, this work aims to show how advanced AI and biosignal analysis can be combined into a BPI with potential applications in neurorehabilitation, assistive devices, and everyday mobility support for people with PD and other motor impairments, like stroke or paralysis.

## Formulation of problem

*How can AI, using multimodal EEG, EMG, and IMU data, be applied to detect motor intentions in real time and restore movement through targeted muscle stimulation, thereby improving mobility and quality of life for individuals with PD?*

---

<sup>5</sup> CNN is an AI-model, which excels in pattern recognition of photos and signals, by filtering and highlight the most important details.

<sup>6</sup> A-SVM is an AI-model, that dynamically adjusts to changes in data, to better classify complex patterns in data.

<sup>7</sup> Transformer-model is an advanced neural network, which uses self-attention to analyse and weigh different parts of the input, parallel to each other.



# Biosignals and Parkinson's Disease

## Parkinson's Disease<sup>8</sup>

PD is a progressive neurodegenerative disorder that primarily affects dopamine-producing neurons in the substantia nigra, a structure within the basal ganglia<sup>9</sup>. Dopamine is a crucial neurotransmitter involved in the brain's regulation and coordination of movement. When dopamine production declines, as is the case in PD, a chemical imbalance arises in the basal ganglia, leading to motor impairments such as tremors, rigidity, bradykinesia (slowness of movement), and postural instability.

Current research on PD focuses on developing treatments aimed at halting disease progression and restoring dopamine production. Other active areas of investigation include advanced therapeutic approaches such as gene therapy, stem cell treatments, neurostimulation, and Deep Brain Stimulation (DBS)<sup>10</sup>.

## Electroencephalography<sup>11</sup>

Electroencephalography (EEG) is a non-invasive technique used to measure the electrical activity generated by the synchronized communication of large groups of neurons in the brain. EEG signals primarily arise from the summation of postsynaptic potentials in the cerebral cortex and reflect the brain's electrical rhythms and functional states. The electrical impulses generated by the brain vary in frequency and are classified into specific frequency bands, each of which is associated with distinct brain functions and mental states. These different frequency bands are illustrated in Figure 1.

---

<sup>8</sup> The section is based on the sources: (Parkinson.dk, u.d.), (Paulson, 2024)

<sup>9</sup> A part of cerebrum, which plays a crucial role for movement and control. Explained further in appendix 5.

<sup>10</sup> DBS is further explained in the "Other solutions"

<sup>11</sup> The section is based on the sources: (Chaddad, Wu, Kateb, & Bouridane, 2023), (Wikipedia, 2024), (Regalado, 2014),

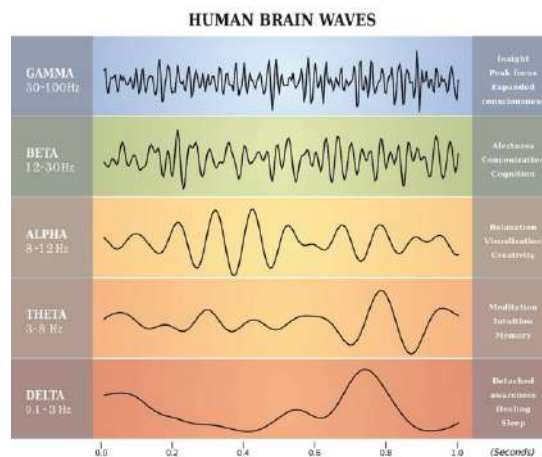


Figure 1: An overview of the different frequency bands<sup>12</sup>

Alphas waves (8 - 12 Hz) relate to relaxation and calm mental states, while beta waves (12 - 30 Hz) relate to focused activity and concentration. Gamma waves (30-100 Hz) are high frequency waves, which typically associate with information processing and conscious attention. Changes can in frequency bands can be observed in PD, e.g. reduced beta-desynchronisation and increased theta- and delta activity, which relate to motoric impairments such as bradykinesia and tremor<sup>13</sup>. Alpha waves over the motoric cortex are also known as Mu-waves.

EEG-signal is measured by placing electrodes on the head scalp in a system known as the international 10/20 system. The system can be seen on Figure 2.

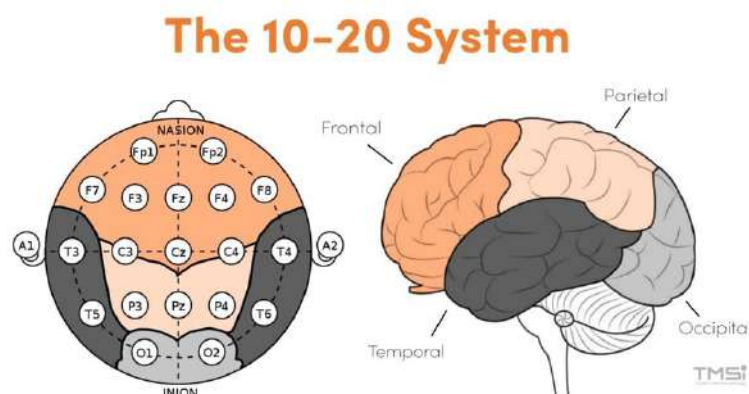


Figure 2: The international 10/20 system for the placement of EEG-electrodes<sup>14</sup>

<sup>12</sup> From <https://coronatoday.com/5-types-of-brain-waves-and-their-link-to-different-states-of-consciousness/>

<sup>13</sup> (Karimi & et al., 2021), (Miladinovic & et al., 2021)

<sup>14</sup> From <https://info.tmsi.com/blog/the-10-20-system-for-egg>

The system was initially developed to ensure the electrodes were placed in a sustainable and logical way. The electrodes are placed on specific position on the head, which corresponds to certain anatomical reference points. This enables precise and comparable measurements of the brain's activity. The letters and numbers in the system are organized as follows:

- Even numbers are on the right hemisphere, uneven numbers on the left hemisphere
- Fp is for prefrontal lobe
- F is for frontal lobe
- P is for parietal lobe
- O is for occipital lobe
- T is for temporal lobe
- C is for central (C3, C4 and Cz are on the primary motor cortex)
- A is the mastoid (the bone behind the ear).

When measuring EEG on a patient, the active electrodes must be placed on the scalp, to measure the signals in specific regions in brain. But a reference electrode (typically on the mastoid, i.e. A1 or A2), and a ground electrode (placed on Fz or nasion), too must be placed to measure the active signal relative to a defined reference.

EEG can measure brain activity in real-time, which is used to analyse different mental states of the user. An example would be using EEG to explore changes in the brain activity, when a person executes movement or are in a resting state. These patterns may then be analysed (i.e. increased or decreased frequency band activity or a change in desynchronization power), to investigate how a disease, such as PD, may affect the brain's structure and functionality.

Figure 3 and Figure 4 shows examples of an electroencephalogram from this project and its corresponding spectrogram. The chosen channel is C3. The electroencephalogram has time on the  $x$ -axis, with the unit of seconds, and amplitude on the  $y$ -axis with the unit of  $\mu V$ . The  $x$ -axis on the

spectrogram is frequency, and the y-axis is the squared amplitude over the frequency, with the unit of  $\left(\frac{\mu V^2}{Hz}\right)$ .

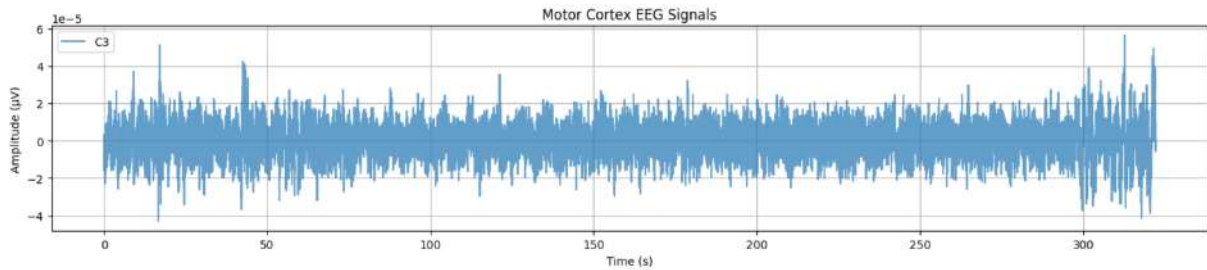


Figure 3: Electroencephalogram based on baseline data from the patient AQ59D analysed from data in (Kueper, et al., 2024)<sup>15</sup>

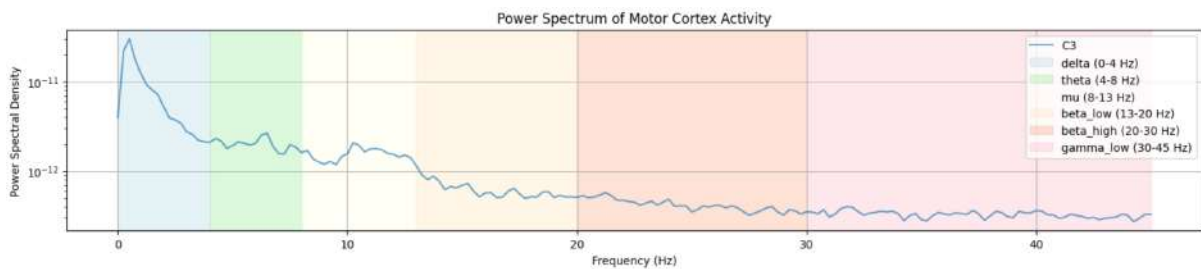


Figure 4: Spectrogram of the C4 electroencephalogram of the patient AQ59D, from (Kueper, et al., 2024)<sup>16</sup>

## Bereitschaftspotential<sup>17</sup>

The Bereitschaftspotential BP<sup>18</sup> is a slowly increasing negative voltage change in the brain's EEG signals, which occurs shortly before a voluntary intentional movement is made. BP represents the brain's motorically planning as is one of the earliest signals on a movement initialization - even before the person is conscious about the intention. The two phases of BP are shown on Figure 5.

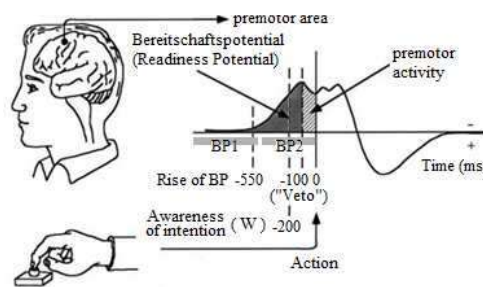


Figure 5: Example of BP<sup>19</sup>

<sup>15</sup> The figure is from a coded visualisation of the EEG data from (Kueper, et al., 2024)

<sup>16</sup> The figure is from a coded visualisation of the EEG data from (Kueper, et al., 2024)

<sup>17</sup> The section is based on the sources: (Wikipedia, 2024), (Georgiev, Lange, Seer, Kopp, & Johanshahi, 2016)

<sup>18</sup> Also known as premotor potential or readiness potential

<sup>19</sup> From [https://www.researchgate.net/figure/Bereitschaftspotential-and-the-Libets-experiment-At-550-ms-the-rise-of-BP-at-200-ms\\_fig14\\_268216375](https://www.researchgate.net/figure/Bereitschaftspotential-and-the-Libets-experiment-At-550-ms-the-rise-of-BP-at-200-ms_fig14_268216375)

The two phases of BP are as follows:

- **The early phase (BP1):** Can be measured approximately 1,5 to 0,5 seconds before the movement and is primary generated in supplementary motoric cortex (SMA). This phase reflects the general preparation of the movement.
- **The late phase (BP2):** Can be measured approximately 500 to 100 milliseconds before the movement, due to the increased activity in the primary motoric cortex. This phase reflects an initialisation of a concrete motoric activity.

In total, this means BP occurs before the conscious intention of a movement. This suggest that the brain begins to plan an action, even before the person experiences the wish of moving. It makes BP relevant for this project, because I aim to predict movement intentions from EEG-data measured in PD patients. A PD patient's EEG-signals are still intact, and the BP's can be measured and analysed, even though the signal may be reduced a bit.

If we instead of voluntary initiated movement, react to an external stimulus, then a classical BP is not generated. This situation is denoted as a stimulus-responsive movement (SRM), where a sensory released response, called an event-related potential (ERP<sup>20</sup>) is generated in the sensory cortex. The signal is sent to the premotor cortex and afterwards to motoric cortex, where the motoric output is coordinated in close collaboration with the basal ganglia.

If we consider the human as a combined sensor and actuator, the difference between ERP and BP may be clearer. Assume I am standing in a completely dark room without any external stimuli, and voluntary decide to begin walking. This movement is self-initiated, and a BP may be measured. If I instead hear my phone ringing, and decide to walk towards it, then the situation is a SRM - and an ERP will dominate in my EEG-signals, while a BP may not be measured.

The difference between BP and SRM is crucial and relevant for this project. I've so far worked with BP signals and voluntary intention, but I wish to explore stimulus-responsive mechanisms further in the future, and incorporate them in my Transformer-model, by including ERP measurements. I'll

---

<sup>20</sup> (Wikipedia, 2025)

also immerse myself in the scientific literature on the interplay between sensor cortex, premotor cortex and the basal ganglia.

## Electromyography<sup>21</sup>

Electromyography (EMG) is a technique capable of measuring the electric signals generated when muscles contract. When a muscle is activated, electric impulses (axon potentials) are sent through the muscle cells, which creates a measurable voltage. The signals are either captured by surface electrodes (placed on the skin) or needle electrodes (inserted directly into the muscle). A visualisation of EMG-measurements from this project, is shown on Figure 6:

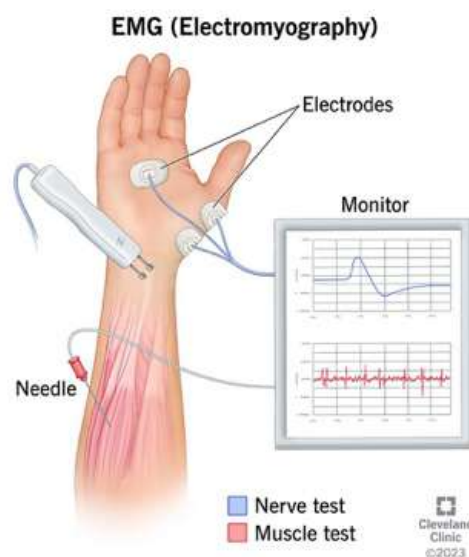


Figure 6: EMG-measurement, with electrodes registering signals from underarm muscles during activation<sup>22</sup>

An EMG-signals reflects a muscle's activity and contains information on:

- The amplitude (the power of muscle activation)
- The timing of the muscle contraction
- Patterns in contraction and rest

An electromyogram is shown on Figure 7. The data is based on a patient who flexes and extends his/her arm. The EMG-signal shows a clear cyclic activation and deactivation, which appears on the signal's characteristic wave shape. The  $x$ -axis is time and has the unit seconds, while the  $y$ -axis is

<sup>21</sup> The section is based on (Johns Hopkins Medicine, u.d.), (wikipedia, 2025), (Cleveland Clinic, 2023)

<sup>22</sup> From <https://my.clevelandclinic.org/health/diagnostics/4825-emg-electromyography>

the amplitude measured in milli voltage. The signal can be used to precisely estimate the movement's timing and intensity.

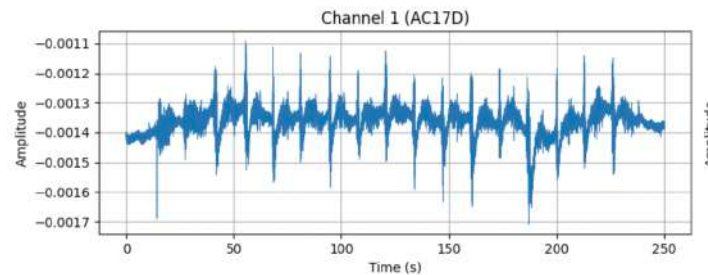


Figure 7: Example of an electromyogram from the project for the subject AC17D from (Kueper, et al., 2024)

EMG can be used to evaluate the changes in muscle activity in PD, because the disease often causes rigidity and bradykinesia, which is reflected in the EMG-patterns as slow or disturbed signals.

## Literature review

This review goes through the current research in EEG/EMG-signal processing, relevant AI-models, EMS, FUS, biochemical aspects and related technologies to this project such as BCI, neuroprosthetics and DBS, which may contribute to the project. In addition to this, changes in PD patients EEG/EMG are highlighted.

The review is split into two parts: current research and already existing solutions related to the project.

### Current research

The review starts on how EEG can be used for movement classification. Then it'll investigate EMG and EEG/EMG combined for movement classification using AI-models. Lastly will changes in EEG through PD be investigated, both motoric and cognitive symptoms are considered.

### EEG-based movement classification

[2] analysed EEG-based movement classification. Subjects were asked to imagine movements, which different AI-models<sup>23</sup> should classify the movements using different feature extraction-

---

<sup>23</sup> A short description on AI-models can be found in appendix 3.

methods<sup>24</sup>. It was shown an A-SVM with Online Recursive Independent Component Analysis (ORICA<sup>25</sup>) together with Common Spatial Patterns (CSP<sup>26</sup>), gave the highest precision (91%). The study shows advanced feature extraction can improve AI-models ability to recognise different intentional movements.

[3] built upon this study, by using a LSTM-RNN model for real-time detection of movement intention. The model achieved a precision of 84-92% precision in an interactive environment, showing a LSTM-RNN can be used to fast and precise classification of movements in EEG-signals.

### *Partial conclusion on EEG-movement classification*

With high precision EEG-based models can classify intentional movement, but they are dependent on feature extraction.

### **EMG-based movement detection and personalisation**

[4] developed a method for automatic movement detection in EMG, by applying a threshold defined as ( $T = \text{Baseline} + 1,2\mu + 2\sigma$ ). They evaluated five different AI models using this approach, with DeepConvNet (D-Conv) demonstrating superior performance for online detection ( $p = 0.001$ ), achieving 100% precision in EMG detection.

[5] demonstrated that EMG signals are unique to everyone. They recorded EMG data from eight muscles in the right leg of 80 participants during walking and cycling. Using SVM, CNN, and Multi-Layer Perceptron's (MLP<sup>27</sup>), they classified the EMG signals to identify individuals. Among these models, the SVM achieved the highest accuracy and fastest performance, with a precision of 99.3%. These findings suggest that personalised AI models may be necessary for my project.

---

<sup>24</sup> Key information is extracted from the raw data to facilitate prediction—such as signal amplitude or dominant frequency components using methods like the Fast Fourier Transform (FFT) or bandpass filtering. This process transforms raw signals into meaningful input features for AI models.

<sup>25</sup> ORICA is a real-time adaptation of ICA used to separate independent signal sources from EEG data. Its adaptive nature makes it well-suited for dynamic EEG environments, particularly for real-time artifact removal.

<sup>26</sup> CSP is a feature extraction technique that enhances the discriminability between two signal states by maximizing the variance differences across spatial filters.

<sup>27</sup> MLP is a neural network, where neurons are organised in layers, and each layer relates to the next one via non-linear activation functions



### *Partial conclusion on EMG-based movement detection and personalisation.*

EMG is effective for movement detection; however, personalized AI models may be necessary, as EMG signals are unique to everyone. AI models can accurately classify EMG signals across different individuals.

### **Combination of EEG/EMG and real-time aspects**

[6] investigated how combining EEG and EMG signals affects the accuracy of movement classification. They employed a LSTM model to analyse data from both brain waves and muscle signals during arm movements and found that the LSTM model performed best when the data were stratified by gender. This suggests that personalized AI models can enhance movement classification.

[7] developed a threshold-based algorithm for detecting the BP from single-channel EEG using the Teager-Kaiser Energy Operator (TKEO<sup>28</sup>). Their method achieved a precision of 91.2%, a sensitivity of 81.1%, and an average latency of -384.9 ms. These results demonstrate its potential for real-time applications, where BP detection could be combined with EMG signals.

### *Partial conclusion on combination of EEG/EMG and real-time aspect*

The combination of EEG and EMG signals can improve classification accuracy, and threshold-based BP detection appears promising for real-time implementation. These methods have the potential to enhance motor control, which is particularly relevant for patients with PD.

The following section will examine how EEG and EMG are applied in clinical contexts.

### **EEG/EMG and Parkinson's Disease**

This section is split into three parts:

- EEG and motoric symptoms (bradykinesia, tremor and Freezing of Gait (FOG<sup>29</sup>))
- Functional connectivity<sup>30</sup> and network changes in PD.
- EEG/EMG for stimulation and treatment

---

<sup>28</sup> TKEO is a signal processing technique that estimates the instantaneous energy of a signal. This approach accentuates changes in both amplitude and frequency, making it particularly effective for detecting rapid variations in signals. Consequently, TKEO is well-suited for applications such as movement classification.

<sup>29</sup> FOG is a situation characterised with difficult initialisation of movement or to stand up. The person freezes in his/her movement.

<sup>30</sup> Functional connectivity refers to the temporal relationship between activities in different brain regions, specifically, whether they oscillate synchronously or exhibit statistical interdependence. Two regions are considered to have high functional connectivity if their EEG signals oscillate in synchrony.

### *EEG and motoric symptoms (bradykinesia, tremor and Freezing of Gait)*

[8] analysed EEG- and EMG-patterns in PD patients with and without FOG. Patients with severe FOG had reduced beta desynchronisation and increased theta activity above the Cz electrode before movement. The study shows EEG-patterns are changed in PD patients.

[9] found Levodopa<sup>31</sup> to better the premotor EEG-desynchronisation in PD patients, which correlates with reduced bradykinesia. This supports the theory on the basal ganglia releasing frontal areas from idling rhythms<sup>32</sup>. The increased desynchronisation correlated with faster movement times above: sensory motoric cortex during simple movements, SMA during hand squeeze and prefrontal cortex during complex or sequential movements.

[10] analysed the interplay between EEG-activity and the PD patients' motor deficit scales. They found high delta- and low alpha-activity to correlate with worse FOG, while high theta- and low beta-activity to relate to a worse UPDRS-III-score<sup>33</sup>. The results suggest EEG-slowness<sup>34</sup> to be a biomarker for motoric deterioration in PD.

[11] analysed if EEG-signals could be used to predict PD patients' resting tremor, before the tremor starts. By analysing data from IMU's, were tremor-onsets identified, and afterwards was the EEG-signals before and during the tremor analysed. Features like form coefficient<sup>35</sup> and entropy<sup>36</sup>, especially in delta- and gamma-bands, were extracted. A K-nearest-neighbour-model (KNN<sup>37</sup>) achieved a predication precision of 73.7%, which increased to 81.3% after using feature-extraction.

### *Partial conclusion on EEG and motoric symptoms (bradykinesia, tremor and FOG)*

Changes in the frequency bands exist in PD patients. EEG may reflect the motoric symptoms in PD. Desynchronisation in the alpha- or beta band before movement, relates to the ability to initiate a

---

<sup>31</sup> Levodopa is medicine, which converts to dopamine in the brain. It is standard treatment against motoric symptoms in Parkinson's disease.

<sup>32</sup> Idling rhythms are the rhythms needed to be damped (desynchronised) to enable motoric activity. These brain signals dominate when the brain is in resting state (you make no movements)

<sup>33</sup> A scale to weigh the severity of Parkinson's disease, where the neurologists tick of boxes depending on the symptoms degree. UPDRS-III refers to the motoric test of PD patients. Look up Se (S. & R., 1987) for the test.

<sup>34</sup> When high frequency waves (alpha, beta and gamma) decrease, while low frequency waves (delta and theta) increase

<sup>35</sup> A quantification for the complexity of a signal. High value → rough and complex, low value → smooth and regular

<sup>36</sup> A quantification of a signal's unpredictability or information content. High value → the signal is chaotic and rich on information, low value → the signal is predictable and structured.

<sup>37</sup> KNN is a model, that classifies new data points by looking at the k nearest neighbour in the training data. The nearest neighbours are decided by a distance function, such as Euclid distance.

movement - which is improved by Levodopa. EEG-slowness (increased delta and theta activity, reduced beta and alpha activity) correlates with worse degree of symptoms. Early changes in EEG may be used to predict resting tremor, which opens a door for real-time adaptive treatment. EEG-changes reflect the symptoms in PD patients.

#### *Functional connectivity and network changes in Parkinson's disease*

[12] analysed EEG-based functional connectivity in PD patients with and without mild cognitive impairment (MCI). The study found MCI-patients to have decreased connectivity in alpha- and delta band. Both PD patients had randomised network topology with lower segregation and increased integration<sup>38</sup>. The decreased integration in the beta band correlated with worse executive function and working memory in MCI-patients.

[13] analysed functional EEG-connectivity in de novo PD patients<sup>39</sup>. The study showed a reduced functional connectivity in the alpha- and beta bands. Conversely, they found an increase in the gamma-band, which is interpreted as a possible compensatory mechanism in the early stages of the disease. Network measurements as assortativity<sup>40</sup> were also decreased in the PD patients.

#### *Partial conclusion on functional connectivity and network changes in Parkinson's disease*

The articles show PD to affect the brain's functional network already in the early stages. A general decrease in functional connectivity in alpha and beta band was observed, which correlated with a worsened motoric and cognitive functionality, while an increased gamma connectivity interprets a cortical compensatory mechanism.

#### *EEG/EMG for stimulation and treatment*

[14] analysed a Machine Learning (ML<sup>41</sup>)-method to distinguish PD patients from healthy individuals by using EEG-signal processing and classification. The EEG-data from PD patients and 16 healthy subjects, were filtered and analysed in which the important features were extracted.

---

<sup>38</sup> Network topology shows how the brain is connected; integration is cross-function cooperation, and segregation is division in specialised areas.

<sup>39</sup> Patients without prior medical treatment.

<sup>40</sup> A network's robustness

<sup>41</sup> ML is a sub-group of artificial intelligence where the computer learns patterns from the data and improves its performance without being explicitly programmed to do it.

Random forest<sup>42</sup> and Extra Trees<sup>43</sup>, had a precision of 97.5%. The study showed that signal processing of EEG and ML, can distinguish PD patients from healthy individuals.

[15] compared different AI-models (MLP, LSTM) capability to predict EMG-signals in PD patients, to improve the efficient in functional electric stimulation (FES<sup>44</sup>). The study showed that AI-models could precisely stimulate and predict EMG-patterns in PD patients, which enables more targeted and adaptive FES-treatment.

[16] analysed a classification-based method for EEG-EMG-corelations in PD patients in temporal periods compared to healthy subjects. They analysed EEG-signals above the frontal and temporal lobe and EMG from the wrist during flexion and extension. An ANN had a precision of 98.8% trained on EEG/EMG, which was higher than model solely trained on either EEG or EMG.

#### *Partial conclusion on EEG/EMG for stimulation and treatment*

The three articles show how advanced signal processing and AI-model, can utilise EEG- and EMG-data to both identify PD and predict muscle activity, which enables a more precise and adaptive treatments methods. With a high precision, it is possible to distinguish PD patients from healthy individuals. EMG-signals in PD patients can be predicted, and multimodal data integration gives a better classification precision.

---

<sup>42</sup> A collection of decision trees, which choose the best split for high precision. Is used in classification.

<sup>43</sup> Is like Random Forest, bust uses random split to increase the variation and decrease overfitting. Is used in classification.

<sup>44</sup> FES is a treatment method, that used electric impulses to activate axons from motor neurons the periphery nerves and stimulate muscles to induce movement.

## Electrical Muscle Stimulation and Functional Electrical Stimulation

Neuromuscular electrical stimulation (NMES) and FES are established techniques to restore or enhance motor function in patients with neurological damage. NMES applies electrical currents directly to muscles or nerves to induce contractions, thereby preventing atrophy<sup>45</sup>, improving strength and maintaining motor control [17]. FES, in contrast, is task-oriented and synchronises stimulation with functional movements such as reaching, grasping, or walking [18], [19].

Recent clinical studies highlight the importance of targeting not only limb but also stabilising musculature. [20] showed that applying FES to both upper limb and interscapular muscles in stroke patients improved reaching movements. Participants receiving FES displayed less trunk flexion, increased shoulder flexion, and greater elbow extension compared to placebo stimulation, as confirmed through motion capture analysis.

This demonstrates that stimulation of stabilising muscle groups can reduce compensatory trunk strategies and improve overall kinematics during functional tasks.

At the systems level, closed-loop FES, where brain or EMG signals trigger stimulation, has been shown to enhance recovery outcomes and drive neuroplasticity [21], [22]. Such approaches are particularly relevant for PD, where bypassing impaired basal ganglia circuits is crucial. Moreover, stimulation frequency and waveform patterns strongly influence performance: research shows that optimised parameters (such as intermediate frequencies, patterned bursts, pulse width and amplitude) can enhance endurance, reduce muscle fatigue, and improve repetitive task performance [23].

In stroke and spinal cord injury, FES has restored grasping and locomotor functions with measurable long-term improvements in independence [18]. Extending these approaches, integrating EEG- and EMG-based detection of motor intention with EMS/FES in PD could enable adaptive, personalised motor support, providing patients with assistance that responds dynamically to their neural and muscular activity.

---

<sup>45</sup> In the context of muscle stimulation, atrophy is the wasting or loss of muscle mass due to reduced activity or nerve input.

### *Partial conclusion on Electrical Muscle Stimulation/Functional Electrical Stimulation*

Electrical stimulation prevents atrophy and restores functional movement. Clinical evidence shows that stimulation of both prime mover and stabilising muscles (e.g., interscapular) improves kinematics, while optimised frequencies and closed-loop FES further enhance endurance and neuroplasticity. For PD, integrating EMS/FES with AI-driven detection of motor intention may provide adaptive, personalised support for motor execution.

### **Focused Ultrasound**

FUS has emerged as a non-invasive neuromodulation technique with deep penetration, high spatial precision, and the ability to modulate mechanosensitive ion channels.

Mechanism of action. Studies show that ultrasonic stimulation activates Piezo1, a mechanosensitive channel expressed in vascular and neuronal tissue. [24] demonstrated that low-intensity ultrasound induced calcium influx and downstream  $\text{Ca}^{2+}$ /CaM/MLCK signalling in endothelial cells<sup>46</sup>, while knockdown of Piezo1 blocked the response. [25] further showed that Piezo1 responses depend strongly on stimulation pattern: long ultrasound bursts triggered robust calcium influx, while short high-frequency bursts failed to do so.

These findings suggest that FUS can modulate neurons and muscles without thermal damage, offering a precise complement to EMS. In PD, FUS arrays could selectively stimulate target muscles based on predicted motor intention, bypassing impaired basal ganglia circuits.

### *Partial conclusion on Electrical Motor Stimulation/Functional Electrical Stimulation*

FUS provides temporally and spatially selective neuromodulation through Piezo1 activation. Its effects depend critically on intensity and burst duration, making it a promising tool for closed-loop, AI-driven therapies in PD together with EMS.

---

<sup>46</sup> Endothelial cells form the thin inner lining of blood vessels, regulating vascular tone, blood flow, and the exchange of substances between blood and surrounding tissues.

## Biochemical Aspects

Dopamine deficiency in the striatum is the biochemical hallmark of PD, and Levodopa (L-dopa) with carbidopa remains the standard therapy.

### **Levodopa prodrugs.**

As reviewed in [26] ester derivatives such as levodopa methyl ester (LDME) and etilevodopa show faster absorption, better solubility, and more stable Central nervous system (CNS) penetration than standard L-dopa. LDME has progressed to Phase III trials with improved bioavailability and reduced gastrointestinal side effects, highlighting prodrugs as a strategy for more continuous dopaminergic stimulation.

### **Combination therapy**

[27] demonstrated that adding entacapone, a COMT inhibitor, to carbidopa/levodopa prolongs L-dopa half-life, increases “on” time, and simplifies treatment through fixed-dose triple therapy (Stalevo®).

### *Partial conclusion on Biochemical Aspects*

While levodopa remains the cornerstone of therapy, prodrug formulations and triple combinations improve stability and duration of dopamine replacement. In this project, such biochemical advances could complement neuromodulation (EMS/FUS), together enabling more continuous and adaptive symptom management.

## Existing solutions related to the project

Other existing solutions related to this project include BCI, neuroprosthetics, and DBS. While these technologies share similarities with the project *From Thought to Movement* (FTtM), they also differ in fundamental ways.

### **Brain Computer Interface<sup>47</sup>**

A BCI is a technology that connects the brain’s electrical activity to an external device, such as a computer, robotic arm, or exoskeleton. BCIs typically use EEG signals to translate the brain’s

---

<sup>47</sup> Sources used in this section: (University of Calgary, 2025), (Wikipedia, 2025)

electrical activity into commands that control external devices. A BCI generally consists of four components:

- 1) A sensor to record brain activity (often EEG)
- 2) A computer to process and analyse the signals
- 3) A device (actuator) to be controlled
- 4) A feedback system, that informs the user about the predicted or executed action

The architecture of a classical BCI system is illustrated in Figure 8:

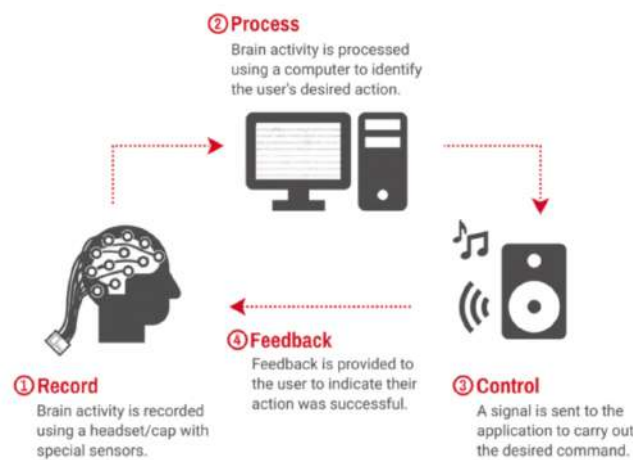


Figure 8: The functional principle of a classical BCI-system<sup>48</sup>

Active participation from the user is required in BCIs, as the system relies on the user consciously focusing on specific thoughts or intentions to initiate movements or actions. An example of such a BCI system is Elon Musk's Neuralink.

The main distinction between BCIs and the FTtM system lies in their objectives. FTtM aims to reactivate the body's natural movements before they are executed, leading to the direct reactivation of the patient's own muscles, particularly in individuals with PD or other MI. In contrast, BCIs are typically used to control external machines.

Because of this fundamental difference, an alternative term for FTtM is a *Brain-Physiological Interface (BPI)*, as the brain signals in this system do not merely control an external device but reintegrate the body's own movements through its bio-signals.

<sup>48</sup> From: <https://cumming.ucalgary.ca/research/pediatric-bci/bci-program/what-bci>



## Neuroprosthetics<sup>49</sup>

Neuroprosthetics is a field of medical technology that employs electronic devices, such as orthoses, prosthetics, or robotic limbs, to replace or restore neurological functions. This is achieved either by stimulating the nervous system (e.g., through electrical impulses) or by interpreting brain signals (commonly via EEG or intracortical measurements) to activate external actuators. Neuroprosthetic systems are typically utilized by individuals with paralysis, amputations, or neurological disorders where natural motor functions are partially or entirely lost.

In contrast, FTtM differs by not replacing bodily functions but by collaborating with the body's existing muscular and nervous systems to enhance or restore movement. FTtM interprets the user's intentions and assists muscle activation without assuming control, thus functioning as an assistive rather than a substitutive technology.

## Deep Brain Stimulation

DBS<sup>50</sup> is a compelling therapeutic approach, one that my father has personally undergone. It involves the surgical implantation of electrodes into specific brain regions to modulate neural activity through controlled electrical stimulation. While DBS does not cure the underlying disease, it adjusts the brain's electrical signals disrupted by conditions such as PD<sup>51</sup>.

In the treatment of PD, the following brain regions are commonly targeted:

- Subthalamic Nucleus (STN)
- Globus Pallidus Internus (GPi)
- Ventral Intermediate Nucleus (VIM) of the thalamus

By delivering high-frequency stimulation, typically around 130 Hz, to these areas, DBS can significantly alleviate motor symptoms such as tremors, rigidity, and bradykinesia. This intervention is particularly beneficial for patients whose symptoms are not adequately managed with medication or who experience severe side effects from pharmacological treatments.

---

<sup>49</sup> Sources used in this section: (Gupta, Vardalakis, & Wagner, 2023), (Friedenberg, et al., 2017), (Wikipedia, 2024)

<sup>50</sup> Sources used in this section: (Wikipedia, 2025), (Johns Hopkins Medicine, 2025), (Hospital, 2014), (Cleveland Clinic, 2022)

<sup>51</sup> A new iteration of DBS is adaptive deep brain stimulation (aDBS), which is a dynamic form of DBS that adjusts in real-time by measuring beta waves. It can stimulate based need, meaning aDBS only stimulates when it is needed [28]

DBS consists of three main components:

Electrodes, a pulse generator (IPG) and connecting wires

- Electrodes are implanted in specific regions of the brain
- The IPG delivers electric impulses to regulate the disrupted neural signals. It is implanted under the skin, typically in the chest or abdomen, and functions similarly to a pacemaker.
- Wires that run under the skin, connecting the IPG to the electrodes implanted in the brain.

An overview of DBS is illustrated in Figure 9. It shows how the neurostimulator (the IPG) is connected via wires to the brain electrodes. The IPG delivers the necessary electrical impulses to modulate the disturbed neural activity. DBS generally reduces beta-band synchronization in the basal ganglia, which facilitates the initiation of movement in PD patients.

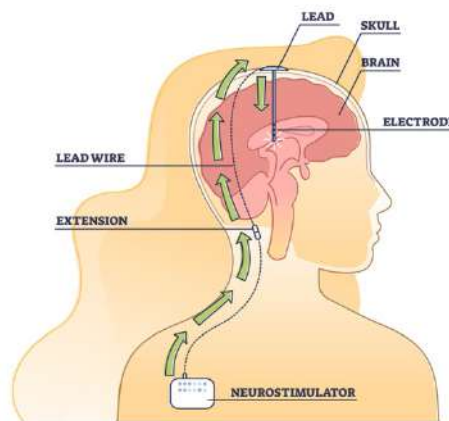


Figure 9: Overview of the DBS system pathway<sup>52</sup>

While DBS shares some parallels with this project, it remains fundamentally different.

DBS suppresses overactive neural activity using high-frequency electrical stimulation, whereas FTtM predicts movements based on intentional brain signals.

Table 1 presents a table summarizing the differences between BCI, neuroprosthetics, DBS and FTtM.

---

<sup>52</sup> From <https://www.ohsu.edu/sites/default/files/2022-05/GettyImages-1324195152-full-size-CROP.jpeg>

Category	Goal	Technology	Degree of invasiveness	The patient	Application of AI	Training
BCI	Communication and control by using brain signals	EEG or implants	Non-invasive (EEG) or invasive (implants)	Neurological disorders	Limited	Comprehensive signal training
Neuroprosthetics	Rehabilitation of motoric functions	EMG/EEG + actuator	Often invasive	Loss of motoric function	Limited	Calibration on muscle activity
DBS	Symptom treatment by brain stimulation	Implanted electrodes and a pulse generator	Very invasive	Parkinson's-disease and tremor	None	Not needed
FTtM	Prediction and active assistance of movement by intention	Wearable EEG with a Transformer-model	Non-invasive	Parkinson's-disease and other mobility disorders	Transformer-model trained on multimodal data	Training on the user's own data

Table 1: Overview of differences and similarities between my project and similar solutions<sup>53</sup>

FTtM distinguishes itself as a non-invasive, wearable system that integrates AI, EEG, EMG and IMU to predict and stabilize motor intentions. FTtM collaborates with the body's natural neuromuscular systems. It employs active AI algorithms and requires patient training, rendering it both unique and potentially adaptable across various applications.

While this review emphasizes EEG and EMG as primary signals for movement prediction in OD patients, alternative technologies exist:

- **Magnetoencephalography<sup>54</sup> (MEG)**: A non-invasive technique that maps neural currents by measuring the magnetic fields generated by brain activity. MEG has demonstrated efficacy in characterizing PD by detecting abnormal phase-amplitude coupling in the brain.
- **Optically pumped magnetometers (OPM<sup>55</sup>)**: An emerging technology that combines the precision of MEG with enhanced portability. OPMs operate at room temperature and can be placed closer to the scalp, providing high signal strength and improved spatial resolution.

In this project, EEG was chosen due to its cost-effectiveness and feasibility for developing a real-time, neurostimulating wearable solution, making it more practical than MEG and OPM-based systems.

<sup>53</sup> Own Work

<sup>54</sup> (Magnetoencephalography, 2024), (Cleveland Clinic, 2025)

<sup>55</sup> (Tierney & et al., 2019), (Virginia Tech, 2021). The researcher Andreas Nørgaard Glud (Clinic lecturer in Institute for Clinical Medicine - Brain- og Back surgery in Aarhus University) suggested me this method.

## Overall conclusion of the literature review

This review shows that multimodal integration of EEG, EMG, and AI provides a robust framework for predicting and supporting movement in PD. EEG captures premotor activity and disease-specific alterations in frequency bands and connectivity, while EMG delivers high-resolution information about muscle activation, albeit requiring personalised calibration. Combined EEG/EMG, especially with advanced models such as LSTM, DeepConvNet, and Transformer architectures, achieves high accuracy and real-time responsiveness, essential for adaptive therapeutic use.

Beyond signal processing, stimulation technologies like EMS/FES and FUS demonstrate that neuromodulation can restore functional movement and enhance neuroplasticity when optimally patterned or closed loop controlled. In parallel, biochemical strategies, including levodopa prodrugs and triple combination therapy with entacapone, extend the pharmacological toolkit to stabilise dopamine levels and complement stimulation-based approaches. Compared with existing solutions such as BCI, neuroprosthetics, and DBS, the FTtM system distinguishes itself by reintegrating natural motor function rather than substituting or externally controlling it.

Taken together, the literature underlines that the most promising path forward lies in hybrid strategies: personalised, AI-driven prediction of motor intention via EEG/EMG/IMU, coupled with adaptive stimulation (EMS, FUS) and supported by pharmacological optimisation, which I call BPI. Such a system holds potential to bypass impaired basal ganglia circuits, reactivate muscle movement, and provide patients with PD more fluent motor control.

## Hypothesis

I hypothesise that an AI Transformer-model trained on multimodal data, specifically EEG, EMG, and IMU signal, can predict intentional movements with a classification accuracy of at least 95%. This hypothesis is based on the Transformer architecture's capability to capture temporal signals and process complex, multimodal datasets effectively.

In practice, the model's output will be used to activate muscles or control mechanical devices, such as robotic arms or exoskeletons, thereby assisting PD patients in their movements. Alternatively, the output could be integrated into a hybrid FUS/EMS system called BPI.

To test this hypothesis, I will undertake the following steps:

1. Train and test various AI models to quantitatively and logically select the most suitable model for my project, based on the results.
2. Collect EEG, EMG, and IMU data from movements performed by myself and in the future my father and/or other test subjects.
3. Train and optimise the Transformer model by applying different feature extraction methods and tuning hyperparameters (e.g., batch size, learning rate). Training and test fold sizes will also be tuned.
4. Evaluate the Transformer's ability to classify movements by comparing its predictions against actual movements from new datasets, both offline and in real time.
5. Build a test setup where I will perform measurements on myself using a custom-built EEG circuit and donated professional equipment. This system will measure the voltage difference between an active electrode and a reference electrode to record EEG signals. Additionally, I will construct a 6-axis robotic arm using a microprocessor, allowing me to demonstrate the system's ability to translate neural intentions into concrete, visible movements in real time.

If the hypothesis stands, the project will show that AI can effectively convert brain intentions into movements, for example, through EMS and FUS, potentially opening new possibilities for neuro-technologies such as my own BPI.

## Design and methodology

Experiments have been conducted in this project, all of which contribute important partial results to the development of the complete system. The experiments build on one another and test the system's robustness and functionality, both through offline analyses and in real-time.

The project is divided into three phases:

### **1. Training and test of AI-models on a public dataset**

I have trained and tested seven different AI models on EEG/EMG data from the article by [29] The subjects were instructed to perform right arm movements using an orthosis while

being monitored. The AI models were programmed to classify the signals as either “movement” or “no movement.” The goal was to identify the most suitable AI model for further development in the project.

## **2. Real-time control of a robot arm using IMU’s**

Next, I built an IMU-based system in which an IMU placed on my arm can control two of the robotic arm’s servos in real time. The goal is to eventually control five servos using three IMUs placed on my forearm, wrist, and upper arm. The purpose is to demonstrate that motion signals from the body can be used directly to control an external device.

## **3. Training and application of the Transformer-model on my own EEG/EMG/IMU-data**

Finally, I will train a Transformer model on my own biosignals. I have programmed the Transformer model to predict intentional movements, identified through BP based on combined EEG, EMG, and IMU inputs. However, I have yet to test and train this model.

I will use my own EEG hardware to record EEG signals and integrate them as input modalities for the Transformer model. The model’s output will consist of binary values that will be translated into specific motor actions of the robotic arm (e.g., contraction or extension). The project will first be implemented offline and later transferred to a real-time setup. In the future, the next version will be applied to data measured from my father.

The most important methodological considerations are presented in the main body of the report, while technical details and experimental logs can be found in Appendices 2, 3, and 4. The following sections describe the choice of AI model, data collection, and measurement setup in more detail.

## Methodical considerations

In this project, I will conduct three experiments to develop and test an AI model for predicting movement in PD. This will follow the three steps outlined in the previous section. It is a complex task that requires a series of sub-goals and intermediate processes. Figure 10 shows a flowchart illustrating how this process will unfold.

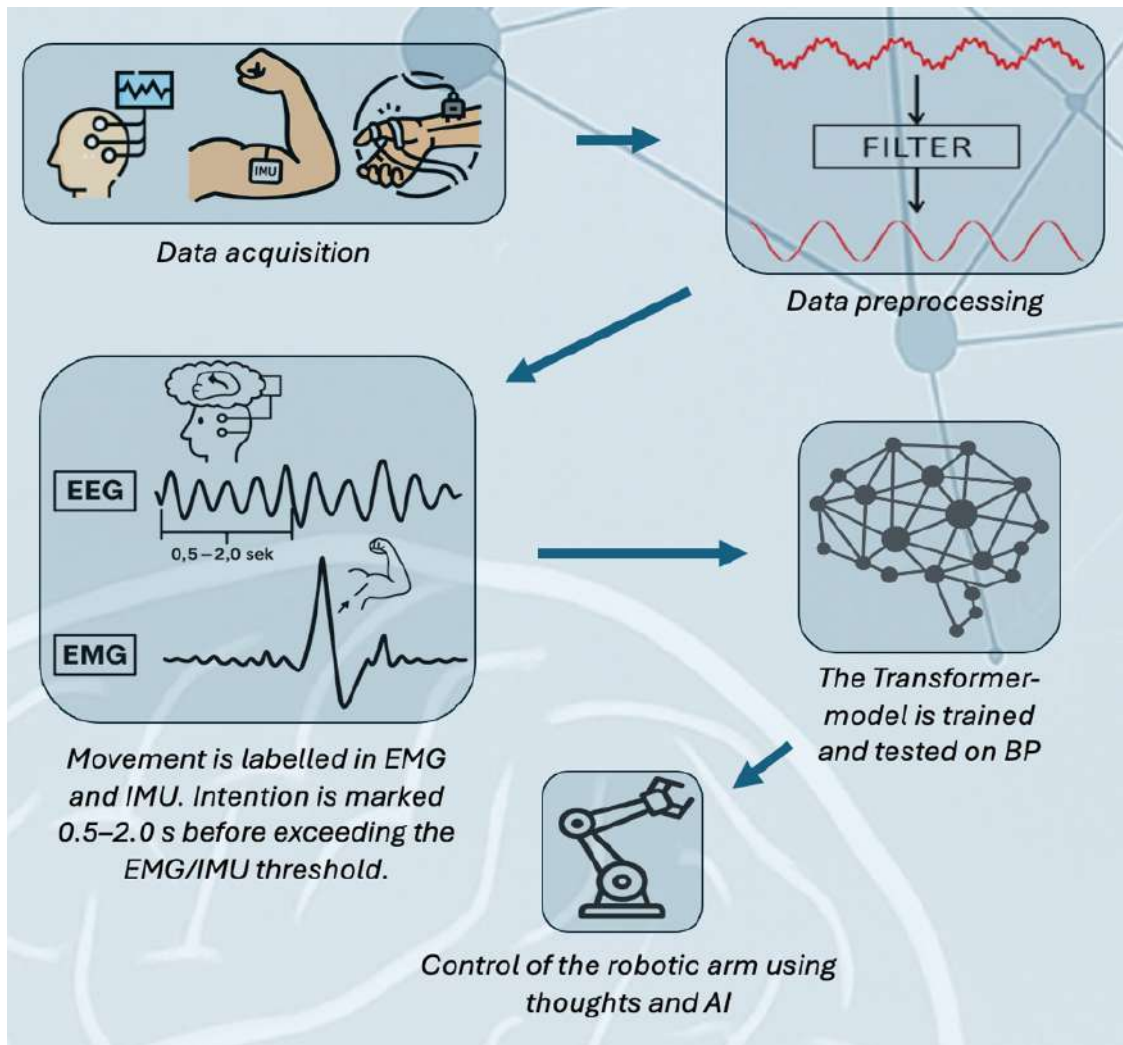


Figure 10: Flow diagram of the project<sup>56</sup>

## Test of AI-models on public dataset

In this experiment, I tested seven different AI models, each selected based on findings from the literature review, to classify an output signal as either movement or no movement. The classification was based on the following predefined threshold value (chosen from (Zhang, et al., 2023))

<sup>56</sup> The author's own work

$$T = \text{Baseline} + 1,2\mu + 2\sigma$$

Where: baseline is the average EMG-signal during rest,  $\mu$  is the average EMG-signal during muscle active and  $\sigma$  is the standard deviation of the EMG-signal during muscle activity.

If the output exceeded this threshold, it was classified as 1 (movement); otherwise, 0 (no movement). The source code for these models is available at: <https://github.com/TobiasBN1005/From-thought-to-movement/tree/main/AI-models>

The dataset used originates from (Kueper, et al., 2024) and contains EEG/EMG data from participants performing right-arm movements with an attached orthosis. The data was bandpass filtered between 0.5 Hz and 45 Hz; notch filtered at 50 Hz to remove noise and finally normalized. To mitigate overfitting, I used 5-fold k-cross-validation. Data from subject AA57D was excluded due to file corruption during upload.

Only the time window from 30 to 230 seconds was analysed, as the signals outside this range were too noisy. The evaluation metrics included precision, confusion matrix, ROC curve, and AUC. Additionally, I measured each model's training time and inference time to assess overall efficiency. Efficiency was defined to yield a value between 0 and 1 (with 1 being optimal), using the following formula:

$$\text{Efficiency} = \left( \alpha \cdot \frac{\text{Precision}^2}{\text{Precision}_{\max}} + \beta \cdot \text{AUC} \right) \cdot \left( 1 - \gamma \cdot \frac{\log(\text{time})}{\log(\text{time}_{\max})} \right)$$

Where<sup>57</sup>:  $\alpha = 0.8$ ,  $\beta = 0.4$ ,  $\gamma = 0.4$ , and

$\text{Precision}_{\max}$  is the highest precision among all AI-models

$\text{time}_{\max}$  is the longest training time among all models.

The following AI models were tested and trained using 5-fold cross-validation (80% training / 20% testing) to prevent overfitting:

---

<sup>57</sup> The coefficients values are chosen to secure that a precise and fast AI-model is weighted most.



1. LSTM-CNN
2. LSTM
3. CNN
4. Transformer
5. SVM
6. A-SVM
7. DeepConvNet

After training and testing, each model's training time, AUC score, precision, and inference time were recorded in an Excel spreadsheet. The efficiency score was automatically calculated using the formula above. The results are shown in Table 2 and Figure 11.

AI-model	Precision	Training time (s)	Time (hh:mm:ss)	AUC	Efficiency	Parameters
<b>A-SVM</b>	85.67%	57	00.00.57	93.36%	79.81%	N/A
<b>CNN</b>	100.00%	1329	00.22.09	100.00%	83.88%	907554
<b>DeepConvNet</b>	99.87%	1063	00.17.43	100.00%	84.86%	1073474
<b>LSTM-CNN</b>	99.92%	3655	01.00.55	100.00%	78.72%	842146
<b>LSTM-RNN</b>	97.58%	14165.18	03.56.05	99.33%	69.54%	548642
<b>SVM</b>	67.29%	8	00.00.08	69.48%	58.44%	N/A
<b>Transformer</b>	98.50%	645	00.10.45	99.97%	85.77%	505410

Table 2: First iteration of AI-model training, using K-fold cross-validation and different amount of parameters . The models might have overfitted in this iteration, because of the high precisions achieved. The models were built to classify between non-movement<sup>58</sup>

<sup>58</sup> The author's own work, made in Excel

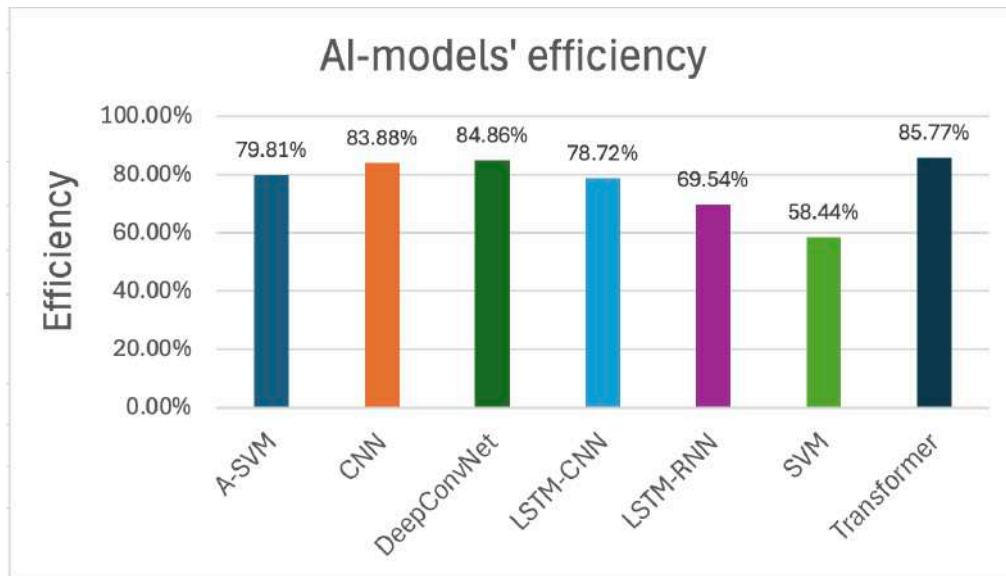


Figure 11: Graph of AI-models' efficiency<sup>59</sup>

I can from the results conclude the following

- **LSTM-RNN** and **LSTM-CNN** performed worst, due to their complexity and long training times.
- **SVM** had the lowest precision (69.48%) and was therefore not selected for further use.
- **CNN** and **DeepConvNet** were both fast and accurate but are not ideal for time-dependent signals like EEG/EMG and thus were excluded.
- **A-SVM** achieved the highest precision but was not selected due to limited presence in the literature and because Transformer models are more advanced and promising in the AI field. Moreover, its precision was 13 percentage points lower than the Transformer-model

Initial results indicated possible overfitting, as evidenced by unusually high precision and AUC scores. To address this, a second iteration was conducted using GroupKFold-validation (same data split), F1-score, and inference time. All models were scaled to ~200,000 parameters for fair comparison. As anticipated, all models exhibited a drop in performance, with the Transformer ranking among the lowest: second to last in inference time and third to last in F1-score. Nevertheless, the Transformer was selected for further development due to its balanced precision, suitability for sequential signals, and strong future potential. Its performance is also likely to improve with more

<sup>59</sup> The author's own work, made in Excel

training data and better hyperparameter tuning. Table 3 show the results from the second iteration while Figure 12 shows a F1-score vs Inference time for the AI-models:

AI-model	Precision	Training time / s	Inference time / s	Time (hh:mm:ss)	AUC	Efficiency	Parameters	F1-score
A-SVM	64.91%	9.89	0.0016	00.00.09	94.04%	58.62%	N/A	73.89%
CNN	96.99%	142.05	0.000712	00.02.22	94.17%	68.56%	229876	90.37%
DeepConvNet	98.25%	103.50	0.00061	00.01.43	96.51%	73.32%	269218	92.68%
LSTM-CNN	92.86%	320.18	0.001545	00.05.20	91.07%	56.99%	191090	86.01%
LSTM-RNN	92.11%	2245.71	0.09465	00.37.25	94.58%	40.33%	243234	89.93%
SVM	50.12%	1.19	0.000051	00.00.01	59.57%	43.66%	N/A	66.78%
Transformer	88.47%	3615	0.018	01.00.15	94.28%	34.37%	227234	83.03%

Table 3: Second iteration of AI-model training, using GroupKFold cross-validation and around the same amount of parameters to better compare different architectures. The precisions have decreased and the models likely did not overfit this time. The models were built to classify between non-movement and movement in EEG and EMG signals<sup>60</sup>

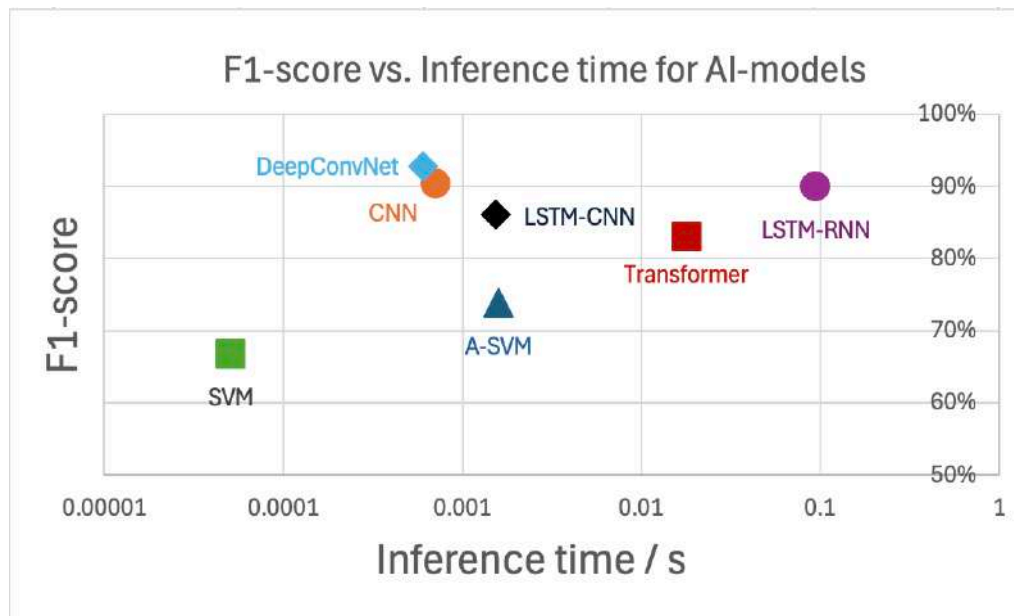


Figure 12: : Graph of AI-models' F1-score vs. Inference time. The x-axis is in a logarithmic scale with base 10. Even though the Transformer performed worse here, I have worked extensively with this model type before, which allows me to keep developing and improving it, especially because it fits well with combining EEG, EMG, and IMU signals in real-time. Its performance is also likely to improve with more training data and better hyperparameter tuning<sup>61</sup>

<sup>60</sup> The author's own work in Excel

<sup>61</sup> The author's own work in Excel

The Transformer model is therefore considered the most suitable for this project due to its balanced precision, strong performance on sequential data, and promising future potential. It will be used for further development in the next phase.<sup>62</sup>.

### Real-time control of a robotic arm by using IMU's

I constructed and built a robotic arm using an Teensy 4.1 platform, consisting of six servos, five of which are active. Each servo controls a specific function of the arm and is numbered from one to six for easy reference. Servo 4 is not used, as it does not correspond to any meaningful physiological movement of the human arm<sup>63</sup>. On Figure 13 is the self-assembled robotic arm for the project, shown.

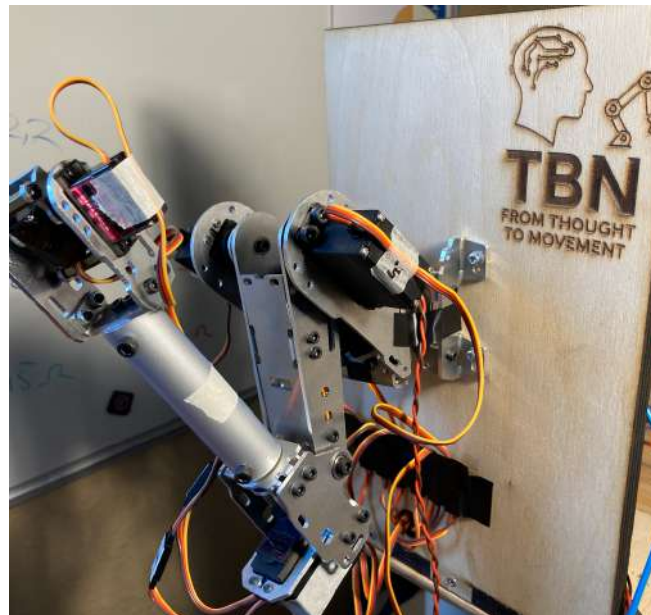


Figure 13: The robotic arm used in this project<sup>64</sup>

I have developed a prototype where each servo can be controlled in real time using data from three IMUs placed on my own arm. The IMUs measure angular velocity and acceleration, which are then translated into movements of the robotic arm. By measuring the angular displacement of each IMU along a selected axis relative to a reference point, it is possible to control the robotic arm simply by

---

<sup>62</sup> A preliminary jury for the Danish science competition *Unge Forskere*, also suggested me to work with a Transformer-model in my project.

<sup>63</sup> Look into Appendix 4 for the experiment's journal. The following link has all the code for the robot arm <https://github.com/TobiasBN1005/From-thought-to-movement-/tree/main/Robotarm>

<sup>64</sup> The author's own work

moving my arm with the IMUs attached. This demonstrates the core concept of my project: translating biosignals into actuator-driven actions. The placement of the IMUs is shown in Figure 14:

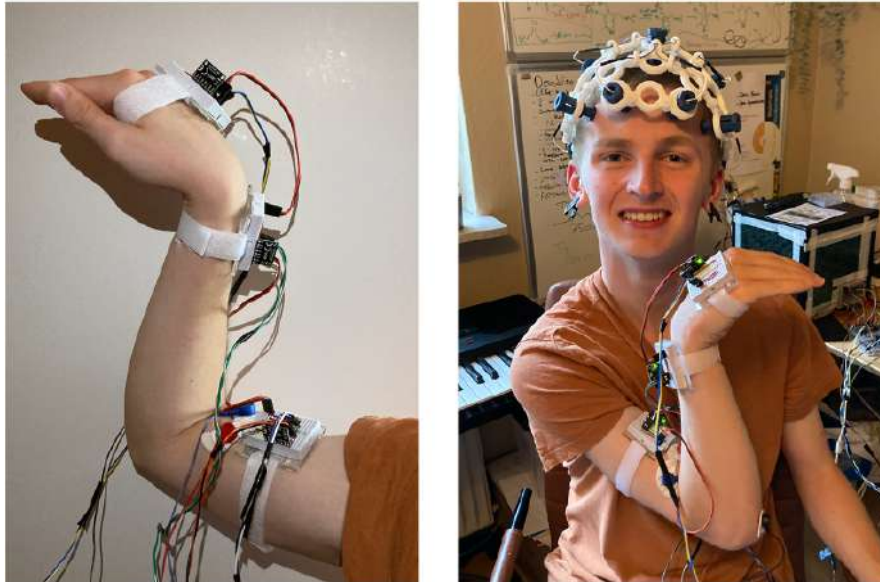


*Figure 14: Three IMUs are mounted on the right arm to track motion dynamics. Surface EMG is recorded from the BB using an active electrode, with a nearby reference electrode and ground placed at the elbow. EEG signals are acquired using the OpenBCI Cyton board and 8-channel EEG headset (donated by OpenBCI)<sup>65</sup>*

The electrical circuit connecting the IMUs to the robotic arm is shown in Figure 15.

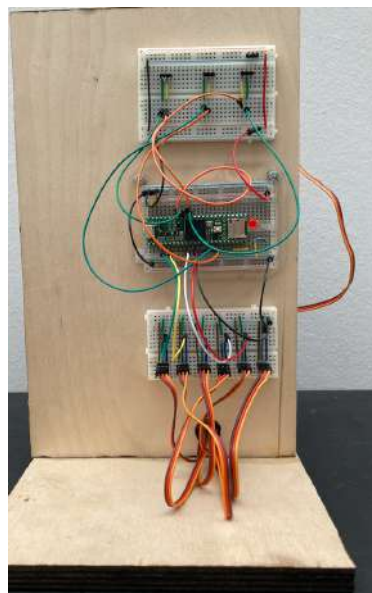


*Figure 15: The circuit for the IMU, robotic arm Teensy 4.1 microcontroller<sup>66</sup>*

---

<sup>65</sup> The author's own work

<sup>66</sup> The author's own work

Once the entire IMU-controlled robotic arm is fully functional, the next step will be to replace the IMUs with signals from my Transformer-based AI model, which processes EEG input directly. The goal is to control the robotic arm in real time based on the user's movement intentions as decoded from brain signals, thereby illustrating a central principle of the project: from intention → to action. It is right now possible for me to control the robotic arm using just my EEG activity. By introducing a threshold for the alpha-activity, I can turn on or turn off the system by either closing or opening my eyes.

In the next phase of the project, the robotic arm will be replaced by an external actuator that directly stimulates the user's own muscles. For example, using FUS combined with EMS, it may be possible to restore movement without relying on the damaged nervous system<sup>67</sup>. The Transformer model, which initially controls the robotic arm, will eventually be used to activate the muscles directly, potentially restoring mobility in individuals with motor impairments due to neurological disorders, such as PD.<sup>68</sup>

## Training and application of the Transformer-model on my own EEG/EMG/IMU-data

The Transformer-model<sup>69</sup> will be trained and tested on three modalities: EEG, EMG, and IMU. Together, these represent the user's intentions (EEG), muscle activity (EMG), and arm movement (IMU), providing a comprehensive view of how brain signals are translated into physical motion. A summary of the experimental setup<sup>70</sup> is presented in Table 4.

Modality	Sensors	Placement	Samplingrate	Function
EEG	Electrodes (at Fp1, Fp2, C3, C4, P7, Cz, O1, and O2)	The scalp	256 Hz	BP/Brain activity/Intention
EMG	Surface electrodes	BB	256 Hz	Muscle activation
IMU	IMU's (Accelerometers + Gyroscopes)	Overarm, Underarm and Wrist	256 Hz	Movement detection

Table 4: Overview of the experimental design and functions<sup>71</sup>

<sup>67</sup> Look at the section "Product ideas" for more information on this

<sup>68</sup> Explained further in the section "Future perspectives"

<sup>69</sup> The code can be found on my Github: [https://github.com/TobiasBN1005/From-thought-to-movement-/tree/main/Main\\_AI\\_model](https://github.com/TobiasBN1005/From-thought-to-movement-/tree/main/Main_AI_model)

<sup>70</sup> Look into Appendix 2 for a journal of this experiment.

<sup>71</sup> The Author's own work



The first modality for the Transformer model is EEG signals recorded from the motor cortex. Electrodes are placed at Fp1, Fp2, C3, C4, P7, Cz, O1, and O2 following the international 10-20 system. The professional EEG hardware donated by OpenBCI is used. This equipment can be seen on Figure 16:

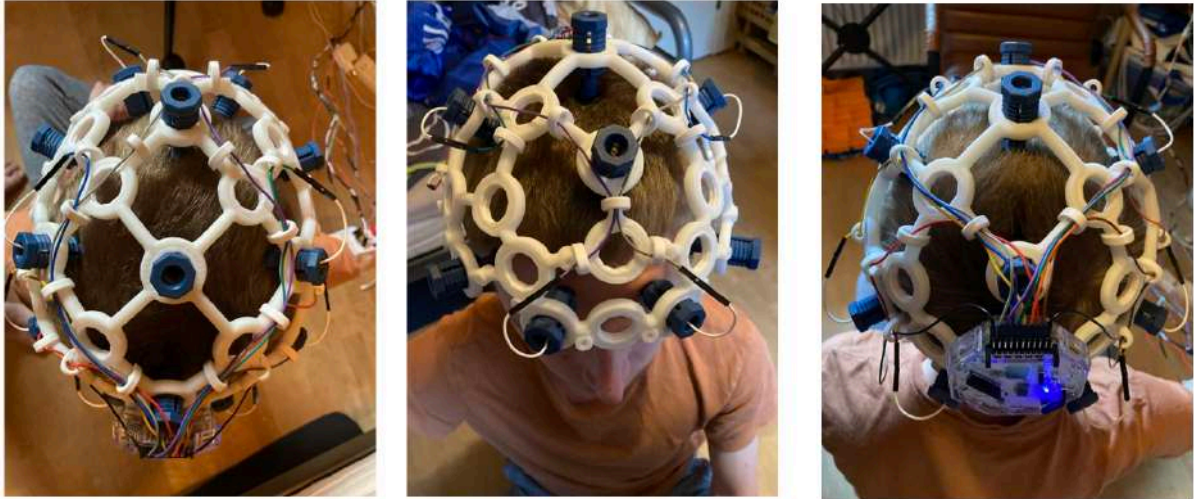


*Figure 16: Electrode placement with EEG-hardware donated by OpenBCI<sup>72</sup>*

The ears serve as the reference electrode, while surface EEG electrodes measure my brain activity. The EEG-signals are measured in real-time and saved as a CSV-file together with EMG and IM-data during training trials. Then I'll perform preprocessing methods such as ICA and bandpass filtering in MATLAB to detect my BP's for specific movements.

The most relevant EEG frequencies lie in the alpha/beta range and the 0-5 Hz band, as these are associated with voluntary movement and the BP respectively. To capture these, a bandpass filter from 0.5 Hz to 45 Hz is applied. The sampling rate is set to 256 Hz, based on recommendations from the literature<sup>73</sup>. Additionally, a notch filter is used to eliminate 50 Hz power line noise and the 10 Hz occipital alpha band.

My self-assembled and corresponding circuit diagrams are shown in Figure 17 and Figure 18 respectively. I took inspiration from (Byrne, 2018)'s master thesis "Development of a low-cost EEG-

---

<sup>72</sup> The author's own work

<sup>73</sup> The sampling rates ranged from 2000 Hz (Kueper, et al., 2024) to 128 Hz (Conti & et al., 2022), but many articles used a sampling rate of 256 Hz, which is why I also use it.

circuit”, where I then modified the circuit to have three active electrodes. My system is very close to be functional. The circuit was used in the first iterations of the project prior to the generous donation by OpenBCI<sup>74</sup>

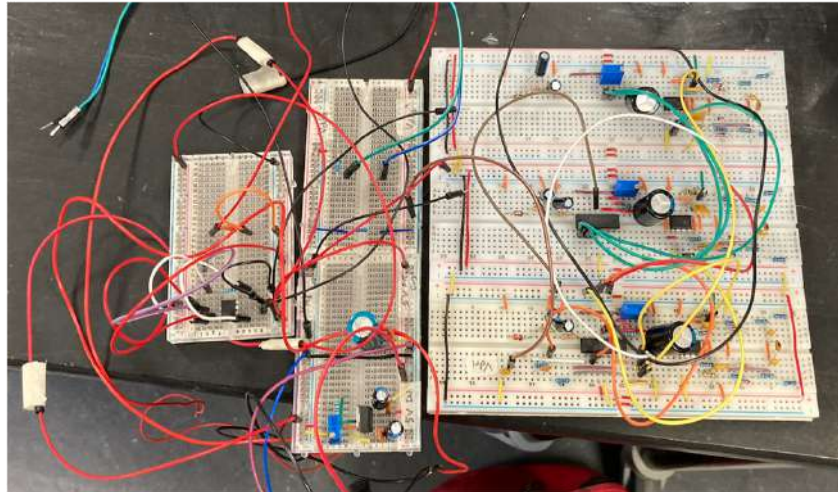


Figure 17: Self-assembled EEG-circuit with 3 active electrodes<sup>75</sup>

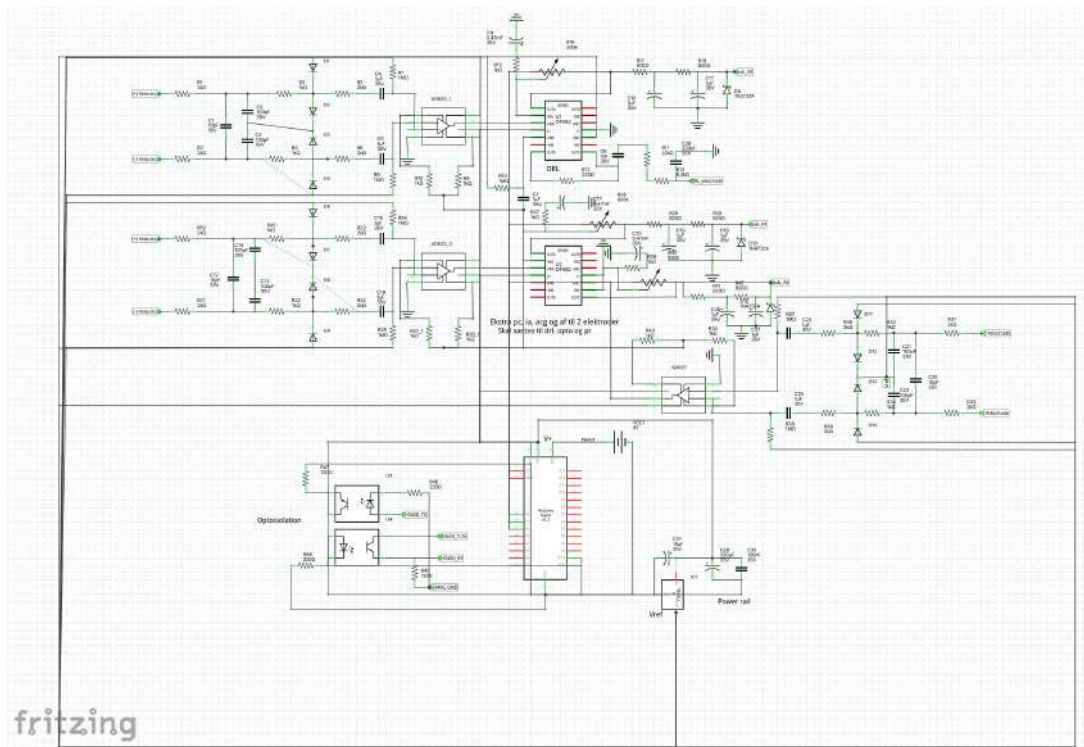


Figure 18: Self-assembled EEG-circuit circuit diagram<sup>76</sup>

<sup>74</sup> Look into Appendix 1 for a walkthrough of the electronics and code behind the EEG-measurements. The code is written in STM32CubeMX, where I used a NucleoF303K8 micro board.

<sup>75</sup> The author’s own work

<sup>76</sup> The author’s own work, made in Fritzing



The circuit is composed of several sub-circuits to ensure a clean and robust EEG signal<sup>77</sup>. The raw EEG data undergoes filtering, amplification, and signal protection before being passed to the Teensy 4.1 microcontroller via its Zar ADC channel for digital processing. The digitized EEG data is then fed into the multimodal Transformer model for further analysis.

The second modality is EMG. I will measure EMG signals from four different muscles in my right arm:

- M. biceps brachii (BB)
- M. triceps brachii (TB)
- M. triceps brachii long head (TBLH)
- M. flexor digitorum superficialis (FDS)

Surface electrodes will be used for the measurements, with the ground electrode placed on the elbow and the reference electrode placed near the biceps. The EMG signals will be used to determine how and when muscles activate, and to define the start time for segmenting BP data.

To reduce impedance and ensure clean signal acquisition, I will take a shower and disinfect the arm to remove dead skin and bacteria before attaching the electrodes. The EMG setup and electrode placement are shown in Figure 19:

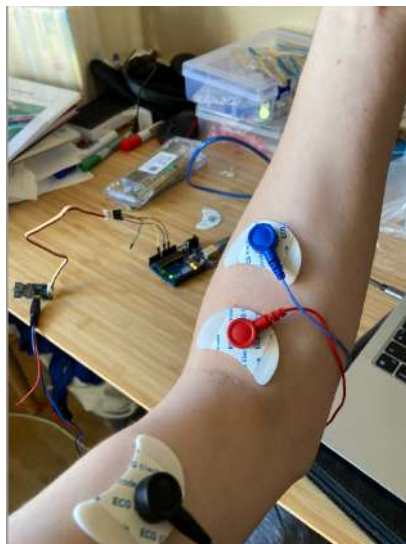


Figure 19: EMG-setup with electrodes on my arm<sup>78</sup>

---

<sup>77</sup> Look into Appendix 1 for a further explanation of the circuit [https://github.com/TobiasBN1005/From-thought-to-movement-/tree/main/EEG\\_code-kopi](https://github.com/TobiasBN1005/From-thought-to-movement-/tree/main/EEG_code-kopi) for the code

<sup>78</sup> The author's own work

In the illustrations:

- The black electrode represents ground
- The red electrode is the active (signal) electrode
- The blue electrode is the reference electrode

The specific muscles where the active electrodes will be placed are shown in Figure 20.

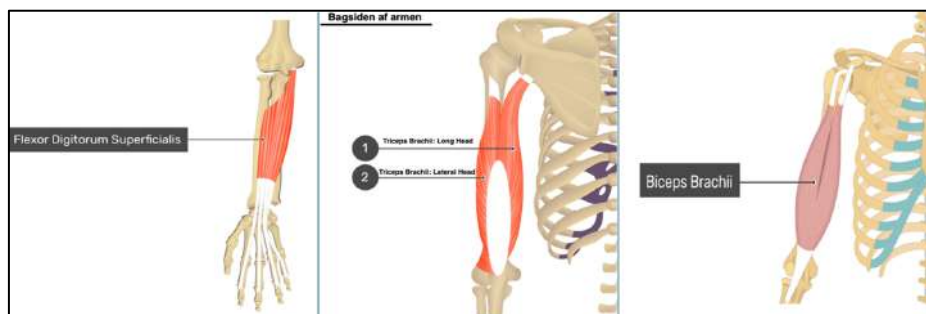


Figure 20: Target muscles for EMG electrode placement<sup>79</sup>

EMG-measurement data during a training session, is shown on Figure 21:

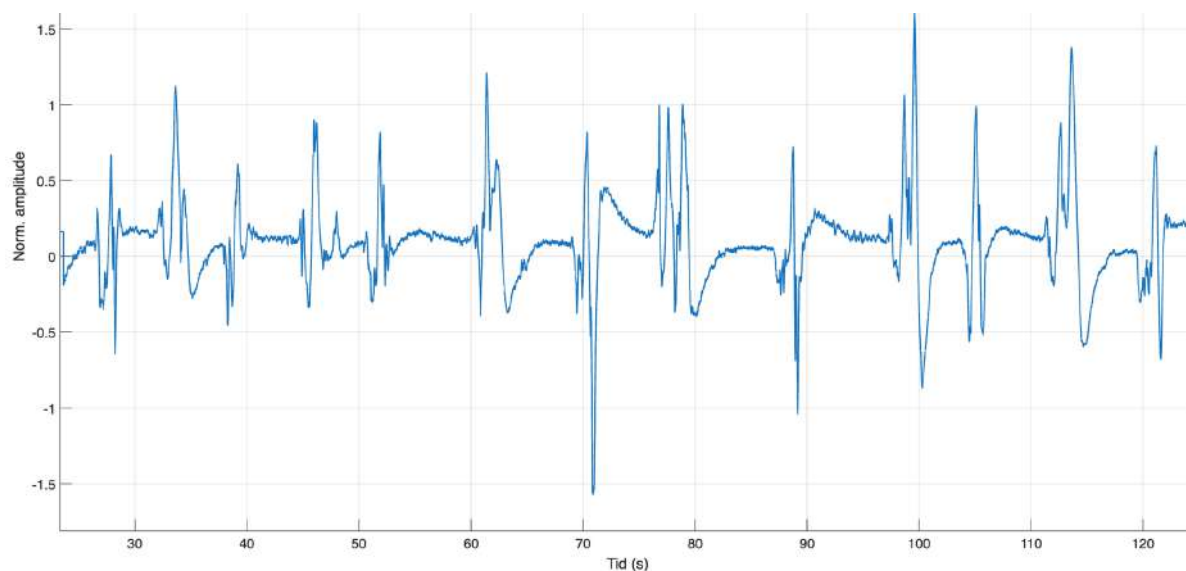


Figure 21: EMG of my own muscle activity during flexion and extension of my right arm<sup>80</sup>

<sup>79</sup> Loaned from <https://www.getbodysmart.com/arm-muscles/>

<sup>80</sup> The author's own work

The third modality involves three IMUs, which will be placed on the forearm, upper arm, and wrist, all on the right arm, just as in the earlier experiment. The IMUs help identify the onset of movement, enabling analysis of the EEG signal before motion begins to identify the BP. In addition to triggering BP analysis, the IMUs enhance the model's robustness and precision by providing real-time data on both movement angle and intensity. The IMU placements are shown in Figure 14.

When a change is detected in the IMU data, a time window from 0.5 to 2 seconds before movement onset is extracted from the EEG signal to identify the BP. Simultaneously, EMG signal deviations are tracked to determine when muscle activation exceeds a predefined threshold. This dual tracking enables the identification of both the start of a movement and the preceding EEG patterns effectively capturing the intention to move. My current MATLAB-code depicting this, is shown in Figure 22.

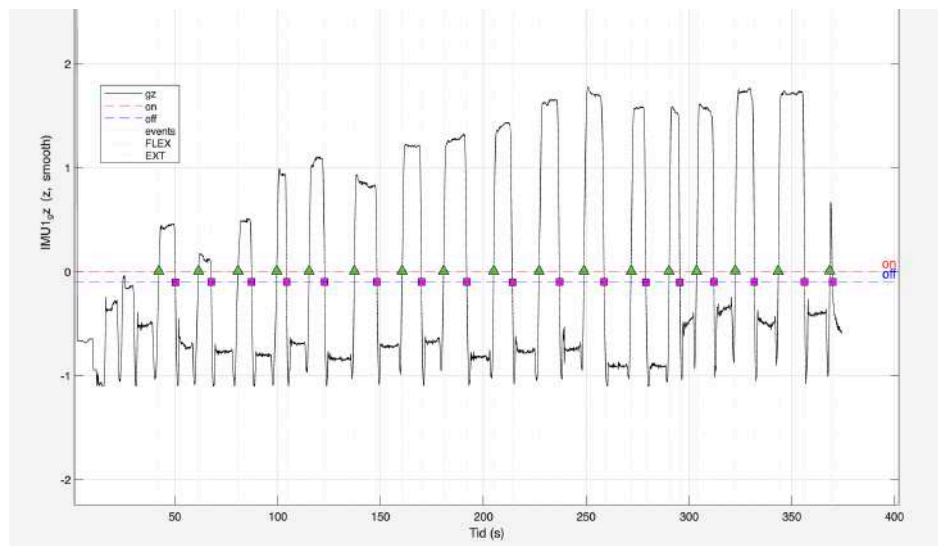


Figure 22: IMU-data during training session with flexion and extension of my right arm<sup>81</sup>

After data collection, all signals will be filtered to reduce noise and optimize quality for training and testing. I will apply a bandpass filter, notch filter, Butterworth filter, and normalize the data around zero to ensure comparability across channels.

<sup>81</sup> The author's own work

During training and testing, I will continuously evaluate whether adjustments in feature extraction are necessary to ensure the model learns from the most robust and informative data structures. Based on this, I will select the most accurate and efficient Transformer model for the project's objectives.

After offline training, the model will be evaluated in real time to assess its ability to detect intentional movements before they occur. The output from the model will be a unique 4-bit binary code for each movement type, classified based on the EEG signal's BP segment. This allows the user's intention to be translated into a specific movement, which will then be executed by the robotic arm.

Current preprocessing of my EEG-data for multiple trials can be seen on:

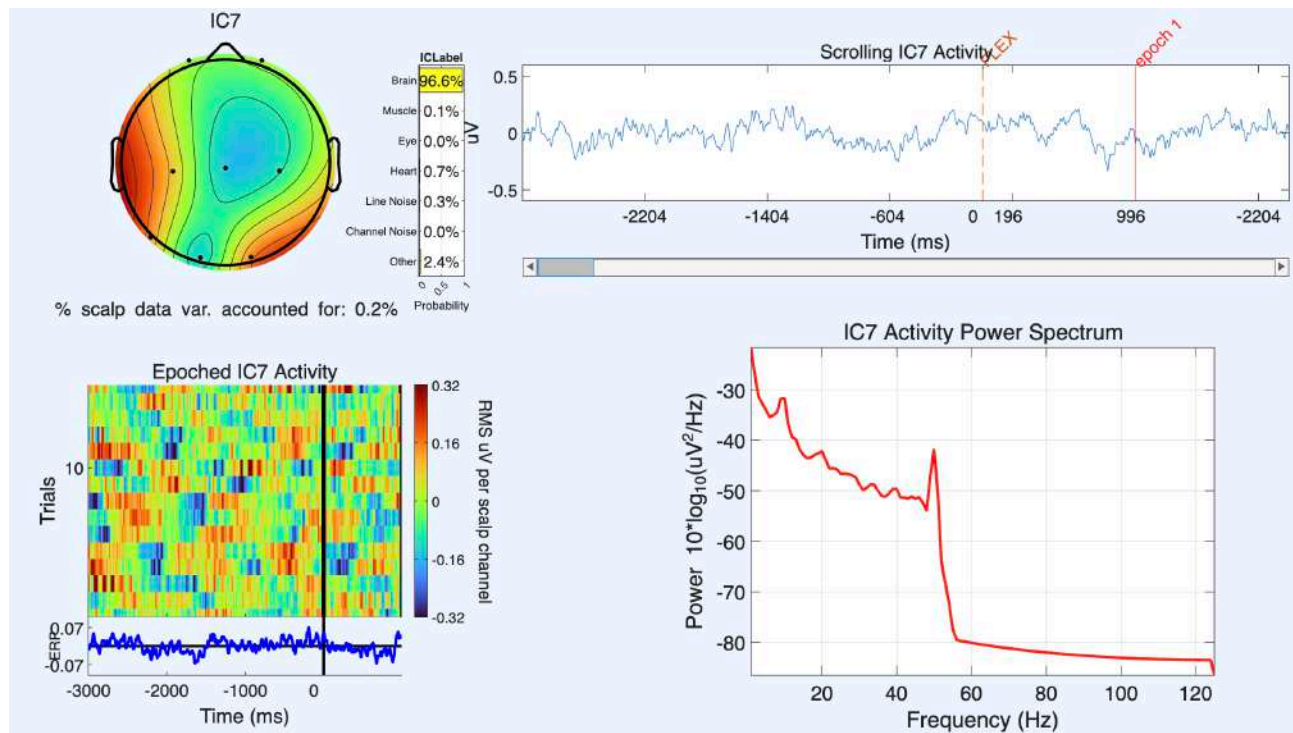


Figure 23: EEG activity, ICA and Power Spectrum of my EEG-signals during a training session<sup>82</sup>.

Table 5 shows the seven primary arm movements used in the training data and experiments, along with their corresponding binary codes. These were selected because they represent the most fundamental arm functions.

<sup>82</sup> The author's own work in MATLAB








Movement	No movement (baseline)	Flexion of underarm	Extension of underarm	Raising of arm	Lowering of arm	Supination of wrist	Pronation of wrist
Photo of Movement							
Binary value	0000	0001	0010	0011	0100	0101	0110

Table 5: The different movement types<sup>83</sup>

These binary values will be serially transmitted to the robotic arm, which will be programmed to interpret each binary sequence as a specific movement in real time.

By combining the three modalities, EEG, EMG, and IMU, the Transformer model will be trained and tested on multimodal data. This integrates intention, muscle activation, and physical movement into a unified architecture, enabling the prediction of movement based solely on the neural signals that reflect intent.

To quantify the model's accuracy, I will log every output generated by the Transformer model and compare it with the actual performed movement. In addition, true positives and false negatives will be recorded, allowing me to create a confusion matrix evaluating the model's classification performance.

As the Transformer model and data collection process are not yet fully completed, no results are available at this stage, but they will be ready for the final presentation!

Based on future results, it is expected that the Transformer model will demonstrate high precision and, importantly, prove that interpreting thought-based intentions is possible using relevant biosignals and a Transformer-based architecture.

<sup>83</sup> The author's own work

### *Sources of error and uncertainties*

This project involves the use of complex biosignals and AI, which naturally introduces potential sources of error and uncertainty. The most important sources of error are outlined below:

#### **1. Quality of EEG/EMG signals**

EEG/EMG signals are highly susceptible to noise, especially from electrical sources, body movements, and poor skin contact. Incorrect electrode placement or high impedance can lead to poor measurements, which is why I use conductive gel and a swim cap to keep the electrodes securely in place.

#### **2. IMU-placement and sensor noise**

IMUs are sensitive to small placement variations and rotational noise. Even minor misplacements during monitoring can lead to incorrect angular calculations, resulting in inaccuracies in the real-time signal.

#### **3. Synchronisation of modalities**

The EEG, EMG, and IMU signals must be recorded with precise time synchronization. This is crucial, as BP and muscle activation need to be correctly aligned with the movement onset for accurate timing matching.

#### **4. Overfitting and data leakage in the AI-model**

The Transformer model may overfit if trained on small or biased datasets, which is why I employ k-fold cross-validation and ensure that the data split is free from overlap to minimize this risk. If signals from the same subject appear in both the training and testing sets, this can artificially inflate precision scores.

#### **5. Homebuilt EEG-hardware and circuit**

The EEG circuit is homebuilt using basic components, which may result in lower signal-to-noise ratios compared to clinical-grade equipment. Potential errors in ADC conversion, filter design, or amplification could interfere with the signal quality.

These sources of error and uncertainty may affect the precision and robustness of the experiment, but they do not invalidate the core concept of the project. Most potential errors have been identified, and efforts have been made to minimize them. The experimental setup is designed to handle noise and variability to the best extent possible.

## Product, future and ethics

### Product

I am in the process of developing a Transformer model that can predict intended movements in real-time based on EEG signals recorded from electrodes placed on the scalp. The goal of this project is to eventually create a wearable, non-invasive device that can incorporate this model. Below are the functional and non-functional requirements<sup>84</sup> for this future product.

### Functional requirements

Functional requirements define the system's concrete functions and capabilities, specifying what the system should do. The functional requirements for the product are presented in Table 6.

Nr.	Functional Requirement
F1	The system must acquire EEG, EMG, and IMU data with high signal quality and effective noise filtration.
F2	The transformer model must predict intentional muscle movements based solely on real-time EEG data.
F3	Electrodes and sensors must be safely and comfortably mounted on the user's head and arm, without causing irritation.
F4	The system must be able to initiate and assist movement using neural intentions alone.
F5	The system must operate in real time: binary movement classification should occur within milliseconds of the user's intention.
F6	The system must be wearable and include a compact transformer model with an integrated battery.
F7	The system must be medically neutral and must not interfere with medications such as Levodopa.
F8	The system must translate the Transformer model's output into physical movement via an actuator (EMS/FUS).
F9	The system must prevent unintended movements. A stop function, either analog or digital, must deactivate the system immediately.
F10	The system must operate continuously for at least 16 hours, allowing overnight recharging for full-day use.

Table 6: The functional requirements of the future product<sup>85</sup>

<sup>84</sup> The source of the definition and difference between functional and non-functional requirements is: (Geeksforgeeks, 2025)

<sup>85</sup> The author's own work



## Non-functional requirements

Non-functional requirements pertain to the quality aspects of the system, such as design, ease of use, and performance, essentially defining how the system should perform. The non-functional requirements for the product are listed in Table 7.

Nr.	Non-functional Requirement
NF1	The final system must be economically accessible and cost-efficient.
NF2	The system must be individualised, supporting person-specific training due to variations in EEG signals and brain structures.
NF3	The system must be scalable: transitioning from personalised models to adaptive models generalisable across different users.
NF4	The user interface (GUI) must be intuitive and user-friendly, allowing easy access for both patients and clinical staff.
NF5	The system must be robust for daily use, including resistance to movement, moisture, humidity, and minor impacts.
NF6	The system must be adjustable to accommodate different body sizes and types of motor impairments.
NF7	The transformer model must provide explainability, e.g., by logging its predictions to a database for post-hoc error analysis.
NF8	User signal data must be processed confidentially and never stored or shared without explicit informed consent.

Table 7: The non-functional requirements of the future product<sup>86</sup>

These requirements ensure that the product must be affordable, smart, and fast, all of which are crucial when implementing the Transformer model in a wearable solution. These different models are discussed in more detail in the next section.

## Product idea: Brain Physiological Interface

### *Focused Ultrasound and Electrical Muscle Stimulation*<sup>87</sup>

My third proposal is a new method for bypassing the motor nervous system and directly activating muscles based on mental intentions. This would be achieved through a hybrid model combining FUS and EMS. I would use ultrasound to prepare the muscle group, after which a concentrated electrical current would activate the muscles, allowing for precise movements. In this case, EMS and FUS would serve as the actuators, replacing the robot arm. The Transformer model would predict the movement based on EEG, with the output providing signals to the ultrasound generator and electrical current generator. A schematic overview of this idea, which I call a BPI, is shown in Figure 24.

---

<sup>86</sup> The author's own work

<sup>87</sup> The section is based on the sources: (Evident, u.d.), (Wikipedia, 2024), (wikipedia, 2025), (Demi, 2018)



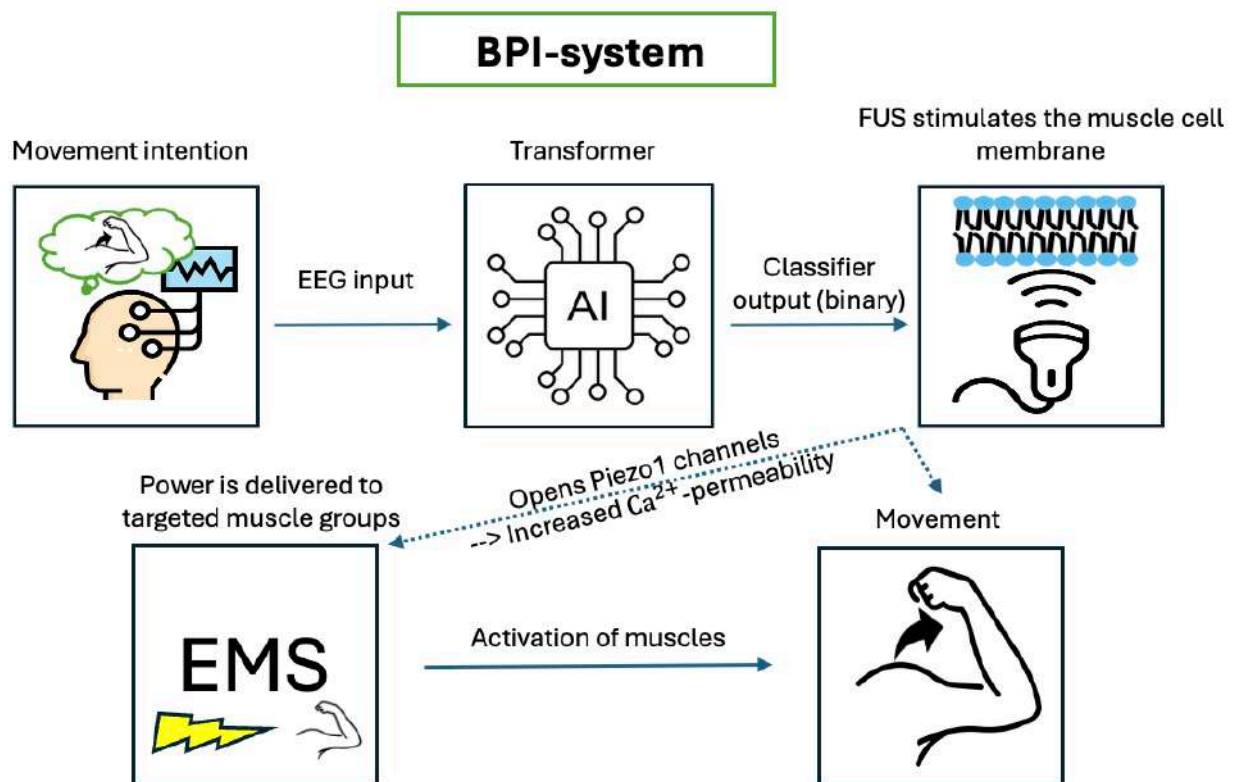


Figure 24: A schematic overview of BPI<sup>88</sup>

EEG signals from the patient's movement intentions would be captured by electrodes placed over the motor cortex and processed by a Transformer model. The model classifies the signals into binary values, which are wirelessly transmitted (e.g., via Bluetooth) to two activation units:

1. A FUS with a 3D-phased array, which targets the signal to the relevant muscle group. Here the Piezo1 channels are stimulated, increasing calcium permeability and preparing the muscle cells for activation
2. An EMS, which sends electrical impulses directly to the muscles

The combination of increased calcium influx and electrical stimulation allows for precise muscle activation, even when the signal pathways in the nervous system are compromised, such as in the case of PD. Thus, my system bypasses the nervous system entirely.

In the following section, I explain more about FUS and EMS.

<sup>88</sup> The author's own work

### Focused Ultrasound for warmup of muscles

FUS will be used in the system to prime selected muscle groups, meaning it will increase their sensitivity to subsequent electrical stimulation. By focusing ultrasound waves precisely on the muscle, the permeability of the cell membrane can be increased. This happens through the activation of calcium ion channels, which lowers the threshold for electrical activation, making muscle contraction easier. The effect depends on the frequency, intensity, and pulse modulation of the ultrasound.

The underlying mechanism involves the mechanosensitive ion channel Piezo1, which opens in response to mechanical stimuli such as stretching, pressure, and vibrations<sup>89</sup>. Piezo1 is a non-selective cation channel, and when it opens, calcium ions flow into the cell. This alters the electrical potential across the cell membrane and makes the muscle cell more excitable to electrical stimuli, making it easier for the muscles to contract.

Figure 25 illustrates this mechanism.

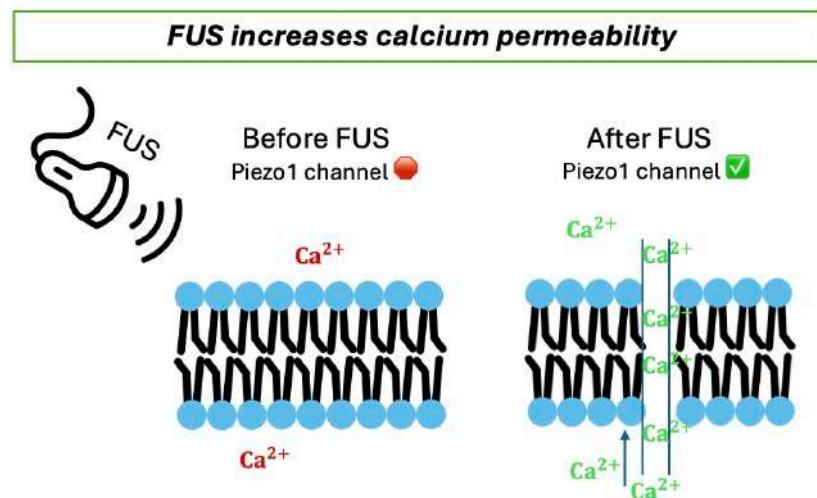


Figure 25: FUS can increase the calcium permeability, which makes it easier for current to activate muscles<sup>90</sup>

In addition to mechanical activation through FUS, the Piezo1 channel can also be activated chemically:

<sup>89</sup> (wikipedia, 2025)

<sup>90</sup> The author's own work

- **Yoda1** is an agonist that binds to Piezo1 and activates it directly without mechanical stimuli
- **Jedi1** and **Jedi2** are newer chemical agonists that offer faster at more reversible activation than Yoda<sup>91</sup>.

On the other hand, Piezo1 can be inhibited by the antagonist Dooku1, which can, among other things, block the action of Yoda1. To ensure high precision in FUS, I will also employ:

- **3D-beamforming**: focusing the sound wave both in-depth and direction<sup>92</sup>
- **Phased array-transducers**: allowing dynamic control of the focus point without physical movement.

The muscles' positions can be mapped using ultrasound scanning (B-mode). Once the muscle coordinates are known, each transducer can be directed at the relevant muscles. The input to the system comes from the Transformer model, which predicts the user's intended movement in real-time based on EEG. This prediction is then converted into signals that control both FUS priming and the subsequent electrical muscle stimulation, enabling the activation of the desired movements.

### Electrical Muscle Stimulation for movement activation

After priming the muscles with FUS, I will use EMS with specific current intensities and frequencies, which will be optimized/selected through experimental work for each muscle and movement type. EMS will be delivered as low-frequency electrical stimulation, triggering muscle contraction. The transducers and electrodes must be strategically placed on the body so that all relevant muscles are within reach, for example, a transducer aimed at the biceps to activate the right arm.

It is important to note that much research is still needed in this field. Therefore, future work will focus on fundamental research into the possibility of accurately activating muscles with FUS/EMS, so that desired movements can be performed. There is still a lot to explore!

### Future perspectives

The future development of the project will focus on making the Transformer model more generalisable. For example, training the Transformer model on larger datasets of EEG/EMG/IMU data

---

<sup>91</sup> Yes! Scientists have named agonist based on Star Wars-characters

<sup>92</sup> By using an array of many small transducers, the direction of the three-dimensional wave can be controlled, allowing it to be directed toward specific muscles. By adjusting the phase differences between the signals sent to each transducer, the focal point can be dynamically shaped and steered, both in depth and laterally, without physically moving the transducer.

from multiple patients to identify patterns across age, gender, and disease stages would be relevant. This would scale the project.

Another possibility could be noise reduction, inspired by noise-cancelling methods from DBS, to filter out tremor noise from EEG/EMG/IMU signals. If the Transformer model can separate intentional movements from tremor patterns, the accuracy of the predictions would also improve.

A third area for improvement could be integrating the system into neuroprosthetics or using it for the rehabilitation of patients with stroke or other motor disorders. The system could also be combined with speech recognition to analyse and improve PD patients speech abilities. This would allow one to predict and even generate speech based on mental intentions.

A future idea I'm working on is called "From Movement to Thought". Because, if thoughts can predict movement, could movements also predict thoughts? Since BP's are roughly unique to actions, reversing the AI-model pipeline may reveal unique thought patterns, opening new perspectives on motor cognition and intention: perhaps revealing a greater link between movements and thoughts. This connection is shown in Figure 26.

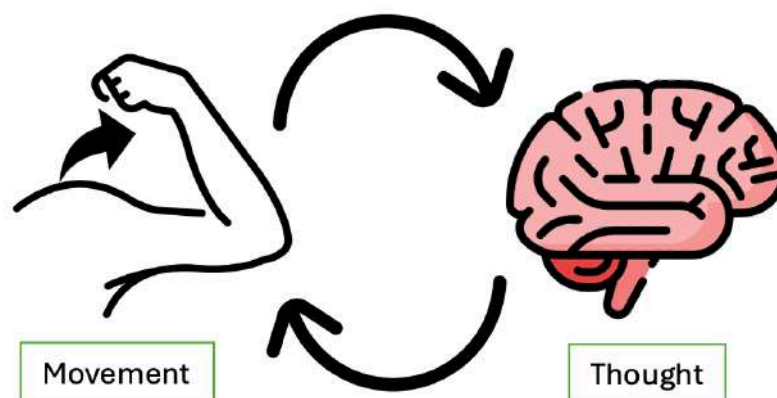


Figure 26: The interplay between brain activity for motor controls and movements may be more intertwined, which From Movement to Thought will explore in the future<sup>93</sup>

EEG also have limitations which could influence the data quality. EEG signals are weak and noisy. Electrodes mainly capture currents orthogonal to the scalp, while much brain activity cancels out or

---

<sup>93</sup> The author's own work

remains hidden. So, a large part of the signal is lost. Alternative methods include Magnetoencephalography, Near-Infrared Spectroscopy or Optically Pumped Magnetometers, but they are less practical for wearable systems. These could be combined with EEG to get a deeper insight into brain activity and movements.

I present a new method to tackle this problem called “Field-Guided Phase Alignment” (FGPA). A weak rhythmic signal that synchronizes cortical activity, so neural currents sum coherently at the scalp. Rather than steering currents toward electrodes, FGPA enhances temporal synchrony, increasing signal-to-noise and exposing intention-related patterns. Like runners pacing together, neurons align to the rhythm, producing a clearer, more decodable EEG signal. The analogy and idea is shown in Figure 27.

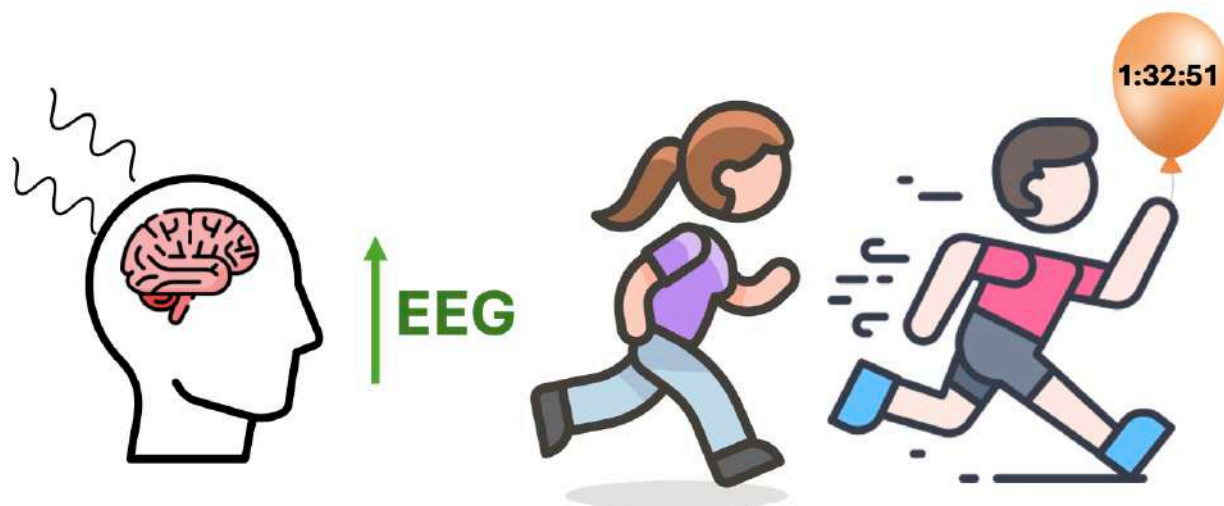


Figure 27: The idea behind FGPA - synchronised waves can enhance EEG activity, just like a runner pacing for you<sup>94</sup>

The project is still in its early phase, and a fully developed product has not yet been realized. However, many ideas are in play, and my work continues with ongoing development and testing. It is a complex project, but I am highly motivated, curious, and open to new inputs that can take the project further.

---

<sup>94</sup> The author's own work

## Ethical considerations of the project

The question of whether AI should assist with motor functions is an important one. PD has significant consequences for patients' quality of life, and any technological solution should, in my opinion, be developed with a focus on the patient's health and needs.

Data collection in this project will take place outside of clinical settings, but with the utmost control and consideration for the patient's well-being. Before testing the Transformer model on my father, I will test the system on myself and consult with my father's neurologist to ensure the experiment does not pose any risks to him.

As the system is further developed for clinical use, it will be necessary to adhere to ethical guidelines for medical research, as well as applicable laws regarding data security and patient rights, including GDPR. The Transformer model must ensure the anonymization of patient data to protect their privacy. While the data collection in this project has not had access to clinical-standard measurement equipment, the results show that the system can function under suboptimal clinical conditions. However, future iterations of the AI will require more precise measurements, either via OpenBCI or other neurotechnology platforms, to ensure higher accuracy and reliability in predictions.

## Conclusion

PD is progressively neurodegenerative, and the patient's mobility worsen as a biproduct of the damaged substantia nigra and brain structure. Existing solutions provide temporary help, but lasting assistance is still needed to enhance the patient's quality of life and voluntary mobility. This project demonstrates that it is possible to predict movement intentions using a Transformer model trained on EEG, EMG, and IMU signals. After testing seven AI architectures, the Transformer was selected for its superior performance on sequential biosignals. A complete signal pipeline was developed, from signal acquisition to real-time robotic control, and validated through 5-fold cross-validation, precision, F1-score, and inference latency.

Biosignals were collected from myself (and in the future from my father) across multiple sessions and varied conditions to simulate different physical and mental states. Data was originally collected by a homebuilt EEG circuit and later with donated equipment from OpenBCI, 3 IMUs placed on my arm, and EMG electrodes on arm muscles.

This diverse dataset will in the future enable the development of a system capable of detecting motor intention and translating it into physical action. The robot arm served as a proof of concept for the fundamental idea behind the project: prediction of movement by AI modelling and biosignals. By combining cutting edge AI and neurotechnology, this project lays the groundwork for future assistive systems that restore mobility, preserve autonomy, and improve quality of life. The goal remains: to turn thought into movement, bringing it one step closer to reality!

## Scientific Articles

- [1] R. Byrne, 'Development of a Low Cost, Open-source, Electroencephalograph-Based Brain-Computer Interface'. Dublin Institute of Technology, May 28, 2018. Accessed: Jan. 10, 2025. [Online]. Available: <https://github.com/RonanB96/Low-Cost-EEG-Based-BCI/blob/master/Thesis/Development%20of%20a%20Low%20Cost%2C%20Open-source%2C%20Electroencephalograph-Based%20Brain-Computer%20Interface.pdf>
- [2] M. J. Antony *et al.*, 'Classification of EEG Using Adaptive SVM Classifier with CSP and Online Recursive Independent Component Analysis', *Sens. Basel*, vol. 22, no. 19, p. 7596, Oct. 2022, doi: 10.3390/s22197596.
- [3] A. Buerkle, W. Eaton, N. Lohse, T. Bamber, and P. Ferreira, 'EEG based arm movement intention recognition towards enhanced safety in symbiotic Human-Robot Collaboration', *Robot. Comput.-Integr. Manuf.*, vol. 70, p. 102137, Aug. 2021, doi: 10.1016/j.rcim.2021.102137.
- [4] D. Zhang, C. Hansen, F. D. Fréne, S. P. Kærgaard, and W. Qian, 'Automated labeling and online evaluation for self-paced movement detection BCI', *Knowl.-Based Syst.*, vol. 265, p. 110383, Feb. 2023, doi: 10.1016/j.knosys.2023.110383.
- [5] J. Aeles, F. Horst, S. Lapuschkin, L. Lacourpaille, and F. Hug, 'Revealing the unique features of each individual's muscle activation signatures', *R. Soc. Publ. Interface*, vol. 18, no. 174, p. 20200770, Jan. 2021, doi: 10.1098/rsif.2020.0770.
- [6] V. del C. Silva-Acosta, I. Román-Godínez, S. Torres-Ramos, and R. A. Salido-Ruiz, 'Automatic estimation of continuous elbow flexion–extension movement based on electromyographic and electroencephalographic signals', *Biomed. Signal Process. Control*, vol. 70, p. 102950, Sept. 2021, doi: 10.1016/j.bspc.2021.102950.
- [7] M. Mahmoodi, Bahador Makkiabadi, M. Mahmoudi, and S. Sanei, 'A new method for accurate detection of movement intention from single channel EEG for online BCI', *Comput. Methods Programs Biomed. Update*, vol. 1, p. 100027, Aug. 2021, doi: 10.1016/j.cmpbup.2021.100027.
- [8] F. Karimi, J. Niu, K. Gouweleeuw, Q. Almeida, and N. Jiang, 'Movement-related EEG signatures associated with freezing of gait in Parkinson's disease: an integrative analysis', *Brain Commun.*, vol. 3, no. 4, p. fcab277, Nov. 2021, doi: 10.1093/braincomms/fcab277.
- [9] H.-C. Wang, A. J. Lees, and P. Brown, 'Impairment of EEG desynchronisation before and during movement and its relation to bradykinesia in Parkinson's disease', *J. Neurol. Neurosurg. Psychiatry*, vol. 66, no. 4, pp. 442–446, Apr. 1999, doi: 10.1136/jnnp.66.4.442.



- [10] A. Miladinović *et al.*, ‘EEG changes and motor deficits in Parkinson’s disease patients: Correlation of motor scales and EEG power bands’, *Procedia Comput. Sci.*, vol. 192, pp. 2616–2623, 2021, doi: 10.1016/j.procs.2021.09.031.
- [11] S. Farashi, A. Sarihi, M. Ramezani, S. Shahidi, and M. Mazdeh, ‘Parkinson’s disease tremor prediction using EEG data analysis-A preliminary and feasibility study’, *BMC Neurol.*, vol. 23, p. 420, Nov. 2023, doi: 10.1186/s12883-023-03468-0.
- [12] A. A. P. Suárez, S. B. Batista, I. P. Ibáñez, E. C. Fernández, M. F. Campos, and L. M. Chacón, ‘EEG-Derived Functional Connectivity Patterns Associated with Mild Cognitive Impairment in Parkinson’s Disease’, *Behav. Sci. Basel*, vol. 11, no. 3, p. 11030040, Mar. 2021, doi: 10.3390/bs11030040.
- [13] M. Conti *et al.*, ‘Brain Functional Connectivity in de novo Parkinson’s Disease Patients Based on Clinical EEG’, *Front. Neurol.*, vol. 13, p. 844745, Mar. 2022, doi: 10.3389/fneur.2022.844745.
- [14] K. Desai, ‘Parkinson’s Disease Detection via Resting-State Electroencephalography Using Signal Processing and Machine Learning Techniques’, *arxiv*, Mar. 2023, doi: 10.48550/arXiv.2304.01214.
- [15] R. A. Zanini, E. L. Colombin, and M. C. F. de Castro, ‘Parkinson’s disease EMG signal prediction using Neural Networks’, *2019 IEEE Int. Conf. Syst. Man Cybern. SMC*, pp. 2446–2453, Sept. 2019.
- [16] A. Saikia, A. Saikia, Amit Ranjan Barua, and S. Paul, ‘EEG-EMG Correlation for Parkinson’s disease’, *Int. J. Eng. Adv. Technol. IJEAT*, vol. 8, no. 6, Aug. 2019, doi: 10.35940/ijeat.F8360.088619.
- [17] B. M. Doucet, A. Lam, and L. Griffin, ‘Neuromuscular Electrical Stimulation for Skeletal Muscle Function’, *Yale J. Biol. Med.*, vol. 85, no. 2, pp. 201–215, June 2012.
- [18] M. Popovic, T. Thrasher, M. Adams, V. Takes, V. Zivanovic, and M. Tonack, ‘Functional electrical therapy: retraining grasping in spinal cord injury’, *Spinal Cord*, vol. 44, pp. 143–151, Mar. 2006, doi: 10.1038/sj.sc.3101822.
- [19] M. Sun *et al.*, ‘FES-UPP: A Flexible Functional Electrical Stimulation System to Support Upper Limb Functional Activity Practice’, *Front. Neurosci.*, vol. 12, no. 449, July 2018, doi: 10.3389/fnins.2018.00449.
- [20] A. Cuesta-Gómez, F. Molina-Rueda, M. Carratala-Tejada, E. Imatz-Ojanguren, D. Torricelli, and J. C. Miangolarra-Page, ‘The Use of Functional Electrical Stimulation on the Upper

Limb and Interscapular Muscles of Patients with Stroke for the Improvement of Reaching Movements: A Feasibility Study', *Front. Neurol.*, vol. 8, May 2017, doi: 10.3389/fneur.2017.00186.

[21] A. Biasiucci *et al.*, 'Brain-actuated functional electrical stimulation elicits lasting arm motor recovery after stroke', *Nat. Commun.*, vol. 9, no. 2421, June 2018, doi: 10.1038/s41467-018-04673-z.

[22] M. A. Khan *et al.*, 'A systematic review on functional electrical stimulation based rehabilitation systems for upper limb post-stroke recovery', *Front. Neurol.*, vol. 14, no. 1272992, Dec. 2023, doi: 10.3389/fneur.2023.1272992.

[23] M. B. Kebaetse, A. E. Turner, and S. A. Binder-Macleod, 'Effects of stimulation frequencies and patterns on performance of repetitive, nonisometric tasks', *J. Appl. Physiol.*, vol. 92, no. 1, pp. 109–116, Jan. 2002, doi: 10.1152/jappl.2002.92.1.109.

[24] L. Zhang *et al.*, 'Activation of Piezo1 by ultrasonic stimulation and its effect on the permeability of human umbilical vein endothelial cells', *Biomed. Pharmacother.*, vol. 131, p. 110796, Nov. 2020, doi: 10.1016/j.biopha.2020.110796.

[25] D. Liao, F. Li, D. Lu, and P. Zhong, 'Activation of Piezo1 Mechanosensitive Ion Channel In HEK293T Cells by 30 MHz Vertically Deployed Surface Acoustic Waves', *Biochem. Biophys. Res. Commun.*, vol. 518, no. 3, pp. 541–547, Oct. 2019, doi: 10.1016/j.bbrc.2019.08.078.

[26] F. Haddad, M. Sawalha, Y. Khawaja, A. Najjar, and R. Karaman, 'Dopamine and Levodopa Prodrugs for the Treatment of Parkinson's Disease', *Molecules*, vol. 23, no. 1, p. 40, Dec. 2017, doi: 10.3390/molecules23010040.

[27] P. Solla, F. Marrosu, and M. G. Marrosu, 'Therapeutic interventions and adjustments in the management of Parkinson disease: Role of combined carbidopa/levodopa/entacapone (Stalevo)', *Neuropsychiatr. Dis. Treat.*, vol. 6, no. 1, pp. 483–490, July 2010.

[28] C. R. Oehr *et al.*, 'Chronic adaptive deep brain stimulation versus conventional stimulation in Parkinson's disease: a blinded randomized feasibility trial', *Nat. Med.*, vol. 30, pp. 3345–3356, Aug. 2019, doi: doi.org/10.1038/s41591-024-03196-z.

[29] N. Kueper *et al.*, 'EEG and EMG dataset for the detection of errors introduced by an active orthosis device', *Front. Hum. Neurosci.*, vol. 18, p. 1304311, Jan. 2024, doi: 10.3389/fnhum.2024.1304311.

# Bibliography

- geeksforgeeks. (2024, Juni 24). *What is LSTM – Long Short Term Memory?* Retrieved Januar 10, 2025, from geeksforgeeks.org: <https://www.geeksforgeeks.org/deep-learning-introduction-to-long-short-term-memory/>
- geeksforgeeks. (2023, Januar 10). *Long short-term memory (LSTM) RNN in Tensorflow*. Retrieved Januar 10, 2025, from geeksforgeeks.org: <https://www.geeksforgeeks.org/long-short-term-memory-lstm-rnn-in-tensorflow/>
- Hamad, R. (2023, December 3). *What is LSTM? Introduction to Long Short-Term Memory*. Retrieved Januar 10, 2025, from medium.com: <https://medium.com/@rebeen.jaff/what-is-lstm-introduction-to-long-short-term-memory-66bd3855b9ce>
- Wikipedia. (2025, Januar 7). *Recurrent Neural Network*. Retrieved Januar 10, 2025, from en.wikipedia.org: [https://en.wikipedia.org/wiki/Recurrent\\_neural\\_network](https://en.wikipedia.org/wiki/Recurrent_neural_network)
- Regalado, A. (2014, Juni 17). *The Thought Experiment*. Retrieved Januar 10, 2025, from technologyreview.com: <https://www.technologyreview.com/2014/06/17/172276/the-thought-experiment/>
- Wikipedia. (2024, December 30). *Electroencephalography*. Retrieved Januar 10, 2025, from en.wikipedia.org: <https://en.wikipedia.org/wiki/Electroencephalography>
- Chaddad, A., Wu, Y., Kateb, R., & Bouridane, A. (2023, Juli 13). Electroencephalography Signal Processing: A Comprehensive Review and Analysis of Methods and Techniques. *Sensors*.
- Parkinson.dk. (n.d.). *Hvad er parkinson?* Retrieved Januar 10, 2025, from parkinson-dk: <https://parkinson.dk/viden-forskning/om-parkinson/hvad-er-parkinson/>
- Paulson, O. B. (2024, Oktober 10). *Parkinsons sygdom*. Retrieved Januar 10, 2025, from lex.dk: [https://lex.dk/Parkinsons\\_sygdom?gad\\_source=1&gclid=CjwKCAiAp4O8BhAkEiwAqv2UqKvBVEG0S1tye5eNw\\_jpHgKSi1qq63S0RQx12dwPH\\_CZ9aiYgT-VuhoCVr0QAvD\\_BwE](https://lex.dk/Parkinsons_sygdom?gad_source=1&gclid=CjwKCAiAp4O8BhAkEiwAqv2UqKvBVEG0S1tye5eNw_jpHgKSi1qq63S0RQx12dwPH_CZ9aiYgT-VuhoCVr0QAvD_BwE)
- Keita, Z. (2023, November 14). *An Introduction to Convolutional Neural Networks (CNNs)*. Retrieved Januar 10, 2025, from datacamp.com: <https://www.datacamp.com/tutorial/introduction-to-convolutional-neural-networks-cnns>
- Mishra, M. (2020, August 26). *Convolutional Neural Networks, Explained*. Retrieved Januar 14, 2025, from towardsdatascience.com: <https://towardsdatascience.com/convolutional-neural-networks-explained-9cc5188c4939>

- Jorgecardete. (2024, Februar 7). *Convolutional Neural Networks: A Comprehensive Guide*. Retrieved Januar 14, 2025, from medium.com:  
<https://medium.com/thedeephub/convolutional-neural-networks-a-comprehensive-guide-5cc0b5eae175>
- ibm. (n.d.). *What are convolutional neural networks?* Retrieved from ibm.com:  
<https://www.ibm.com/think/topics/convolutional-neural-networks>
- Gupta, A., Vardalakis, N., & Wagner, F. B. (2023, Januar 6). Neuroprosthetics: from sensorimotor to cognitive disorders. *Communications Biology*.
- Nicolas-Alonso, L. F., & Gomez-Gil, J. (2012, Januar 31). Brain Computer Interfaces, a Review. *Sensors*.
- Byrne, R. (2018). *Development of a Low Cost, Open-source, Electroencephalograph-Based Brain-Computer Interface*. Honours Degree in Electrical and Electronic Engineering (DT021A) of the Dublin Institute of Technology.
- Kueper, N., Chari, K., Bütetür, J., Habenicht, J., Rossol, T., Kim, S. K., . . . Kirchner, E. A. (2024, Januar 22). EEG and EMG dataset for the detection of errors introduced by an active orthosis device . *Brain-Computer Interfaces*.
- Wikipedia. (2024, November 28). *Motor cortex*. Retrieved Januar 22, 2025, from en.wikipedia.org:  
[https://en.wikipedia.org/wiki/Motor\\_cortex](https://en.wikipedia.org/wiki/Motor_cortex)
- Knierum, J. (2020, Oktober 20). *Motor Systems*. Retrieved Januar 22, 2025, from nba.uth.tmc.edu:  
<https://nba.uth.tmc.edu/neuroscience/s3/chapter03.html>
- Ackermann, S. (1992). *Major Structures and Functions of the Brain*. Retrieved from ncbi.nlm.nih.gov: <https://www.ncbi.nlm.nih.gov/books/NBK234157/>
- wikipedia.org. (2024, December 26). *Savitzky-Golay filter*. Retrieved Januar 25, 2025, from en.wikipedia.org: [https://en.wikipedia.org/wiki/Savitzky%E2%80%93Golay\\_filter](https://en.wikipedia.org/wiki/Savitzky%E2%80%93Golay_filter)
- Jensen, P. M., & Jensen, C. M. (2019, Oktober). *Sensorer - Anvendt el-lære*. Retrieved 2022, from sensorer.systime: <https://sensorer.systime.dk/?id=1>
- Google colab. (n.d.). *Fourier Transform*. Retrieved from colab.research.google.com:  
<https://colab.research.google.com/github/jinglescode/python-signal-processing/blob/main/tutorials/Fourier%20Transform.ipynb>
- Google colab. (n.d.). *Signal Filters*. Retrieved from colab.research.google.com:  
[https://colab.research.google.com/github/iotanalytics/IoTTutorial/blob/main/code/preprocessing\\_and\\_decomposition/Signal\\_Filters.ipynb](https://colab.research.google.com/github/iotanalytics/IoTTutorial/blob/main/code/preprocessing_and_decomposition/Signal_Filters.ipynb)

- geeksforgeeks. (2022, Januar 19). *Plotting a Spectrogram using Python and Matplotlib*. Retrieved Januar 25, 2025, from geeksforgeeks.org: <https://geeksforgeeks.org/plotting-a-spectrogram-using-python-and-matplotlib/>
- Wikipedia. (2024, November 1). *Bereitschaftspotential*. Retrieved Januar 26, 2025, from en.wikipedia.org: <https://en.wikipedia.org/wiki/Bereitschaftspotential>
- Wikipedia. (2025, Januar 25). *Deep Brain Stimulation*. Retrieved Februar 7, 2025, from en.wikipedia.org: [https://en.wikipedia.org/wiki/Deep\\_brain\\_stimulation](https://en.wikipedia.org/wiki/Deep_brain_stimulation)
- Johns Hopkins Medicine. (2025). *Deep Brain Stimulation*. Retrieved Februar 7, 2025, from hopkinsmedicine.org: <https://www.hopkinsmedicine.org/health/treatment-tests-and-therapies/deep-brain-stimulation>
- Hospital, B. o. (Director). (2014). *Deep Brain Stimulation mod Parkinsons sygdom - hvordan foregår det, hvorfor virker det?* [Motion Picture].
- Cleveland Clinic. (2022, Maj 23). *Deep Brain stimulation*. Retrieved Februar 7, 2025, from my.clevelandclinic.org: <https://my.clevelandclinic.org/health/treatments/21088-deep-brain-stimulation>
- Wikipedia. (2025, Februar 5). *Brain-Computer-Interface*. Retrieved Februar 7, 2025, from en.wikipedia.org: [https://en.wikipedia.org/wiki/Brain%E2%80%93computer\\_interface](https://en.wikipedia.org/wiki/Brain%E2%80%93computer_interface)
- Friedenberg, D. A., Schwemmer, M. A., Landgraf, A. J., Annetta, N. V., Bockbrader, M. A., Bouton, C. E., . . . Sharma, G. (2017, August 21). Neuroprosthetic-enabled control of graded arm muscle contraction in a paralyzed human. *Nature*.
- Wikipedia. (2024, November 30). *Neuroprosthetics*. Retrieved Februar 7, 2025, from en.wikipedia.org: <https://en.wikipedia.org/wiki/Neuroprosthetics>
- Parkinson.org. (2025). *Statistics*. Retrieved from parkinson.org: <https://www.parkinson.org/understanding-parkinsons/statistics>
- Zhang, D., Hansen, C., De Fréne, F., Kærgaard, S. P., Qian, W., & Chen, K. (2023, April 8). *Automated labeling and online evaluation for self-paced movement detection BCI*. Retrieved Februar 10, 2025, from sciencedirect.com: <https://www.sciencedirect.com/science/article/pii/S0950705123001338?via%3Dihub>
- Georgiev, D., Lange, F., Seer, C., Kopp, B., & Johanshahi, M. (2016, Juni 6). *Movement-related potentials in Parkinson's disease*. Retrieved from sciencedirect.com: <https://www.sciencedirect.com/science/article/abs/pii/S1388245716300219>

Johns Hopkins Medicine. (n.d.). *Electromyography (EMG)*. Retrieved from hopkinsmedicine.org: <https://www.hopkinsmedicine.org/health/treatment-tests-and-therapies/electromyography-emg>

wikipedia. (2025, Februar 7). *Electromyography*. Retrieved Januar 15, 2025, from en.wikipedia.org: <https://en.wikipedia.org/wiki/Electromyography>

Cleveland Clinic. (2023, Oktober 2). *EMG (Electromyography)*. Retrieved Januar 17, 2025, from my.clevelandclinic.org: <https://my.clevelandclinic.org/health/diagnostics/4825-emg-electromyography>

Antony, M. J., Sankaralingam, B. P., Mahendran, R. K., Gardezi, A. A., Shafiq, M., Choi, J.-G., & Hamam, H. (2022, Oktober 7). *Classification of EEG Using Adaptive SVM Classifier with CSP and Online Recursive Independent Component Analysis*. Retrieved Februar 13, 2025, from pmc.ncbi.nlm.nih.org: <https://pmc.ncbi.nlm.nih.gov/articles/PMC9573537/>

3Blue1Brown. (2024, December 12). *Neural Networks*. Retrieved Februar 18, 2025, from youtube.com: [https://www.youtube.com/playlist?list=PLZHQObOWTQDNU6R1\\_67000Dx\\_ZCJB-3pi](https://www.youtube.com/playlist?list=PLZHQObOWTQDNU6R1_67000Dx_ZCJB-3pi)

Wikipedia. (2025, Februar 18). *Transformer (Deep learning architecture)*. Retrieved Februar 18, 2025, from en.wikipedia.org: [https://en.wikipedia.org/wiki/Transformer\\_\(deep\\_learning\\_architecture\)#Full\\_transformer\\_architecture](https://en.wikipedia.org/wiki/Transformer_(deep_learning_architecture)#Full_transformer_architecture)

Geeksforgeeks. (2024, December 6). *Transformers in Machine Learning*. Retrieved Februar 18, 2025, from geeksforgeeks.org: <https://www.geeksforgeeks.org/getting-started-with-transformers/>

Sachinsoni. (2024, September 5). *Transformer Architecture Part-1*. Retrieved Februar 18, 2025, from pub.towards.ai.net: <https://pub.towardsai.net/transformer-architecture-part-1-d157b54315e6>

Geeksforgeeks. (2025, Januar 27). *Support Vector Machine (SVM) algorithm*. Retrieved Februar 18, 2025, from geeksforgeeks.org: <https://www.geeksforgeeks.org/support-vector-machine-algorithm/>

Singh, R. (2024, Oktober 17). *Support Vector Machines (SVM)*. Retrieved Februar 18, 2025, from medium.com: <https://medium.com/@RobuRishabh/support-vector-machines-svm-27cd45b74fbb>

- Wikipedia. (2025, Februar 17). *Support Vector Machine*. Retrieved Februar 18, 2025, from en.wikipedia.org: [https://en.wikipedia.org/wiki/Support\\_vector\\_machine](https://en.wikipedia.org/wiki/Support_vector_machine)
- IBM. (n.d.). *What is a Neural Network?* Retrieved Februar 19, 2025, from ibm.com: <https://www.ibm.com/think/topics/neural-networks>
- Geeksforgeeks. (2024, December 6). *What is a Neural Network?* Retrieved Februar 19, 2025, from geeksforgeeks.org: <https://www.geeksforgeeks.org/neural-networks-a-beginners-guide/>
- Hansen, S. (2002). *Fra neuron til neurose*. Gads Forlag.
- Wikipedia. (2024, November 21). *Huber loss*. Retrieved Februar 19, 2025, from en.wikipedia.org: [https://en.wikipedia.org/wiki/Huber\\_loss](https://en.wikipedia.org/wiki/Huber_loss)
- Wikipedia. (2025, Februar 16). *Mean absolute error*. Retrieved Februar 19, 2025, from en.wikipedia.org: [https://en.wikipedia.org/wiki/Mean\\_absolute\\_error](https://en.wikipedia.org/wiki/Mean_absolute_error)
- IBM. (2024, Juli 12). *What is a loss function?* Retrieved Februar 19, 2025, from ibm.com: <https://www.ibm.com/think/topics/loss-function>
- Magnetoencephalography*. (2024, November 22). Retrieved Marts 23, 2025, from en.wikipedia.org: <https://en.wikipedia.org/wiki/Magnetoencephalography>
- Cleveland Clinic. (2025). *Magnetoencephalography (MEG)*. Retrieved Marts 23, 2025, from my.clevelandclinic.org: <https://my.clevelandclinic.org/health/diagnostics/17218-magnetoencephalography-meg>
- Tierney, T. M., & et al., I. (2019, Oktober 1). *Optically pumped magnetometers: From quantum origins to multi-channel magnetoencephalography*. Retrieved Marts 23, 2025, from pmc.ncbi.nlm.nih.gov: <https://pmc.ncbi.nlm.nih.gov/articles/PMC6988110/>
- Virginia Tech. (2021, Maj 12). *Virginia Tech launches 'next generation' human brain imaging lab*. Retrieved Marts 23, 2025, from news.vt.edu: <https://news.vt.edu/articles/2021/05/virginia-tech-launches--next-generation--human-brain-imaging-lab.html>
- Miladinovic, A., & et al., I. (2021). *EEG changes and motor deficits in Parkinson's disease patients: Correlation of motor scales and EEG power bands* Author links open overlay panel. Retrieved Marts 23, 2025, from sciencedirect.com: <https://www.sciencedirect.com/science/article/pii/S1877050921017683>
- Conti, M., & et al., I. (2022, Marts 15). *Brain Functional Connectivity in de novo Parkinson's Disease Patients Based on Clinical EEG*. Retrieved Marts 23, 2025, from frontiersin.org: <https://www.frontiersin.org/journals/neurology/articles/10.3389/fneur.2022.844745/full>

- Peláez Suárez, A. A., & et al., I. (2021, Marts 23). *EEG-Derived Functional Connectivity Patterns Associated with Mild Cognitive Impairment in Parkinson's Disease*. Retrieved Marts 23, 2025, from pmc.ncbi.nlm.nih.gov: <https://pmc.ncbi.nlm.nih.gov/articles/PMC8005012/>
- Desai, K. (2023, Marts 29). *Parkinsons Disease Detection via Resting-State Electroencephalography Using Signal Processing and Machine Learning Techniques*. Retrieved Marts 23, 2025, from arxiv.org: <https://arxiv.org/abs/2304.01214>
- Wang, H.-C., & et al., I. (1999). *Impairment of EEG desynchronisation before and during movement and its relation to bradykinesia in Parkinson's disease*. Retrieved Marts 23, 2025, from pmc.ncbi.nlm.nih.gov: <https://pmc.ncbi.nlm.nih.gov/articles/PMC1736289/>
- Farashi, S., & et al., I. (2023). *Parkinson's disease tremor prediction using EEG data analysis-A preliminary and feasibility study*. Retrieved Marts 13, 2025, from link.springer.com: <https://link.springer.com/article/10.1186/s12883-023-03468-0>
- Zanini, R., & et al., I. (2019, September). *Parkinson's disease EMG signal prediction using Neural Networks*. Retrieved Marts 13, 2025, from researchgate.net: [https://www.researchgate.net/publication/336890507\\_Parkinson's\\_disease\\_EMG\\_signal\\_prediction\\_using\\_Neural\\_Networks](https://www.researchgate.net/publication/336890507_Parkinson's_disease_EMG_signal_prediction_using_Neural_Networks)
- Saikia, A., & et al., I. (2019, September). *EEG-EMG Correlation for Parkinson's disease*. Retrieved Marts 13, 2025, from researchgate.net: [https://www.researchgate.net/publication/335620895\\_EEG-EMG\\_Correlation\\_for\\_Parkinson's\\_disease](https://www.researchgate.net/publication/335620895_EEG-EMG_Correlation_for_Parkinson's_disease)
- Oehrn, C. R., & et al., I. (2024). *Chronic adaptive deep brain stimulation versus conventional stimulation in Parkinson's disease: a blinded randomized feasibility trial*. Retrieved Marts 13, 2025, from nature.com: <https://www.nature.com/articles/s41591-024-03196-z#Ack1>
- Andrusca, A. (2023, Oktober 30). *Basal ganglia pathways*. Retrieved Marts 25, 2025, from kenhub.com: <https://www.kenhub.com/en/library/anatomy/direct-and-indirect-pathways-of-the-basal-ganglia>
- Hunt, W., & Sugano, Y. (2020, Juni 30). *The Basal Ganglia*. Retrieved Marts 25, 2025, from teachmeanatomy.info: <https://teachmeanatomy.info/neuroanatomy/structures/basal-ganglia/>
- Buerkle, A., & et al. (2021, August). *EEG based arm movement intention recognition towards enhanced safety in symbiotic Human-Robot Collaboration*. Retrieved Februar 14, 2025, from sciencedirect.com: <https://www.sciencedirect.com/science/article/pii/S0736584521000223>



- Karimi, F., & et al. (2021, November 24). *Movement-related EEG signatures associated with freezing of gait in Parkinson's disease: an integrative analysis*. Retrieved Februar 13, 2025, from academic.oup.com:  
[https://academic.oup.com/braincomms/article/3/4/fcab277/6437995?utm\\_source=chatgpt.com&login=false](https://academic.oup.com/braincomms/article/3/4/fcab277/6437995?utm_source=chatgpt.com&login=false)
- S., F., & R., E. (1987). *Parkinson's Disease Research, Education and Clinical Centers*. Retrieved Marts 26, 2025, from parkinsons.va.gov:  
<https://www.parkinsons.va.gov/resources/UPDRS.asp>
- Geeksforgeeks. (2025, Januar 8). *Functional vs. Non Functional Requirements*. Retrieved Marts 27, 2025, from geeksforgeeks.org: <https://www.geeksforgeeks.org/functional-vs-non-functional-requirements/>
- Silva-Acosta, V. D., & et al. (2021, September). *Automatic estimation of continuous elbow flexion–extension movement based on electromyographic and electroencephalographic signals*. Retrieved Februar 13, 2025, from sciencedirect.com:  
<https://www.sciencedirect.com/science/article/pii/S1746809421005474>
- Mahmoodi, M., & et al., I. (2021, August 18). *A new method for accurate detection of movement intention from single channel EEG for online BCI*. Retrieved from sciencedirect.com:  
<https://www.sciencedirect.com/science/article/pii/S2666990021000264>
- wikipedia. (2025, Februar 11). *PIEZO1*. Retrieved Marts 31, 2025, from en.wikipedia.org:  
<https://en.wikipedia.org/wiki/PIEZO1>
- Evident. (n.d.). *What Is a Phased Array Transducer?* Retrieved Marts 31, 2025, from ims.evidentscientific.com: <https://ims.evidentscientific.com/en/learn/ndt-tutorials/transducers/phased-array-transducer>
- Wikipedia. (2024, Oktober 29). *Phased array ultrasonics*. Retrieved Marts 31, 2025, from en.wikipedia.org: [https://en.wikipedia.org/wiki/Phased\\_array\\_ultrasonics](https://en.wikipedia.org/wiki/Phased_array_ultrasonics)
- Demi, L. (2018, August 31). *Practical Guide to Ultrasound Beam Forming: Beam Pattern and Image Reconstruction Analysis*. Retrieved Marts 31, 2025, from mdpi.com:  
<https://www.mdpi.com/2076-3417/8/9/1544>
- University of Calgary. (2025). *What is a Brain Computer Interface?* Retrieved April 4, 2025, from cumming.ucalgary.ca: <https://cumming.ucalgary.ca/research/pediatric-bci/bci-program/what-bci>
- Brodal, P. (1995). *Sentral Nerve Systemet* (2 ed.). Oslo: Tano.

- Wikipedia. (2025, Marts 25). *Event-related potential*. Retrieved April 5, 2025, from en.wikipedia.org: [https://en.wikipedia.org/wiki/Event-related\\_potential](https://en.wikipedia.org/wiki/Event-related_potential)
- Aeles, J., & et al. (2021, Januar 13). Revealing the unique features of each individual's muscle activation signatures. *Journal of the Royal Society Interface*, 18(174). Retrieved Februar 13, 2025, from pmc.ncbi.nlm.nih.gov: <https://pmc.ncbi.nlm.nih.gov/articles/PMC7879771/>
- Silva-Acosta, V. D., & et al. (2021, September). *Automatic estimation of continuous elbow flexion–extension movement based on electromyographic and electroencephalographic signals*. Retrieved Februar 13, 2025, from sciencedirect.com: <https://www.sciencedirect.com/science/article/pii/S1746809421005474>
- Mahmoodi, M., & et al., l. (2021, August 18). *A new method for accurate detection of movement intention from single channel EEG for online BCI*. Retrieved from sciencedirect.com: <https://www.sciencedirect.com/science/article/pii/S2666990021000264>

## Appendix A - Background Theory

Appendix A documents the theory of the project more in-depth than the report and further explains more related aspects and corners of the project. Relevant theory, mathematics and AI-models used in the project, are all introduced and explained.

### The Brain and Basal Ganglia<sup>95</sup>

The brain is one of the most complex organs in the body and is responsible for regulating both conscious and unconscious functions. It consists of various structures and regions, each with specific functions. The motor cortex, located in the frontal lobe, plays a central role in controlling voluntary movements. It sends electrical signals to the muscles via the spinal cord, enabling precise and coordinated actions. Figure 28 shows the different regions of the brain :

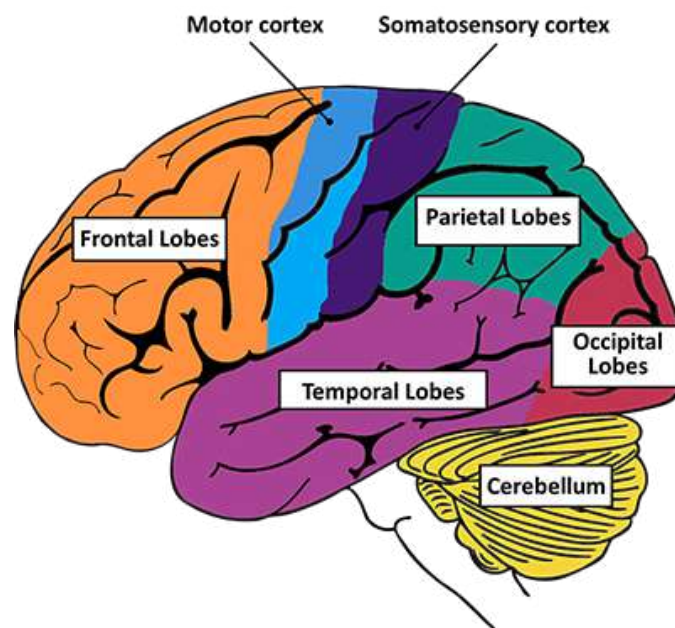


Figure 28: Overview of the brain's structure and different regions<sup>96</sup>

The basal ganglia<sup>97</sup> are central to motor control and function as a complex circuit that integrates signals from the cortex and sends processed output back via the thalamus. The system primarily

---

<sup>95</sup> The section is based on the sources: (Hansen, 2002, s. 1 - 45), (Andrusca, 2023) og (Hunt & Sugano, 2020)

<sup>96</sup> From <https://www.ninds.nih.gov/health-information/public-education/brain-basics/brain-basics-know-your-brain>

<sup>97</sup> Also known as basal nuclei

consists of: the striatum (putamen and caudate nucleus), globus pallidus (GPe and GPi), substantia nigra (pars compacta (SNc) and pars reticulata (SNr)), and the subthalamic nucleus (STN).

### **Striatum**

Receives signals from the cortex and dopamine from the substantia nigra. The striatum is crucial for initiating and adjusting movements, acting as a "gatekeeper" for motor activity.

### **GPe/GPi**

The GPe participates in the indirect pathway, which inhibits movement. The GPi is the final output center of the basal ganglia-it sends inhibitory signals to the thalamus.

### **Thalamus**

Functions as a motor relay station. When not inhibited by the GPi, it sends excitatory signals back to the cortex, enabling movement execution.

To control, adjust, and modulate movements, the basal ganglia employ three main pathways:

- **The direct pathway:** facilitates movement by increasing excitation of the motor cortex (dopamine → receptors).
- **The indirect pathway:** inhibits movement by increasing inhibition of the motor cortex (dopamine → suppression via D2 receptors in the striatum).
- **The hyperdirect pathway:** rapidly inhibits movement via cortex → STN → GPi → Thalamus (not dopamine-modulated).

By using excitatory (glutamate) and inhibitory (GABA) neurotransmitters, the overall effect can be finely modulated. To better understand these pathways, imagine a person wishing to move their legs to go for a walk. Figure 29 shows the direct and indirect pathway of the basal ganglia.

# Basal Ganglia

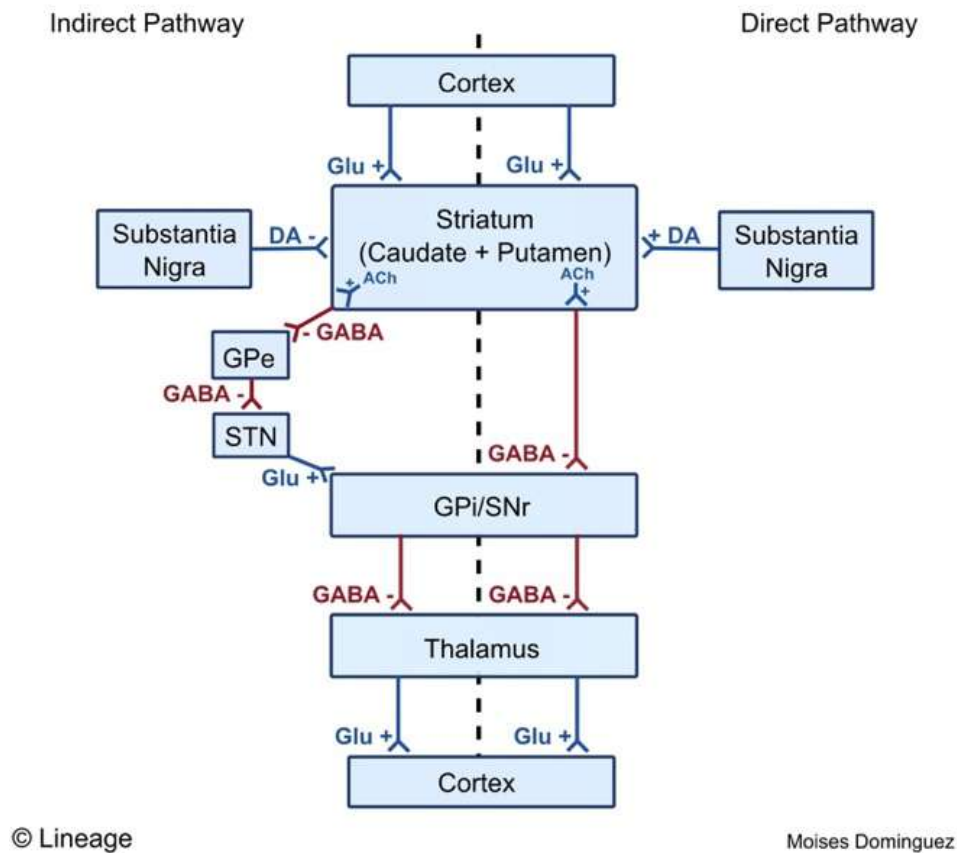


Figure 29: The direct and indirect pathways in the basal ganglia<sup>98</sup>

## Direct Pathway

The direct pathway facilitates movement: The cortex sends glutamate signals to the putamen, which via GABA inhibits the inhibitory output neurons in the GPi and SNr. Since these normally inhibit the thalamus, this inhibition leads to disinhibition of the thalamus, which can now excite the motor cortex again - thus initiating movement.

Dopamine from the SNc modulates this pathway by activating D1 receptors in the striatum, which strengthens the excitatory effect on movement. Without sufficient dopamine (as in PD), activity in the direct pathway is reduced, resulting in motor hypokinesia and bradykinesia.

<sup>98</sup> From <https://step1.medbullets.com/neurology/113008/basal-ganglia>

In the direct pathway, a positive feedback occurs because two inhibitory synapses are connected in series. This means GABA from the putamen suppresses GABA from the GPi, thereby reducing the inhibitory effect of the GPi on the thalamus, a process called disinhibition. In other words, an inhibitory neuron inhibits another inhibitory neuron, producing a net activating effect.

### **Indirect Pathway**

Alongside the direct pathway, the indirect pathway of the basal ganglia can also be active. Here, the motor cortex first sends glutamate to the putamen (as in the direct pathway). The putamen then sends inhibitory GABA signals to the GPe.

This inhibits the GPe, which normally inhibits the STN. When the GPe is inhibited, disinhibition of the STN occurs, allowing it to send excitatory glutamate signals to the GPi and SNr. These in turn inhibit the thalamus via GABA. When the thalamus is inhibited, excitatory output to the motor cortex is reduced, thereby suppressing movement.

Dopamine from the SNc modulates this pathway by binding to D2 receptors in the striatum, which reduces the activity of the indirect pathway. Thus, dopamine weakens movement suppression and promotes movement. With dopamine deficiency (as in PD), the indirect pathway becomes overactive, contributing to bradykinesia and rigidity.

### **Hyperdirect Pathway**

Glutamate is sent directly from the motor cortex to the STN, which delivers strong excitatory signals to the GPi and SNr. Since the GPi sends inhibitory GABA to the thalamus, the net effect is inhibition of the thalamus, reducing excitatory output to the motor cortex and thereby suppressing movement. The hyperdirect pathway plays an important role in rapid movement inhibition, for example when suppressing an initiated movement or an impulsive action - a kind of “emergency brake.”. Figure 30 depicts the hyperdirect pathway.

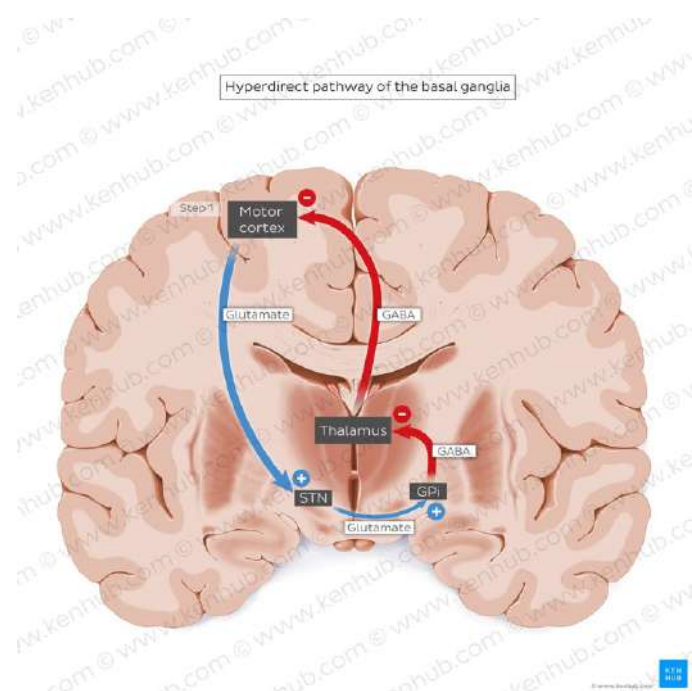


Figure 30: The hyperdirect pathway in the basal ganglia<sup>99</sup>

## Relation to PD

A central cause of the motor symptoms in PD is the loss of dopamine-producing neurons in the substantia nigra pars compacta. This dopamine depletion weakens the direct pathway of the basal ganglia (which normally facilitates movement via D1 receptors) and strengthens the indirect pathway (which inhibits movement via D2 receptors). The result is over-inhibition of the thalamus, reducing excitatory output to the motor cortex and thereby impairing movement initiation. Movements thus become slow, rigid, or absent.

This dysfunction in the basal ganglia is also reflected in the brain's electrical activity. In PD, there is typically a reduction in high-frequency oscillations (alpha, beta, and especially gamma), which are normally associated with movement preparation and flexible network communication [9], [10], [12], [13]. At the same time, an increase in low-frequency bands (especially delta and theta) is observed, indicating more rigid and less responsive network activity.

High-frequency waves require a certain degree of desynchronization between neuronal populations to enable flexible signal processing. This desynchronization depends on both sufficient excitation (e.g., from the thalamus) and energy availability both of which are weakened in dopamine

<sup>99</sup> From <https://www.kenhub.com/en/library/anatomy/direct-and-indirect-pathways-of-the-basal-ganglia>

deficiency. As a result, neural networks remain in synchronized resting activity, preventing the buildup of goal-directed motor activity.

In short: Dopamine deficiency leads to imbalance in the basal ganglia circuitry, reduces excitatory feedback to the motor cortex, impairs cortical desynchronization, and shifts oscillatory activity toward low-frequency bands, all of which contribute to the motor symptoms of PD.

However, in the early stages of PD, gamma connectivity can be increased as a compensatory mechanism, even as dopamine levels begin to decline. This is because cortical networks still have sufficient excitation and flexibility to sustain high-frequency communication. But as dopamine deficiency worsens, excitatory input to the cortex through the thalamus decreases, and gamma activity collapses. This leads to reduced network flexibility and increased dominance of low-frequency and pathological bands, correlating with the motor symptoms in advanced PD.

## Signal Preprocessing Methods<sup>100</sup>

### Fourier transformation

Sometimes it is more relevant to describe a function in the frequency domain rather than in the time domain. The Fourier transform provides a method to transform a time-dependent function,  $f(t)$ , into a frequency-dependent function  $F(\omega)$ .

The idea behind the Fourier transform is that all signals can be decomposed into a sum of sine and cosine functions with different frequencies and amplitudes. If we write the function  $f(t)$  in complex form, we have:

$$f(t) = \frac{1}{2\pi} \int_{-\infty}^{\infty} F(\omega) \cdot e^{i\omega t} d\omega$$

Here,  $i$  is the imaginary unit ( $\sqrt{-1}$ ), and  $\omega$  is the angular frequency defined as  $\omega = 2\pi f$ , where  $f$  is the frequency in Hz.

---

<sup>100</sup> Sources used in this section: (wikipedia.org, 2024), (Jensen & Jensen, 2019), (Google colab, u.d.) (Google colab, u.d.) (geeksforgeeks, 2022)



The Fourier transform is defined as:

$$\mathcal{F}\{f(t)\} = F(\omega) = \int_{-\infty}^{\infty} f(t) \cdot e^{-i\omega t} dt$$

Similarly, one can go the other way, from the frequency domain back to the time domain, by applying the inverse Fourier transform:

$$\mathcal{F}^{-1}\{F(\omega)\} = f(t) = \frac{1}{2\pi} \int_{-\infty}^{\infty} F(\omega) \cdot e^{i\omega t} d\omega$$

The Fourier transform is a bijective transformation, which means that there exists a unique inverse transformation (the inverse Fourier transform) that reconstructs the original signal without loss.

### Fast Fourier Transform (FFT)

Usually discrete data is used, an example could be an EEG-measurement, where the numeric algorithm FFT is used. FFT is an efficient method to calculate the Fourier transformation of discrete data points, and enables signals to be analysed quickly and precise.

In practice, discrete data are often used, for example from an EEG recording, and here the numerical algorithm FFT is applied. FFT is an efficient method for calculating the Fourier transform of discrete data points and makes it possible to analyse signals quickly and accurately.

Figure 31 shows FFT used on a C-major chord with added noise, to demonstrate the power of FFT.

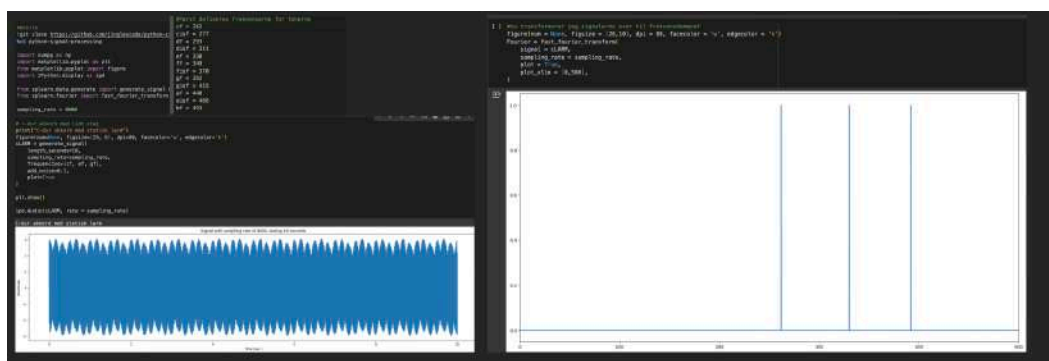


Figure 31: FFT used on a C-major chord<sup>101</sup>

<sup>101</sup> The author's own work

### *Practical application*

With the help of Fourier transforms, signals such as EEG can be analyzed. For example, specific frequencies related to the brain's Bereitschaftspotential can be identified, or noise can be filtered. FFT makes it possible to analyze large datasets quickly and accurately. Fourier transforms and FFT are therefore essential tools in this project.

### *Noise filtering*

Filtering is an essential part of signal processing, especially when working with biological signals such as EEG and EMG, which often contain significant amounts of noise. The purpose of filtering is to improve signal quality by suppressing noise without losing relevant characteristics of the dataset. Several methods are used depending on the source of noise and the desired outcome.

### *Bandpass filtering*

Bandpass filtering is used to isolate specific frequency bands by allowing frequencies within a given range to pass while attenuating the rest. This can be useful for isolating relevant frequencies in EEG or EMG signals, for example,  $\mu$ -waves and beta waves. High-pass and low-pass filters are often used to focus on specific frequencies in the dataset.

### *Baseline correction*

Baseline correction is used to normalize the signal by adjusting it to a baseline period, typically defined as a period before a stimulus (from  $-0.2$  to  $0$  seconds). This ensures that the signal is adjusted for any systematic drift.

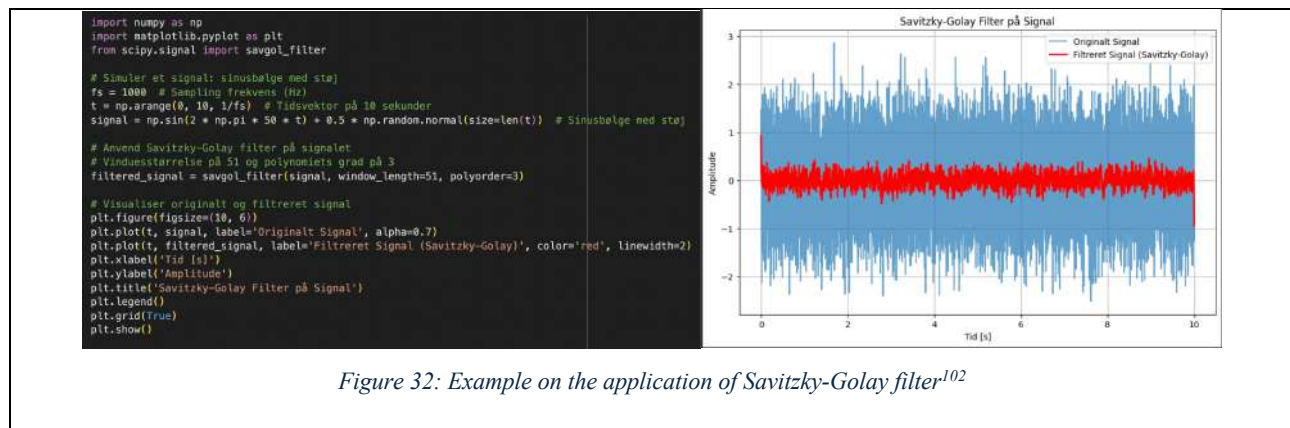
### *Notch filter*

A notch filter is a narrowband filter that attenuates a specific frequency without significantly affecting nearby frequencies. It is often used to remove electrical noise at 50/60 Hz from mains power.

### *Savitzky-Golay filter*

The Savitzky-Golay filter is a method used to smooth a signal and remove noise by fitting a polynomial to the signal over a moving window. This filter is effective at removing high-frequency noise

while preserving the main structures of the signal. Figure 32 shows an example of the Savitzky-Golay filter in use.



### Spectrogram (Time-frequency analysis)

The spectrogram is a method for analyzing signals in both time and frequency. It divides the signal into short time windows and calculates the FFT for each section, making it possible to visualize how the frequency components of the signal change over time. This is especially useful for identifying time-dependent frequency patterns in EEG or EMG data.

## Neural Network<sup>103</sup>

A neural network is a ML model inspired by the structure and function of the human brain. The model consists of interconnected neurons that process data in order to learn, recognize patterns, and classify information.

The most important components of an NN are:

- **Neurons:** units that receive data and are activated by an activation function
- **Connections/synapses:** links between neurons, controlled by weights and biases
- **Weights and biases:** parameters that determine the strength and influence of connections
- **Activation functions:** functions that process data and transfer it through the layers
- **Learning rule:** the method that adjusts weights and biases during training to improve accuracy.

<sup>102</sup> The author's own work

<sup>103</sup> Based on the sources: (3Blue1Brown, 2024), (IBM, u.d.), (Geeksforgeeks, 2024)

A neural network consists of input, hidden, and output layers that work together to learn patterns in data. The input layer receives raw data, where each neuron represents a feature (e.g., a pixel value or variable). The hidden layers then process the data using weights, biases, and activation functions such as ReLU or sigmoid. These layers identify complex patterns, such as edges in images or trends in time series. Figure 33 illustrates the structure of an NN.

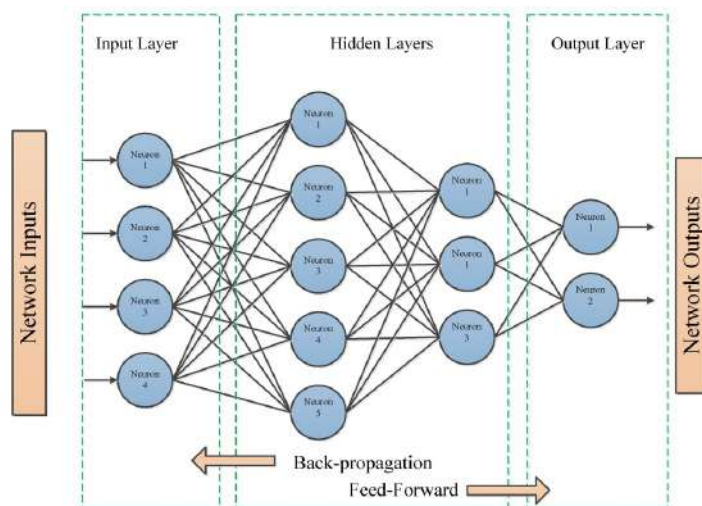


Figure 33: The architecture of a NN<sup>104</sup>

The output layer generates the final result. The number of neurons here depends on the task: classification usually requires one neuron per class, while regression typically uses a single neuron for a continuous value.

The network learns through an iterative process. During **forward propagation**, data passes one way through the layers to produce a prediction. The error between the prediction and the correct result is calculated, and during **backpropagation**, weights and biases are adjusted to minimize this error. Over many iterations, the network gradually improves its accuracy and ability to recognize patterns.

Evaluation of the NN's output is done using a loss function, which measures the difference between the NN's output and the expected result.

<sup>104</sup> From <https://www.linkedin.com/pulse/feedforward-vs-backpropagation-ann-saffronedge1/>

## Recurrent Neural Network & Long Short-Term Memory<sup>105</sup>

An Recurrent Neural Network (RNN) is a neural network designed to handle sequential data, where the order of inputs matters. Unlike standard feedforward networks, which only take one input at a time, RNNs include feedback loops that allow the network to “remember” information from previous points in the sequence. This is achieved through a hidden state, called the memory state, which is updated at each time step and retains important information from earlier inputs.

Figure 34 shows the difference between a feedforward network and an RNN.

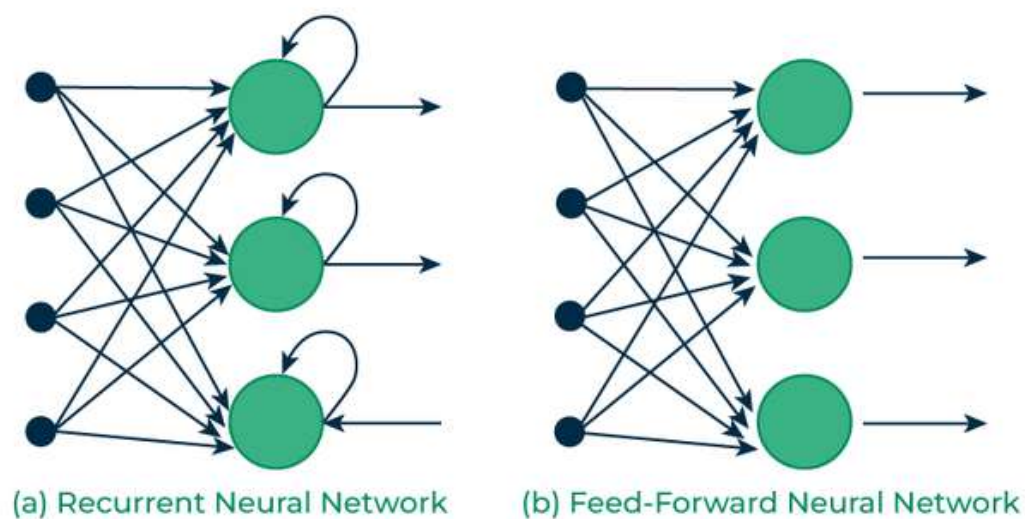


Figure 34: The difference between feedword network and RNN<sup>106</sup>

However, RNNs struggle with long sequences, as the memory state gradually loses important information. This is due to the **vanishing gradient problem**, where the gradients used to update weights during training become very small. This prevents the network from learning long-term dependencies in sequences.

To solve this, **LSTM** networks were introduced. LSTMs include a memory cell that can preserve information over long periods. Memory is regulated by three gates that determine which information to store or discard:

<sup>105</sup> Based on the sources: (Hamad, 2023), (geeksforgeeks, 2024), (geeksforgeeks, 2023), (Wikipedia, 2025).

<sup>106</sup> From <https://www.geeksforgeeks.org/introduction-to-recurrent-neural-network/>

- **Input gate** ( $i_t, \hat{C}_t, C_t$ ): controls which information is added to the memory cell
- **Forget gate** ( $f_t$ ): decides which information to retain or delete, based on past inputs
- **Output gate** ( $o_t$ ): controls which information is output from the memory cell

LSTMs are especially useful for tasks such as language modeling (e.g., ChatGPT) or time-series analysis with long intervals, which is relevant for this project. Figure 35 shows the architecture of an LSTM.

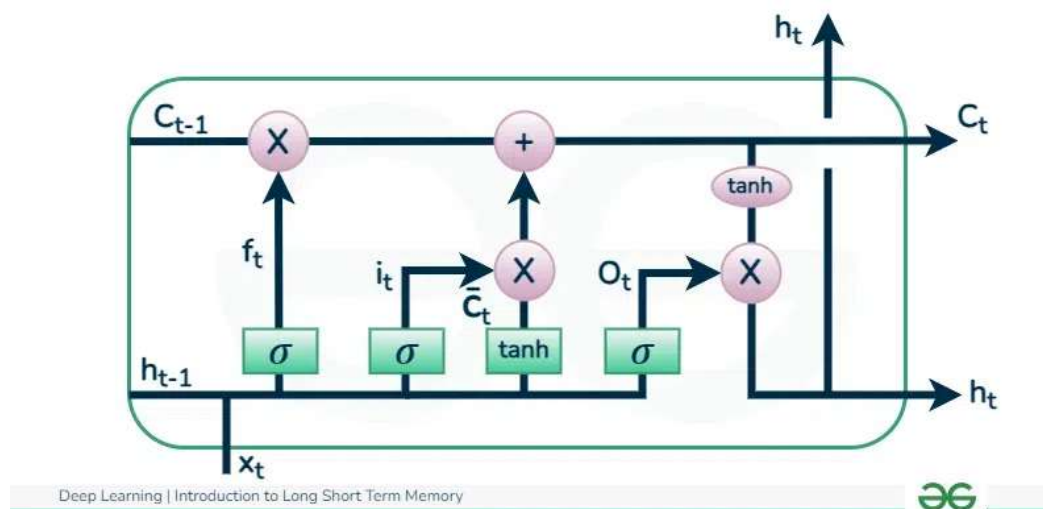


Figure 35: The architecture behind an LSTM<sup>107</sup>

## Convolutional Neural Network<sup>108</sup>

A CNN is a type of neural network specialized for processing grid-like data structures, such as images or sensor signals. CNNs are designed to mimic the human visual system, where neurons respond to specific regions called receptive fields. In CNNs, simple patterns like lines and edges are identified first, followed by more complex features like shapes and objects across multiple layers.

Figure 36 shows the architecture of a CNN.

<sup>107</sup> From <https://www.geeksforgeeks.org/deep-learning-introduction-to-long-short-term-memory/>

<sup>108</sup> The sections is based on the sources: (Keita, 2023), (Jorgecardete, 2024), (ibm, u.d.), (Mishra, 2020)

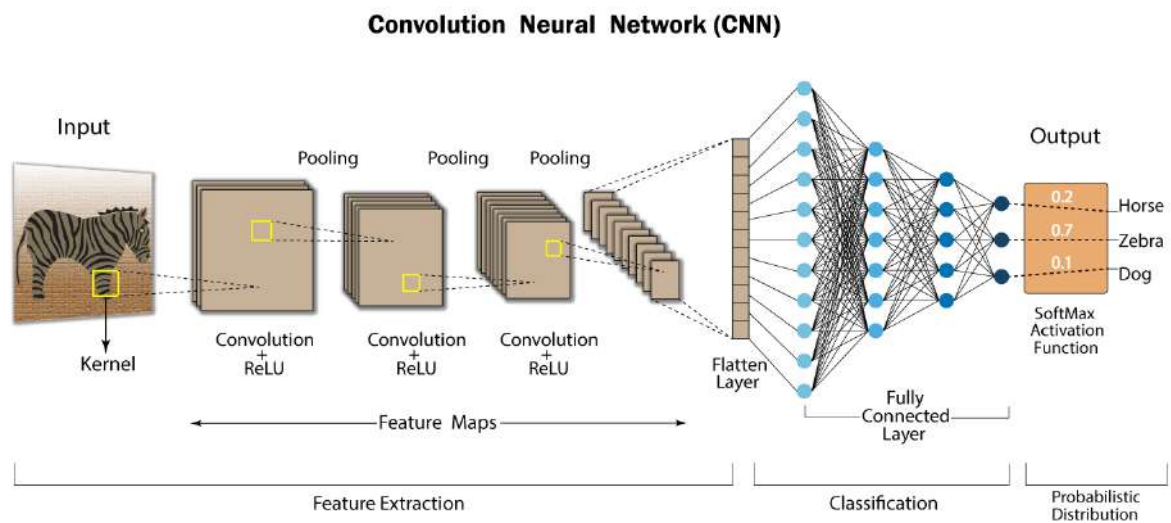


Figure 36: The architecture behind a CNN<sup>109</sup>

A CNN typically consists of three main layers:

- **Convolution layer:** Performs convolution using small, learnable filters (kernels) that scan the data grid to highlight patterns. The result is an activation map representing the detected patterns.
- **Pooling layer:** Reduces the size of activation maps by summarizing nearby values, often through max-pooling. This reduces data size and creates more robust representations.
- **Fully connected layer:** Combines the extracted features and links input to output, typically used for classification or regression.

<sup>109</sup> From <https://ai.plainenglish.io/deep-dive-into-the-world-of-cnns-8cf22cd84e7>



## Transformer-model<sup>110</sup>

A Transformer is a sophisticated deep neural network that processes data in parallel, unlike LSTMs which work sequentially. It does this through self-attention, which allows the model to focus on the most important parts of the data, regardless of their position. This makes it highly effective at understanding long-range dependencies.

The different groups of data the model receives are called modalities. For example, if EEG, EMG, and IMU signals are used, each represents its own modality, making the model multimodal. Importantly, each modality often requires different preprocessing steps before being fused in the Transformer:

- **EEG:** low-pass filtering, notch filtering (50/60 Hz noise), ICA (to remove eye-blink artifacts)
- **EMG:** envelope extraction is common, ICA is rarely used
- **IMU:** typically requires signal derivation for velocity and acceleration, not ICA or envelope extraction

A Transformer works with vectors, so modalities are transformed into vector representations. These are normalized and projected into a shared vector space via linear transformations. In this way, all signals are represented as d-vectors, where d is the “embedding dimension.” An embedding is the transformation of raw inputs (e.g., sensor data) into semantically meaningful vectors in a high-dimensional space, where similar inputs lie closer together.

Since temporal information is not inherently preserved, positional encoding is introduced. This provides relative positions for each token in the Transformer, typically through sine/cosine functions or learnable position embeddings.

The tokens are then passed through the Transformer encoder, consisting of multiple encoding blocks, each containing:

---

<sup>110</sup> Sources: (3Blue1Brown, 2024), (Wikipedia, 2025), (Geeksforgeeks, 2024), (Sachinsoni, 2024)



- **Multi-Head Self-Attention (MHSA):** input vectors are transformed into Query, Key, and Value. Attention scores are calculated as weightings between Query and Key, and applied to Value, enabling the model to focus on the most relevant parts of the sequence across modalities.
- **Feedforward Neural Network (FNN):** processes the attention output token-wise, transforming embeddings into more abstract representations.
- **Residual Connections & Layer Normalization:** ensure stable training, preserve information flow, and improve convergence.

These encoding blocks are stacked (typically 4-6 layers) to learn progressively deeper representations.

After encoding, modalities can be combined either by concatenation (directly joining embeddings) or via cross-modal attention, where the Transformer learns dynamic weighting across modalities. The final sequence representation can be extracted through a CLS-token, average pooling, or a weighted sum.

- **Flatten & Concatenation:** outputs from all three modalities are merged into a single vector.
- **Dense Layers & Softmax:** a fully connected neural network layer makes predictions based on the processed embeddings.

Output examples:

- Classification: type of movement-
- Regression: angle of a movement

Figure 37 shows the data flow of a Transformer-model.

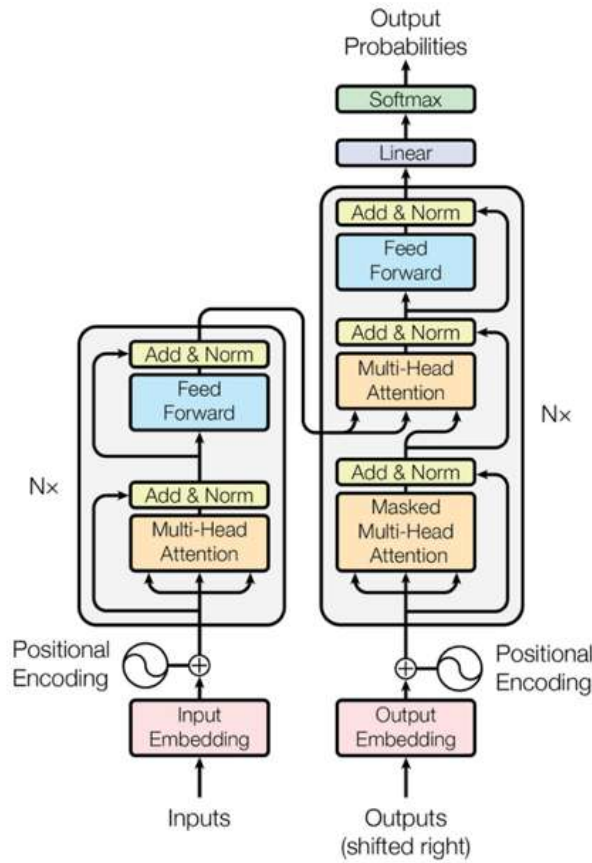


Figure 37: Overview of the dataflow in a Transformer-model<sup>111</sup>

In this project, the Transformer is designed to classify EEG signals as specific movements, where the output is a binary value representation of each movement. The model's modalities are EEG, EMG, and IMU.

## Some of the Mathematics behind the Project<sup>112</sup>

### Forward Propagation

The mathematics of forward propagation:

$$z = \sum_{i=1}^n w_i \cdot x_i + b$$

<sup>111</sup> From <https://pub.towardsai.net/transformer-architecture-part-1-d157b54315e6>

<sup>112</sup> Sources: (IBM, 2024), (Wikipedia, 2025), (Wikipedia, 2024)

Where:

- $z$  is the total activation input to a neuron, the linear combination of weighted inputs plus bias
- $w_i$  is the weight associated with input  $x_i$ . Weights determine how much each input contributes to the overall output
- $x_i$  is the  $i$ -th input value (e.g., a pixel or a sensor reading)
- $b$  is a bias term, a constant that shifts the activation level to allow the neuron to learn offsets in the data

After  $z$  is calculated, it is passed through an **activation function** so the neuron can learn non-linear patterns.

### Activation functions

Activation functions introduce non-linearity into deep neural networks and are crucial for learning complex patterns. They determine the neuron's output given its input.

A simple analogy is a circuit where the activation function decides if the circuit is ON or OFF based on the input signals.

### ReLU (Rectified Linear Unit)

The most common activation function in deep networks is ReLU, defined as:

$$f(z) = \max(0, z)$$

This means

$$f(z) = \begin{cases} 0, & \text{if } z \leq 0 \\ z, & \text{if } z > 0 \end{cases}$$

The derivative (and therefore gradient):

$$f'(z) = \begin{cases} 0, & \text{if } z < 0 \\ 1, & \text{if } z > 0 \end{cases}$$

Which shows ReLU is non-differentiable at  $z = 0$ . ReLU sets all negative inputs to 0 while leaving positive values unchanged. It is computationally efficient but can lead to “dying ReLUs” (neurons

permanently inactive). A variant, Leaky ReLU, assigns a small slope to negative inputs to mitigate this. Figure 38 shows a ReLU graph:

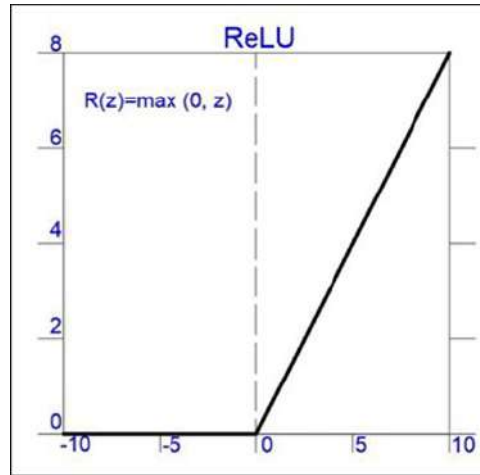


Figure 38: ReLU graph<sup>113</sup>

### Properties with ReLU

Range:

$$f(z) \in [0, \infty)$$

Which means all negative input are set as 0, while positive values remain unchanged.

### Efficient calculation:

ReLU is quick to evaluate in comparison to sigmoid or tanh-function, because it requires only a simple maximum operation.

Backward propagation:

During training of a NN must the activation function be differentiated in the backward propagation.

For ReLU this is:

If  $z > 0$ , the gradient is 1

If  $z < 0$ , the gradient is 0

If  $z = 0$ , the gradient is defined but is typically set as either 0 or 1

<sup>113</sup> From [https://www.researchgate.net/figure/Activation-function-ReLu-ReLu-Rectified-Linear-Activation\\_fig2\\_370465617](https://www.researchgate.net/figure/Activation-function-ReLu-ReLu-Rectified-Linear-Activation_fig2_370465617)

This makes the ReLU less sensitive towards gradient problems but can lead to the “dying ReLU” problem, where neurons can become permanent inactive if their weights lead to negative inputs. To help with this, can Leaky ReLU be used where negative gets a small slope instead of being set equal to 0.

### Sigmoid:

Another activation function is the Sigmoid:

$$\sigma(z) = \frac{1}{1 + e^{-z}}$$

It maps values into the range (0,1), making it useful when outputs represent probabilities, such as binary classification. However, it suffers from the vanishing gradient problem for large positive/negative inputs, slowing learning in deep networks.

Figure 39 shows the Sigmoid function and its differentiated version

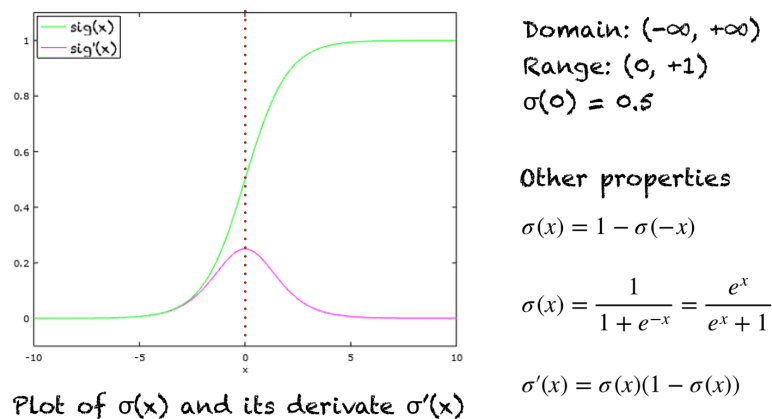


Figure 39: Sigmoid function and differentiated function<sup>114</sup>

### Properties with the Sigmoid Function

The output is always in the interval of 0 to 1 which makes it suitable for problems where one wishes a probability as output, like classification of data or photos. Because  $\sigma(0) = 0.5$ , the function is symmetrical around  $z = 0$ . This means positive values are pushed toward 1 while negative toward 0.

<sup>114</sup> From <https://machinelearningmastery.com/a-gentle-introduction-to-sigmoid-function/>

As an activation function is the Sigmoid used to introduce non-linearity in binary classification in the output layer of a NN. Sigmoid is then used in the last neuron in the network to classify between two classes. Because the output is always between 0 and 1, it can be interpreted as a probability for a sample belongs to a defined class. Sigmoid is also used in logistical regression to estimate the probability of a binary occurrence.

A problem of the Sigmoid activation function is when  $z$  is very big or very small. Under these circumstances will the "The vanishing gradient problem" show, where the gradients in the backwards propagation become extremely small. This suppresses the learning rate in deep NN because the weight adjustments become minimal. And because of this problem is the ReLU used more frequently than the Sigmoid activation function.

### Loss functions<sup>115</sup>

Evaluation of a neural network's output is carried out using a loss function, which measures the difference between the network's predicted output and the actual values. In this project, the following loss functions have been used:

#### Mean Absolute Error (MAE)

Loss functions evaluate how well a neural network's predictions match the target values. In this project:

$$MAE = \frac{1}{n} \sum_{i=1}^n |y_i - \hat{y}_i|$$

Where

- $n$  amount of data points
- $y_i$  the actual values
- $\hat{y}_i$  the predicted values
- $|\hat{y}_i - y_i|$  the absolute mistake

---

<sup>115</sup> (IBM, 2024)

Measures average absolute error. Robust but less sensitive to large errors. MAE is used in NN to minimise mistakes between predicted and actual output values by optimising the weights of the network so the MAE is reduced over time.

A high MAE indicates that there is a big difference between predicted and actual output, while a small MAE indicates a more precise model. Henceforth must the MAE be as low as possible to ensure an usable and precise model.

MAE has its limitations. It punishes big mistakes less than MSE, which can be a problem if big mistakes are problematic (or very prone in the predictions). MAE is also non-differentiable in  $z = 0$ , which can make gradient based optimisation algorithms less effective.

### Mean Squared Error (MSE)

Like MAE, MSE is a loss functions that is used in NN and regression models to measure the difference between predicted and actual values. MSE calculates the average of squared error between predicted and actual values:

$$MSE = \frac{1}{n} \sum_{i=1}^n (y_i - \hat{y}_i)^2$$

Where

- $n$  amount of data points
- $y_i$  the actual values
- $\hat{y}_i$  the predicted values
- $|\hat{y}_i - y_i|$  the absolute mistake

Penalizes large errors more strongly than MAE.

MSE in NN is used to minimise mistakes by optimising weights, making the average squared mistake reduced over time. A low MSE indicates a precise model, while a high MSE indicates the model makes big mistakes.

A limitation with MSE is it punishes big mistakes more heavily than MAE because the mistakes squares. If the data set includes outliers, can these dominate the loss and lead to an unstable learning

rate. MSE also has its unit output squared compared to the input data, making it more difficult to interpret.

### Huber Loss

Huber Loss is a combination of MSE and MAE, switching between the two depending on a predefined threshold  $\delta$ . It is often used in regression models where one wants to penalize large errors more strongly than MAE, but without letting outliers dominate the learning process, as can happen with MSE.

Huber Loss is defined as:

$$L(y, \hat{y}) = \begin{cases} \frac{1}{2}(y - \hat{y})^2, & \text{if } |y - \hat{y}| \leq \delta \\ \delta \cdot |y - \hat{y}| - \frac{1}{2}\delta^2, & \text{if } |y - \hat{y}| > \delta \end{cases}$$

Where:

- $y$ : the actual value
- $\hat{y}$ : the predicted value
- $\delta$ : the threshold determining when the loss switches from MSE to MAE
- For **small errors** ( $|y - \hat{y}| \leq \delta$ ), Huber Loss behaves like MSE:

$$L(y, \hat{y}) = \frac{1}{2}(y - \hat{y})^2$$

This squares small errors, ensuring smooth gradients and precise learning.

- For **large errors** ( $|y - \hat{y}| > \delta$ ), Huber Loss behaves like MAE:

$$L(y, \hat{y}) = \delta |y - \hat{y}| - \frac{1}{2}\delta^2$$

This switches to a linear penalty, making it less sensitive to outliers.

**In summary:** Huber Loss is an efficient loss function that balances precision with robustness by combining MSE and MAE into a single function with a smooth transition between them.



### Adam (Adaptive Moment Estimation)

Adam is an adaptive optimization algorithm that combines momentum-based gradient updates ( $\beta_1$ ) with RMSProp-like learning rate adaptation ( $\beta_2$ ), resulting in stable and fast convergence. It computes an adaptive learning rate for each parameter.

$$\begin{aligned}m_t &= \beta_1 m_{t-1} + (1 - \beta_1) \nabla \theta_t \\v_t &= \beta_2 v_{t-1} + (1 - \beta_2) (\nabla \theta_t)^2\end{aligned}$$

Where:

- $m_t$  and  $v_t$  are the first and second moment estimates of the gradient
- $\beta_1$  and  $\beta_2$  are exponential smoothing factors
- $\nabla \theta_t$  is the gradient of the loss function with respect to the parameters

The learning rate for updating the parameter  $\theta$  is then adjusted as:

$$\theta_t = \theta_{t-1} - \frac{\alpha}{\sqrt{v_t} + \epsilon} m_t$$

Where:

- $\alpha$  is the initial learning rate
- $\epsilon$  is a small constant to prevent division by zero

### Summary

These methods form the foundation of the project: signal processing optimizes EEG input, neural networks classify movement patterns, and the Transformer model enables multimodal analysis. Together, this combination ensures robust and accurate detection of intentional movements in people with motor impairments.

## Appendix B - Self-assembled EEG-hardware

This appendix documents the completed EEG instrument, which was constructed and tested. The system is almost fully functional and ready to be used in real time for EEG data acquisition to compare between self-assembled EEG-hardware and professional equipment from OpenBCI.

To build my EEG instrument, I drew inspiration from the following source:

<https://github.com/RonanB96/Low-Cost-EEG-Based-BCI>

I modified the circuit so that three active electrodes could measure EEG signals. The article states that the Driven Right Leg (DRL), opto-isolation, and microcontroller could be reused if a new channel were to be added. Therefore, I extended the design by adding two extra components: protection circuits, instrumentation amplifiers, an AC gain stage, and a power rail for the entire circuit.

### Circuit diagrams

#### Reference article circuit

Below are the circuit diagrams from the reference article, which served as inspiration for the construction of my EEG system.

#### Image of the instrument from the reference article

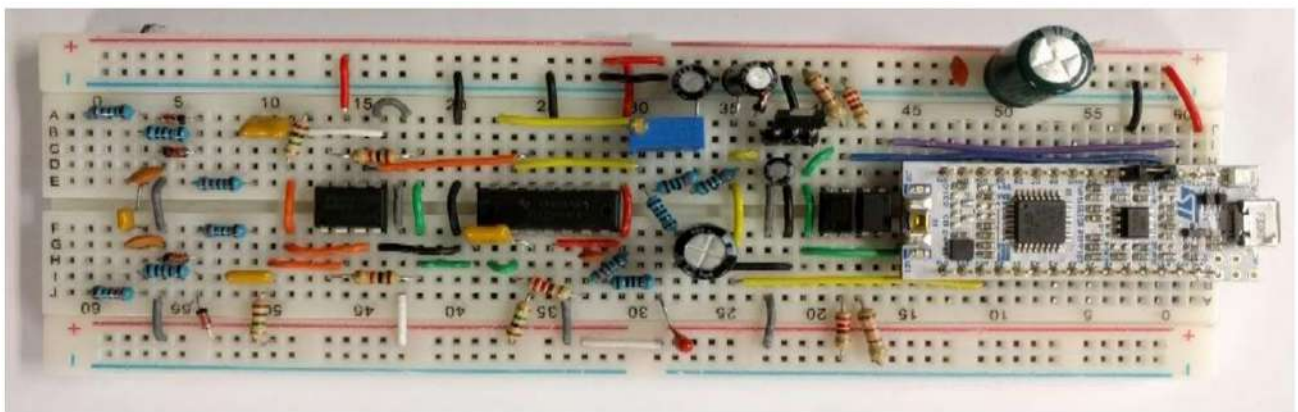


*Figure 40: The EEG-circuit from the reference article, here without electrodes, USB-adpater and battery<sup>116</sup>*

---

<sup>116</sup> (Byrne, 2018)'s work

## Circuit diagram from reference article

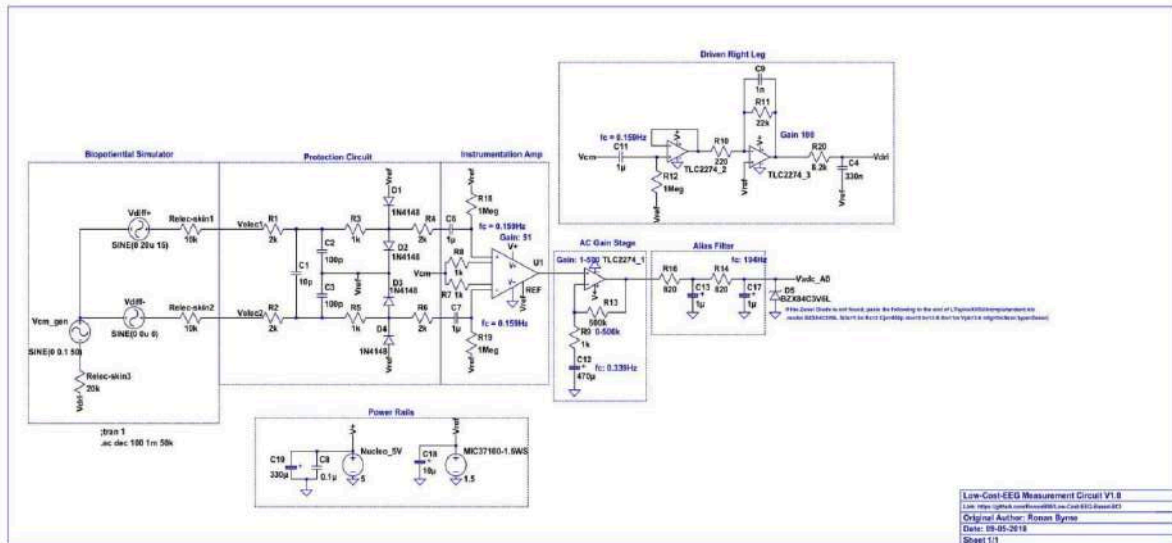


Figure 41: Circuit diagram for the reference article<sup>117</sup>

## Optoisolation circuit diagram from reference article fra

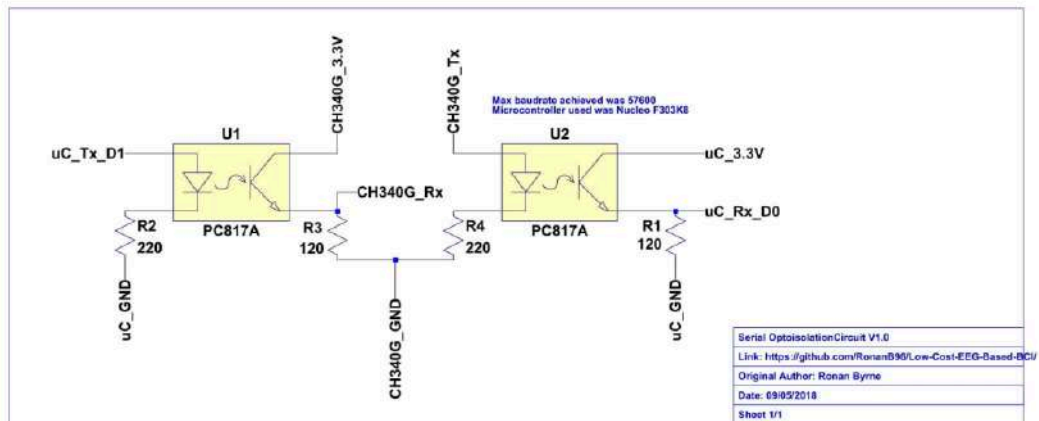


Figure 46 LTSpice diagram of optoisolation circuit

Figure 42: Circuit diagram for optoisolation circuit from the reference article<sup>118</sup>

<sup>117</sup> (Byrne, 2018)'s work

<sup>118</sup> (Byrne, 2018)'s work

## My Own Circuits

A picture of my own EEG-circuit, in which I modified (Byrne, 2018)'s system to have three active electrodes (C3, C4 and Cz), can be found on Figure 17, while the circuit diagram is to be found on Figure 18.

## Component list

This is an overview of the used components for the EEG-instrument.

Component	Amount	Link
NUCLEO-F303K8	1	<a href="https://dk.farnell.com/stmicroelectronics/nucleo-f303k8/dev-board-nucleo-32-mcu/dp/2500224">https://dk.farnell.com/stmicroelectronics/nucleo-f303k8/dev-board-nucleo-32-mcu/dp/2500224</a>
TLC2274ACN Quad Operation Amplifier	2	<a href="https://elektronik-lavpris.dk/p81636/tlc274cn-4xop-amp-cmos-316v-lp-ln-dip14/">https://elektronik-lavpris.dk/p81636/tlc274cn-4xop-amp-cmos-316v-lp-ln-dip14/</a>
MIC37100-1.5WS 1.5V Regulator	1	<a href="https://uk.farnell.com/microchip/mic37100-1-8ws/lto-volt-reg-1a-1-8v-sot-223-3/dp/2510064?srltid=Afm-B0oo3qqaKl973Czm7dZ3Yi2I5xva6krqyqloaKxCIEO0r-Qoy2pts">https://uk.farnell.com/microchip/mic37100-1-8ws/lto-volt-reg-1a-1-8v-sot-223-3/dp/2510064?srltid=Afm-B0oo3qqaKl973Czm7dZ3Yi2I5xva6krqyqloaKxCIEO0r-Qoy2pts</a>
AD623AN Instrumentation amplifier	3	<a href="https://elektronik-lavpris.dk/p136258/ad623anz-analog-devices-ic-instr-amp-800khz-110db-8dip/">https://elektronik-lavpris.dk/p136258/ad623anz-analog-devices-ic-instr-amp-800khz-110db-8dip/</a>
USB-TTL Converter	1	<a href="https://elektronik-lavpris.dk/p147229/sbc-ttl-usb-interface-converter/">https://elektronik-lavpris.dk/p147229/sbc-ttl-usb-interface-converter/</a>
PC817N Opto-Coupler	2	<a href="https://elektronik-lavpris.dk/p129954/pc817x4nsz1b-optokoblere-5kv-80v-50ma-300-dip-4-tpc817d/">https://elektronik-lavpris.dk/p129954/pc817x4nsz1b-optokoblere-5kv-80v-50ma-300-dip-4-tpc817d/</a>
Diode	12	Loaned from Egaa Gymnasium
Zener Diode	3	<a href="https://elektronik-lavpris.dk/p78506/bzx84c0039-smd-zenerdiode-03w-39v-sot23/">https://elektronik-lavpris.dk/p78506/bzx84c0039-smd-zenerdiode-03w-39v-sot23/</a>
9V battery	1	Loaned from Egaa Gymnasium
9V battery snap	1	Loaned from Egaa Gymnasium
Breadboard	5/6	Loaned from Egaa Gymnasium
10p Ceramic Condensator	3	Loaned from Egaa Gymnasium

Component	Amount	Link
100p Ceramic Condensator	6	<a href="https://uk.farnell.com/vishay/1c10c0g101j100b/cap-100pf-100v-5-c0g-np0/dp/1612162?srsId=AfmBOoq5v5y8b-3E6UZvHNZjMfKd0eCFIdQ4LkaOzQI_h7Hm8aFXv-wD">https://uk.farnell.com/vishay/1c10c0g101j100b/cap-100pf-100v-5-c0g-np0/dp/1612162?srsId=AfmBOoq5v5y8b-3E6UZvHNZjMfKd0eCFIdQ4LkaOzQI_h7Hm8aFXv-wD</a>
1n Ceramic Condensator	3	Loaned from Egaa Gymnasium
100n Ceramic Condensator	3	<a href="https://elektronik-lavpris.dk/p85224/kenf100-cer-capacitor-100nf-50v-p508-20-80-y5v/">https://elektronik-lavpris.dk/p85224/kenf100-cer-capacitor-100nf-50v-p508-20-80-y5v/</a>
330n Ceramic Condensator	3	<a href="https://elektronik-lavpris.dk/p147820/sr215e334zaa-mlc-capacitor-330nf-50v-z5u-p508/">https://elektronik-lavpris.dk/p147820/sr215e334zaa-mlc-capacitor-330nf-50v-z5u-p508/</a>
1u Ceramic Condensator	9	<a href="https://elektronik-lavpris.dk/p143435/ec08we0105mda-mlc-capacitor-10uf-100v-z5u-p508/">https://elektronik-lavpris.dk/p143435/ec08we0105mda-mlc-capacitor-10uf-100v-z5u-p508/</a>
1u Electrolytic Condensator	6	Loaned from Egaa Gymnasium
10u Electrolytic Condensator	3	Loaned from Egaa Gymnasium
330u Electrolytic Condensator	3	<a href="https://uk.farnell.com/rubycon/63rx30330mg412-5x25/cap-330-f-63v-20/dp/2342132?srsId=Afm-BOoojUvpckolabgnCnpb4yV9G_1Y9dtp100NHe0AtAeX4s-5uCEwE">https://uk.farnell.com/rubycon/63rx30330mg412-5x25/cap-330-f-63v-20/dp/2342132?srsId=Afm-BOoojUvpckolabgnCnpb4yV9G_1Y9dtp100NHe0AtAeX4s-5uCEwE</a>
470u Electrolytic Condensator	3	Loaned from Egaa Gymnasium
120 $\Omega$ Resistor	6	<a href="https://dk.farnell.com/multicomp-pro/mcre000026/res-120r-5-125mw-axial-carbon/dp/1700225">https://dk.farnell.com/multicomp-pro/mcre000026/res-120r-5-125mw-axial-carbon/dp/1700225</a>
220 $\Omega$ Resistor	9	Loaned from Egaa Gymnasium
820 $\Omega$ Resistor	6	Loaned from Egaa Gymnasium
1 k $\Omega$ Resistor	15	Loaned from Egaa Gymnasium
2 k $\Omega$ Resistor	12	Loaned from Egaa Gymnasium
8,2 k $\Omega$ Resistor	3	Loaned from Egaa Gymnasium
22 k $\Omega$ Resistor	3	Loaned from Egaa Gymnasium

Component	Amount	Link
1 M $\Omega$ Resistor	9	Loaned from Egaa Gymnasium
500 k $\Omega$ Potentiometer	3	<a href="https://dk.farnell.com/en-DK/bourns/3296w-1-504lf/trimmer-25-turn-500k/dp/9353313?srltid=AfmBOo-pAH4LEJm7vCso_wcaJcKg6tj3cxu_KVmpi2-ZdGUpq0Fy3Ep5c">https://dk.farnell.com/en-DK/bourns/3296w-1-504lf/trimmer-25-turn-500k/dp/9353313?srltid=AfmBOo-pAH4LEJm7vCso_wcaJcKg6tj3cxu_KVmpi2-ZdGUpq0Fy3Ep5c</a>
Golden EEG-Electrodes	9	<a href="https://shop.openbci.com/products/openbci-gold-cup-electrodes">https://shop.openbci.com/products/openbci-gold-cup-electrodes</a>
Electrogel	1	<a href="https://shop.cephalon.eu/OneStep-AbrasivPlus-EEG-Gel-(120-g-tube)/VareDetaljer.aspx?9=DK&amp;5=HH10200&amp;11=1950">https://shop.cephalon.eu/OneStep-AbrasivPlus-EEG-Gel-(120-g-tube)/VareDetaljer.aspx?9=DK&amp;5=HH10200&amp;11=1950</a>
Swimming cap	1	<a href="https://www.sportsworld.dk/slazenger-silicone-swimming-cap-adults-885040#colcode=88504003">https://www.sportsworld.dk/slazenger-silicone-swimming-cap-adults-885040#colcode=88504003</a>

## The Function of the System

The EEG instrument records the brain's electrical signals through three electrodes (C3, Cz, and C4). The signals are processed through several circuit blocks: protection circuit, instrumentation amplifier, AC amplification stage, anti-aliasing filter, power supply, opto-isolation circuit, and a Driven Right Leg (DRL) circuit. The signal is then sent to a microcontroller and transferred via USB to a computer for analysis.

To ensure reliable and noise-free measurements, both low-pass and high-pass filtering are applied, as well as active noise compensation through the DRL. The power supply is stabilized and filtered, and the entire system is galvanically isolated from the computer. The updated circuit with correctly numbered components is available here: <https://github.com/TobiasBN1005/From-thought-to-movement-/tree/main>

### Protection circuit

The protection circuit safeguards the components from overvoltage, overcurrent, and unwanted noise. It also limits current in fault situations.

Since EEG signals are very weak, sensitive amplifiers are required, which can easily be distorted by noise or damaged by unexpected high voltages. Therefore, the protection circuit is essential.

The two signals from the electrodes first pass through a differential and a common-mode low-pass filter. The common-mode filter consists of R11, C31, R21, and C21, while the differential filter is formed by R11, R21, and C11, creating a second-order low-pass filter on each signal line. Resistors R31 and R5 also reduce current.

Diodes D11, D21, D31, and D41 clamp the signals between Vref and GND, ensuring they do not exceed  $V_{ref} \pm 0.7$  V. This protects the amplifier from overvoltage.

Resistors R41 and R61 further limit current in the case of unexpected voltages before the signals are passed to the instrumentation amplifier.

### Instrumentation amplifier

The instrumentation amplifier amplifies the weak differential signal between two electrodes while suppressing common-mode noise. The signal path first includes a first-order high-pass filter (C61, R181 and C71, R191) to remove DC offset caused by half-cell potentials. This prevents distortion in the amplifier.

Resistors R181 and R191 are  $1\text{ M}\Omega$  to maintain a high input impedance.

Once the DC components are removed, the relevant AC components are amplified via R71 and R81. The common-mode voltage  $V_{cm}$  (the time-varying common-mode signal between body and ground) is measured here and sent to the DRL circuit. The purpose of DRL is to reduce  $V_{cm}$  and improve the system's Common Mode Rejection Ratio (CMRR), which should be above 80 dB. Component tolerances, however, reduce CMRR in practice, which DRL helps to compensate for.

### AC amplification stage and anti-aliasing filter

After the instrumentation amplifier, the signal from the AD623 is passed to an AC gain stage, based on a TLC2274 quad-op amp. Here, a variable AC gain between 1 and 501 is achieved using the adjustable resistor R131 (trimmer). The DC component passes without amplification, while AC components are amplified. Capacitor C131 is charged via R91 and R131 to Vref.

After amplification, the signal is sent to a passive low-pass filter (R161, R141, C131, C171), which reduces high-frequency components before the ADC and minimizes aliasing. A Zener diode ensures that the output voltage does not exceed 3.3 V, the maximum for the ADC input.

### DRL circuit

The DRL circuit uses  $V_{cm}$  from the instrumentation amplifier, which after high-pass filtering (C11 and R12) is sent to a buffer (Ua) that provides a clean AC version of  $V_{cm}$ . The signal is processed by a low-pass filter (R10, C9, and R11), then passed to an inverting amplifier (Ub), which amplifies  $V_{cm}$  by a factor of  $-100$ .

C9, R20, and C4 ensure that the inverted  $V_{cm}$  is in phase with the original, which is necessary for effective noise cancellation. Resistor R20D limits current to the body. The signal is sent to the body via a dedicated DRL electrode, thereby reducing common-mode noise from the body and environment, and improving CMRR.

### Power supply

The circuit is powered by 5 V,  $V_{ref}$ , and GND.

The 5 V comes from the Nucleo board's 5 V pin and is stabilized by C19 and C8. C19 acts as a large buffer tank absorbing slow variations in voltage, while C8 removes high-frequency noise.

$V_{ref}$  at 1.5 V is generated via a MIC37100 regulator and used as the reference voltage for signal processing and as the maximum touch voltage for user safety. 1.5 V was chosen since it is the mid-point between GND and 3.3 V (the ADC input range). Capacitor C18 at the regulator output ensures fast response to load changes.

GND is the common reference of the system, shared across the entire circuit, and comes from the Nucleo board.

### Opto-isolation circuit

To ensure galvanic isolation between the EEG system and the computer, data is transmitted through an optocoupled serial interface. The microcontroller's UART TX and RX are connected to an



optocoupler, which transfers the signal to a USB-TTL converter (CH340G) and then to the computer. Resistors R1O, R2O, R3O, and R4O ensure fast switching of the phototransistor. The baud rate is 57,600, and the sampling rate is 256 Hz.

## Summary

In total, this circuit filters, protects, and amplifies EEG signals from three active electrodes, enabling later data processing and use in my Transformer model.

## Code and software

The code can be found here: <https://github.com/TobiasBN1005/From-thought-to-movement-/tree/main>.

The EEG instrument software was developed in STM32CubeIDE, an integrated development environment designed for STM32 microcontrollers by STMicroelectronics. I used it together with a Nucleo F303K8 board, which serves as the central unit of the measurement system. I used the graphical tool STM32CubeMX to generate initialization code based on the hardware configuration. This included configuration of peripheral units such as ADC, UART, DMA, and TIM2.

Figure 43 below shows the pinout and configuration of my F303K8 board:

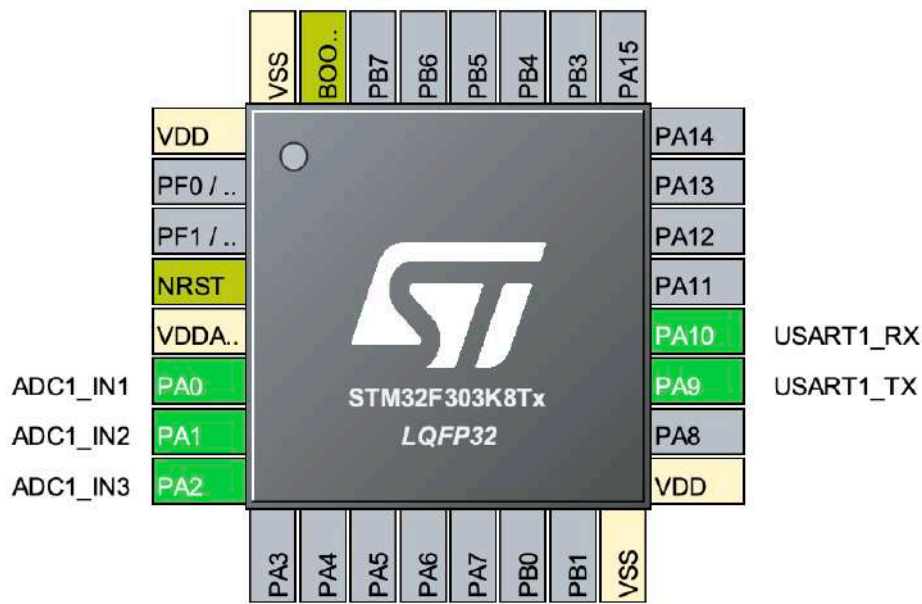


Figure 43: The configuration of the F303K8 NucleoSTM32 microcontroller<sup>119</sup>

Let's go through why I chose this specific configuration.

To collect EEG data from the three active electrodes, C3, C4, and Cz, I configured ADC1 (Analog-to-Digital Converter 1) on the Nucleo F303K8. The electrodes measure voltage variations from the motor cortex and are connected to the three analog input channels on the microcontroller: PA0, PA1, and PA2.

In STM32CubeMX, I configured these pins as:

- PA0 → ADC1\_IN1
- PA1 → ADC1\_IN2
- PA2 → ADC1\_IN3

The signals come directly from the analog outputs of my EEG circuit (where they are amplified, filtered, and protected).

## ADC1 configuration

All the ADC1 settings can be seen on Figure 44.

<sup>119</sup> The author's own work in STM32CubeMX

Function	Setting	Comment
Mode	Independent mode	ADC1 is independent of ADC2, since only one ADC is used for EEG data
Clock Prescaler	ADC Asynchronous mode	ADC runs with a clock independent from the system clock
Resolution	ADC 12-bit resolution	ADC runs with a clock independent from the system clock
Data Alignment	Right alignment	Resolution: 12-bit (4096 levels) — sufficient for EEG signals
Scan Conversion Mode	Enabled	Least Significant Bit aligned to the right → easy handling in integer variables
Continuous Conversion Mode	Disabled	Sequential sampling of multiple channels → needed for 3 electrodes
Discontinuous Conversion Mode	Disabled	Conversion triggered only by an external trigger (Timer 2) → no polling loop
DMA Continuous Mode	Enabled	Entire channel sequence converted in one cycle → consistent signal flow
End of Conversion Mode	End of single conversion	ADC results automatically sent to RAM via DMA
Overrun Behaviour	Overrun data overwritten	End-of-conversion (EOC) flag set when a single channel conversion is complete
Low Power Auto Wait	Disabled	Newest data overwrites old if not read in time (not relevant with continuous DMA sampling)
Enable Regular Conversions	Enable	Conversion round includes all three channels:
Number of Conversions	3	ADC runs with a clock independent from the system clock
External Trigger Conversions Source	Timer 2 Trigger Out event	Resolution: 12-bit (4096 levels) - sufficient for EEG signals
External Trigger Conversions Edge	Trigger detection on the rising edge	Least Significant Bit aligned to the right → easy handling in integer variables
SequencerNbRanks	1	Sequential sampling of multiple channels → needed for 3 electrodes
Rank	1, Channel 1, Sampling time: 61,5 Cycles	First electrode (C3)
Rank	2, Channel 2, Sampling time: 61,5 Cycles	Second electrode (C4)
Rank	3, Channel 3, Sampling time: 61,5 Cycles	Third electrode (Cz)

Figure 44: Settings for ADC1<sup>120</sup>

All channels (IN1, IN2, IN3) are set to single-ended mode, which is standard for EEG since measurements are made relative to a common reference.

ADC1 runs in scan conversion mode, meaning all three channels are converted sequentially at each sampling step. Sampling is triggered in real time by Timer 2 (TIM2). Data is automatically transferred via DMA to memory, minimizing CPU load. The ADC runs at 12-bit resolution with right alignment for precise and efficient processing. This setup enables stable and synchronous real-time acquisition of EEG data from all three electrodes.

<sup>120</sup> The author's own work in STM32CubeMX

## TIM2 Configuration

All the TIM2 settings can be seen on Figure 45.

Function	Setting	Comment
Slave Mode	Disabled	Timer runs independently
Trigger Source	Disabled	No external trigger used
Clock Source	Internal Clock	TIM2 uses the <b>internal clock</b> as its source
Channel 1-4	Disabled	No PWM applied - only TRGO output is used
Combined Channels	Disabled	No channels are utilized
Prescaler (PSC 16 bits value)	1125	Timer clock frequency is divided down to a suitable frequency
Counter Mode	Up	Timer counts from 0 to the <b>ARR value (Auto Reload Register)</b>
Counter Period	249	When the counter reaches 249, an update event is generated, used as the ADC trigger
Internal Clock	No Division	No additional clock division
Auto-reload preload	Disable	ARR updates immediately
Master / Slave Mode	Disable	TIM2 acts as the <b>master</b> and sends TRGO without external synchronization
Trigger Event Selection TRGO	Update Event	Each time the counter rolls over, the ADC is triggered

Figure 45: Settings for TIM2<sup>121</sup>

TIM2 serves as the trigger source for ADC1, ensuring stable and precise sampling. It generates an update event at a fixed frequency, forwarded as a TRGO signal to ADC1. In this project, the sampling rate is set to 256 Hz (PSC = 1406, ARR = 199), a common rate for EEG analysis.

## USART Configuration

All the USART settings can be seen on Figure 46. Figure 44

---

<sup>121</sup> The author's own work in STM32CubeMX

Function	Setting	Comment
Mode	Asynchronous	Used for serial communication with the computer via USB-TTL
Hardware Flow Control (RS232)	Disable	Only TX/RX pins are used
Baud Rate	56700 bits / s	Standard baud rate (fixed, stable)
Word Length	8 bits (including parity)	Standard 8-bit data word, no parity
Parity	None	Simple format, standard UART settings
Stop Bits	1	Supports both transmitting and receiving signals
Data Direction	Receive and transmit	Ensures precision and noise robustness during data transfer
Over Sampling	16 samples	Standard sampling applied
Signal Sample	Disable	TX/RX signals are not inverted
Auto Baud rate	Disable	Data stream is not inverted
TX/RX Pin Active Level Inversion	Disable	TX and RX lines are not swapped
Data Inversion	Disable	Allows new data to overwrite old if not read in time (important for real-time streaming)
TX and RX Pins Swapping	Disable	DMA continues even in case of receiver errors
Overrun	Enable	Data is sent LSB first
DMA on RX error	Enable	Used for serial communication with the computer via USB-TTL
MSB First	Disable	Only TX/RX pins are used

Figure 46: Settings for USART<sup>122</sup>

USART1 is configured in asynchronous mode to transmit EEG data from the STM32 to a PC via a USB-TTL converter.

- Baud rate: **57,600 bps** (chosen for stable real-time transmission)
- Data format: 8 data bits, no parity, 1 stop bit
- Data is sent LSB first, with error handling (overrun/DMA errors) enabled to ensure robust streaming.

<sup>122</sup> The author's own work in STM32CubeMX

## DMA Configuration

All the DMA settings can be seen on Figure 47. Figure 44

Function	Setting	Comment
Mode	Circular	Continuous operation: circular buffer mode ensures uninterrupted sampling
Increment Address	Memory	Memory address increments after each conversion → necessary to store samples sequentially in the buffer
Data Width	Half Word	16-bit width (required for 12-bit ADC output) → correct data formatting
DMA Request	ADC1	DMA responds to completed ADC conversions and automatically transfers the data
Channel	DMA1 Channel 1	Specific channel assigned to ADC1 on STM32F303K8 → hardware routing
Direction	Peripheral to Memory	Data flows from ADC (peripheral) to RAM
Priority	High	Ensures ADC data transfers are prioritized over lower-priority DMA processes

Figure 47: Settings for DMA<sup>123</sup>

To enable real-time EEG acquisition without CPU overhead, **DMA1 Channel 1** is configured to transfer data from ADC1 into a RAM buffer.

- Mode: *circular*, so the buffer continuously updates without manual intervention
- Data width: 16-bit (half-word), matching the 12-bit ADC output
- Direction: peripheral-to-memory with auto-increment, so each new sample is placed correctly in memory

This ensures stable and efficient data handling for EEG signals from C3, C4, and Cz.

---

<sup>123</sup> The author's own work in STM32CubeMX

## NVIC Configuration

All the NVIC settings can be seen on Figure 48

Function	Setting	Comment
Priority Group	4 bits for pre-empt	Fine-grained control of interrupt priorities
Force DMA Channels Interrupts	Enable	Allows DMA to trigger interrupts (e.g., transfer complete) → essential for real-time dataflow
Non maskable interrupt	Enable	Critical faults enabled:
Hard fault interrupt	Enable	Handles memory access errors
Memory management fault	Enable	Catches unauthorized memory reads/writes
Pre-fetch, fault, memory access fault	Enable	Reports errors if the program attempts to execute invalid code
Undefined instruction or illegal state	Enable	Allows software-based system calls
System service call via SWI instruction	Enable	Supports debugging with external tools
Debug monitor	Enable	Enables low-priority interrupts for multitasking
Pendable request for system service	Enable	Used for time management (SysTick)
Time base: System tick timer	Enable (pre-emption priority: 15)	Not needed: power monitoring
PVD interrupt through EXTI line 16	Disable	Not relevant: Flash interrupts (not used)
Flash global interrupt	Disable	Clock control interrupt (not used)
RCC global interrupt	Disable	Used to fetch finished ADC data from DMA to RAM → essential in the EEG system
DMA1 channel1 global interrupt	Enable	DMA manages the continuous dataflow
ADC1 and ADC2 interrupts	Disable	TIM2 not used for interrupts (it is only a trigger source)
TIM2 global interrupt	Disable	Allows detection of received/transmitted data over UART
USART1 global interrupt / USART1 wake-up interrupt through EXTI line 25	Enable	Not necessary: FPU interrupts (not used on STM32F303K8)
Floating point unit interrupt	Disable	Allows software-based system calls

Figure 48: Settings for NVIC<sup>124</sup>

The NVIC is configured to allow interrupts from DMA and USART1, enabling automatic transfer of EEG data from ADC → RAM → PC without disrupting the main program. SysTick interrupts are used for timekeeping but set to lowest priority. Error interrupts are enabled for robust fault handling.

## Summary

In summary, I built a system where an STM32 Nucleo F303K8 microcontroller synchronously acquires EEG signals from three electrodes (C3, Cz, C4) via ADC1 (PA0, PA1, PA2). Sampling is precisely triggered by TIM2 at 256 Hz, and data is transferred via DMA in circular mode, allowing continuous acquisition without CPU overload. Data is then transmitted through USART1 over a USB-TTL converter to a PC, where it can be processed in real time. The EEG data is then used as input to a Transformer model to classify movement intentions. In this way, a fully integrated system

<sup>124</sup> The author's own work in STM32CubeMX

is created, where thoughts and intentions can be translated into action through signal processing and AI.

After configuring the code in STM32CubeMX, I generated the base code and continued development in STM32CubeIDE, where all relevant files (main.c, main.h, etc.) were implemented and uploaded to the Nucleo F303K8 microcontroller.

## Project Data Book

The Project Data Book is a different document for this project, which is my the figure numbering is unique to just this section. Don't confuse "Figure 1" in Project Data Book with "Figure 1" in the Research Paper/Appendices — they are two different figures.



# From Thought to Movement -

## A Brain Physiological Interface for Motor Impairments

Author: Tobias Bendix Nielsen

School: Egaa Gymnasium

Year: 2025

Mostratec 2025 - Biomedical Engineering

## Timeline

December 2024: Project idea development began learning Python and AI models in Google Colab. Initial planning of robotic arm and EEG system.

January 2025: Wrote first research paper. Tested various AI architectures. Built first version of the robotic arm with Arduino and servos. Initiated contact with relevant researchers.

February: Optimized the robotic arm. Started developing a custom EEG circuit inspired by R. Byrne (2018). Started to code in Spyder 6 (Python), Arduino UNO (C++) and STM32 (C).

March: Integrated IMUs for precise motion tracking. Conducted literature review. Programmed seven AI architectures. Presented at the Danish National Youth Science Fair semifinals (Unge Forskere). Collaborated with EEG and neuroscience researchers. Added EMG measurements to the system.

April: Completed a 3-channel EEG circuit. Developed IMU-based real-time control of the robotic arm (using quaternions, non-Euclidian coordinates to avoid Gimbal Lock etc.). Presented at the Unge Forskere finals.

May: Received donated 8-channel OpenBCI equipment. Improved EEG hardware in collaboration with Aarhus University. Redesigned robotic arm setup.

June: Enhanced design and implemented EEG-based control of the robotic arm.

July: Summer break and research on EMS/FUS integration to develop a BPI in the future.

August: Began collecting EEG, EMG, and IMU data. Updated literature review with literature on EMS/FUS.

September: Training and optimization of the Transformer model on my own multimodal data, to create a direct pipeline from thought to movement.

## Experimental observations

### Journal - Choice of AI-model

This appendix documents the AI models tested in the project for analysing and classifying EEG/EMG data. Training time and accuracy of each model were examined to select the best-performing model for experiments with my own biosignals.

Each model includes a short description of its architecture and training process. After this, the accuracy of each AI model is briefly reported, and finally, the models' performances are summarised and compared to identify the most suitable model for the project.

The appendix is divided into two parts:

- A **journal** of how the AI models were tested
- An **overview and code** for the different AI models

Finally, the selected AI model for the project is concluded.

### Journal: Orthosis arm movement with public data (28<sup>th</sup> of February)

*Conducted by: Tobias Bendix Nielsen*

*Purpose: Test a prototype AI model on public datasets*

#### **Before the experiment**

##### **Initial ideas and hypotheses**

Questions:

- Can an AI model predict movement vs. non-movement based on EEG and EMG data?
- How can the model be optimized to improve accuracy?

The expectation was to find a moderate correlation between EEG and EMG, despite datasets being collected from different individuals with unique brain structures. The hypothesis was that the model

could predict movement vs. non-movement and thus form the basis for further optimization and eventual application in Parkinson's patients.

At the project's start, data from previous studies (Kueper et al., 2024) were used to test and iterate the AI model. All methodological descriptions in this journal are therefore drawn from that article.

## Method description

### *Experimental setup*

Participants performed 15 repetitions of flexion and extension with the right arm. EEG data were recorded from 64 channels, with focus on C3, C4, and Cz (motor cortex). EMG was recorded from:

- M. biceps brachii
- M. triceps brachii (lateral and long head)
- M. flexor digitorum superficialis

To minimize eye artifacts, subjects were instructed to fixate on a black cross during the experiment.

### *Variable control:*

- Electrodes placed according to the international 10/20 system and standard protocols for consistency
- Noise-free data and trials without orthosis errors were used to establish a baseline

### *Materials / apparatus*

- **EEG system:** LiveAmp64 with 64 channels (Brain Products GmbH), ActiCap slim electrodes, sampling rate 500 Hz, reference FCz, ground AFz
- **EMG system:** ANT mini eego amplifier, sampling rate 1000 Hz, bipolar electrodes placed using SENIAM guidelines
- **Orthosis:** Active elbow orthosis with torque sensors
- **Synchronization:** Event Trigger Board for precise alignment of EEG and EMG

### *Safety considerations*

Subjects were asked to remain still and avoid sudden movements.

## After the Experiment

### Procedure

The data was collected from 8 subjects with EEG-electrodes placed on the scalp and EMG-electrodes on the mentioned muscles on both arms. These muscles are crucial for the flexion and extension of the arm. Figure 49 shows these muscles.

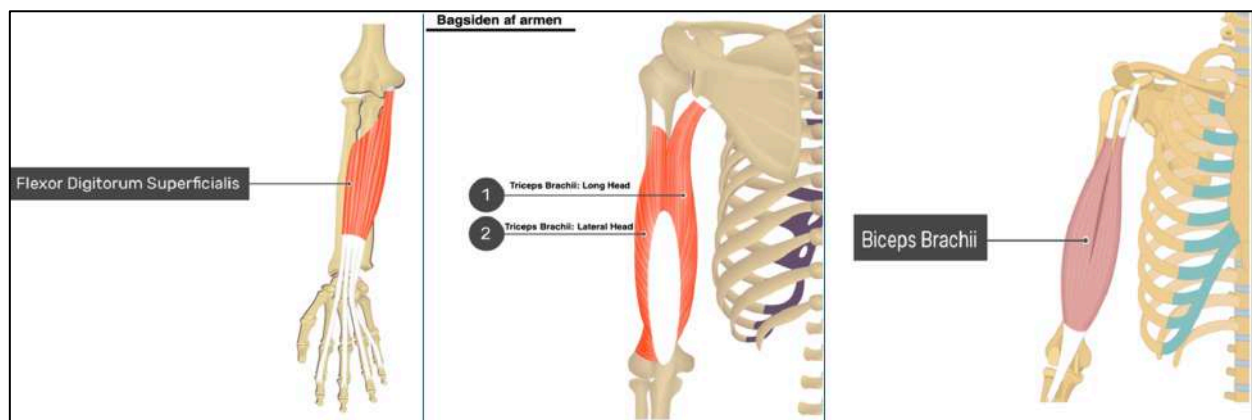


Figure 49: The different muscles where EMG-electrodes were placed<sup>125</sup>

Data were collected from eight subjects with electrodes on the scalp and the above muscles. Participants performed 15 repetitions of extension and flexion with the right arm while fixating on a cross to minimize eye artifacts. Experiments were cued by verbal stimuli. Only baseline data (without induced orthosis errors) were used.

EEG was recorded at 500 Hz with a 0.0-131 Hz bandpass filter. EMG was sampled at 1000 Hz with SENIAM placements. EEG and EMG were synchronized using an Event Trigger Board, achieving an average timing difference below 8.5 ms.

### AI-models

All models (codes included at the end of this appendix) were trained on the dataset from Kueper et al. (2024). EEG channels used: C3, C4, Cz. EMG: first 4 channels only. Analysis window: 30-210

<sup>125</sup> Loaned from: <https://www.getbodysmart.com/arm-muscles/>

seconds (earlier data were too noisy). EEG was aligned to EMG activity by looking 200 ms before movement onset.

Validation: Group-K-fold Cross-validation

Precision: Confusion matrix and ROC curve

## Observation, results and data analysis

AI models were trained on EEG and EMG data. To compare across models, accuracy and speed were evaluated. Metrics were normalized with an efficiency score:

$$\text{Efficiency} = \alpha \cdot \frac{\text{Accuracy}^2}{\text{Accuracy}_{\max}} + \beta \cdot \text{AUC} - \gamma \cdot \frac{\log(\text{time})}{\log(\text{time}_{\max})}$$

with  $\alpha = 0.8$ ,  $\beta = 0.5$ ,  $\gamma = 0.7$ . Accuracy was weighted highest, but computation time also mattered. The results can be seen on

AI-model	Precision	Training time (s)	Time (hh:mm:ss)	AUC	Efficiency	Parameters
A-SVM	85.67%	57	00:00:57	93.36%	79.81%	N/A
CNN	100.00%	1329	00:22:09	100.00%	83.88%	907554
DeepConvNet	99.87%	1063	00:17:43	100.00%	84.86%	1073474
LSTM-CNN	99.92%	3655	01:00:55	100.00%	78.72%	842146
LSTM-RNN	97.58%	14165.18	03:56:05	99.33%	69.54%	548642
SVM	67.29%	8	00:00:08	69.48%	58.44%	N/A
Transformer	98.50%	645	00:10:45	99.97%	85.77%	505410

Table 8: The results from the AI-models

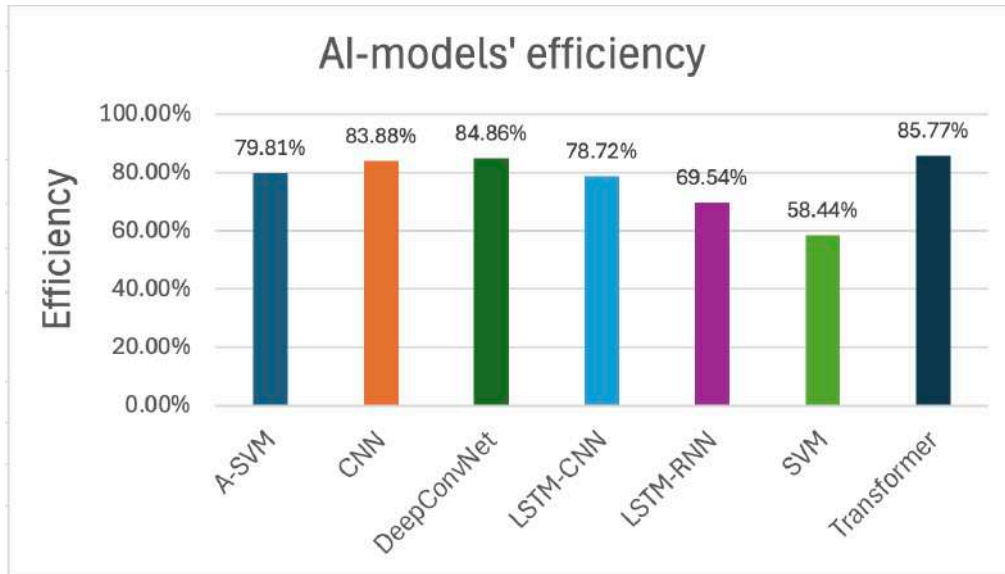


Figure 50: The efficiency of the different AI-models

## Results

AI-model	Precision	Training time (s)	Time (hh:mm:ss)	AUC	Efficiency	Parameters
<b>A-SVM</b>	85.67%	57	00.00.57	93.36%	79.81%	N/A
<b>CNN</b>	100.00%	1329	00.22.09	100.00%	83.88%	907554
<b>DeepConvNet</b>	99.87%	1063	00.17.43	100.00%	84.86%	1073474
<b>LSTM-CNN</b>	99.92%	3655	01.00.55	100.00%	78.72%	842146
<b>LSTM-RNN</b>	97.58%	14165.18	03.56.05	99.33%	69.54%	548642
<b>SVM</b>	67.29%	8	00.00.08	69.48%	58.44%	N/A
<b>Transformer</b>	98.50%	645	00.10.45	99.97%	85.77%	505410

Table 9: First iteration of AI-model training, using K-fold cross-validation and different amount of parameters . The models might have overfitted in this iteration, because of the high precisions achieved. The models were built to classify between non-movement<sup>126</sup>

<sup>126</sup> The author's own work, made in Excel

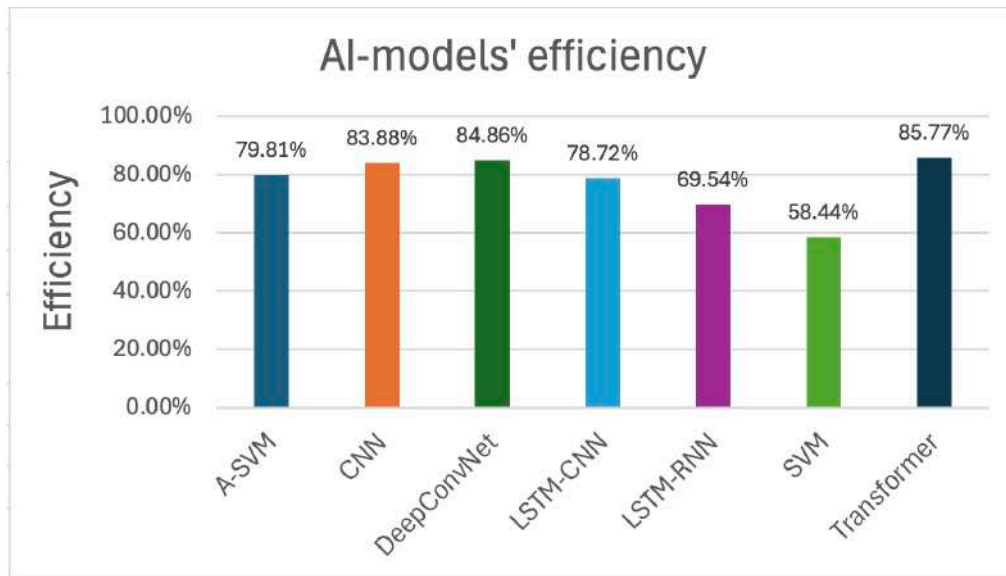


Figure 51: Graph of AI-models' efficiency

I can from the results conclude the following

- **LSTM-RNN** and **LSTM-CNN** performed worst, due to their complexity and long training times.
- **SVM** had the lowest precision (69.48%) and was therefore not selected for further use.
- **CNN** and **DeepConvNet** were both fast and accurate but are not ideal for time-dependent signals like EEG/EMG and thus were excluded.
- **A-SVM** achieved the highest precision but was not selected due to limited presence in the literature and because Transformer models are more advanced and promising in the AI field. Moreover, its precision was 13 percentage points lower than the Transformer-model

Initial results indicated possible overfitting, as evidenced by unusually high precision and AUC scores. To address this, a second iteration was conducted using GroupKFold-validation (same data split), F1-score, and inference time. All models were scaled to ~200,000 parameters for fair comparison. As anticipated, all models exhibited a drop in performance, with the Transformer ranking among the lowest: second to last in inference time and third to last in F1-score. Nevertheless, the Transformer was selected for further development due to its balanced precision, suitability for sequential signals, and strong future potential. Its performance is also likely to improve with more training data and better hyperparameter tuning. Table 3 show the results from the second iteration while Figure 52 shows a F1-score vs Inference time for the AI-models:



AI-model	Precision	Training time / s	Inference time / s	Time (hh:mm:ss)	AUC	Efficiency	Parameters	F1-score
A-SVM	64.91%	9.89	0.0016	00:00.09	94.04%	58.62%	N/A	73.89%
CNN	96.99%	142.05	0.000712	00:02.22	94.17%	68.56%	229876	90.37%
DeepConvNet	98.25%	103.50	0.00061	00:01.43	96.51%	73.32%	269218	92.68%
LSTM-CNN	92.86%	320.18	0.001545	00:05.20	91.07%	56.99%	191090	86.01%
LSTM-RNN	92.11%	2245.71	0.09465	00:37.25	94.58%	40.33%	243234	89.93%
SVM	50.12%	1.19	0.000051	00:00.01	59.57%	43.66%	N/A	66.78%
Transformer	88.47%	3615	0.018	01:00.15	94.28%	34.37%	227234	83.03%

Table 10: Second iteration of AI-model training, using GroupKFold cross-validation and around the same number of parameters to better compare different architectures. The precisions have decreased, and the models likely did not overfit this time. The models were built to classify between non-movement and movement in EEG and EMG signals<sup>127</sup>

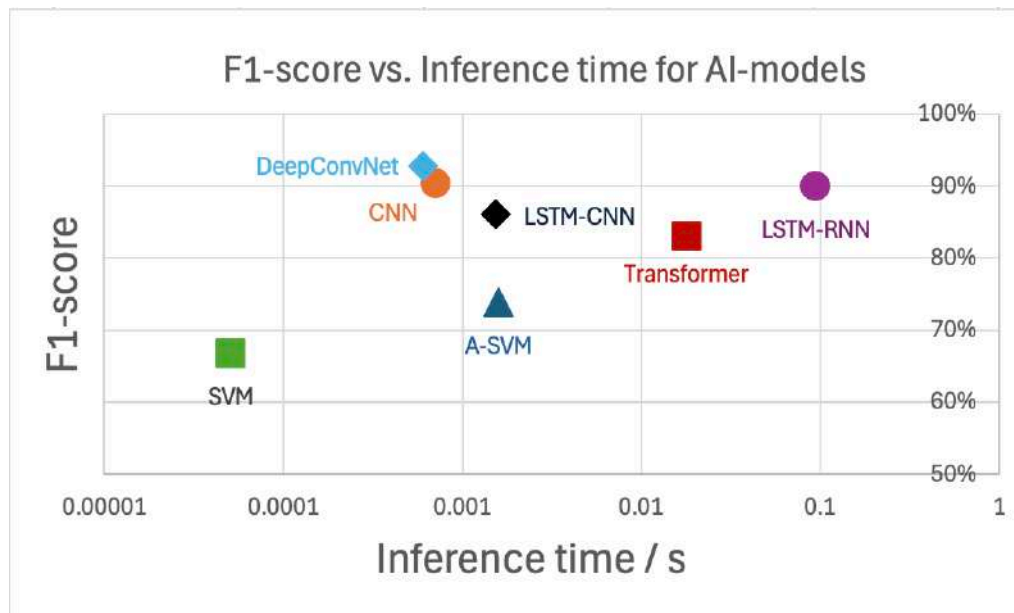


Figure 52: Graph of AI-models' F1-score vs. Inference time. The x-axis is in a logarithmic scale of 10. Even though the Transformer performed worse here, I have worked extensively with this model type before, which allows me to keep developing and improving it, especially because it fits well with combining EEG, EMG, and IMU signals in real-time. Its performance is also likely to improve with more training data and better hyperparameter tuning<sup>128</sup>

The Transformer model is therefore considered the most suitable for this project due to its balanced precision, strong performance on sequential data, and promising future potential. It will be used for further development in the next phase.<sup>129</sup>

<sup>127</sup> The author's own work in Excel

<sup>128</sup> The author's own work in Excel

<sup>129</sup> A preliminary jury for the Danish science competition *Unge Forskere*, also suggested me to work with a Transformer-model in my project.

## *Discussion*

Results align partially with literature but highlight limitations:

- Models were trained on non-Parkinson's data from multiple subjects, not individualized datasets
- Brain structure varies between individuals, so signals differ significantly
- My own future data (from custom-built EEG/EMG/IMU) will be noisier and less precise than the research-grade setups

## *Reflection*

The journal shows that AI models can predict movement vs. non-movement from EEG/EMG, but with room for improvement. This represents an important first step toward technology supporting Parkinson's patients. Future work should include more precise data, advanced methods, and individualized training for clinical use.

## *Overview of AI models*

The following AI models were tested:

- Model 1: LSTM-CNN
- Model 2: LSTM
- Model 3: CNN
- Model 4: Transformer
- Model 5: SVM
- Model 6: A-SVM
- Model 7: DeepConvNet

All were evaluated with k-fold cross-validation, AUC, confusion matrix, and accuracy.

Source code: <https://github.com/TobiasBN1005/From-thought-to-movement->

<https://github.com/TobiasBN1005/From-thought-to-movement->

## Model descriptions

### LSTM-CNN

Combines CNN's feature extraction with LSTM's long-term memory to predict EMG signals and movements.

### LSTM-RNN

An RNN variant with memory cells (LSTM), useful for time-series like EEG/EMG. Can learn temporal dependencies and predict future values.

### CNN

Convolutional Neural Network specialized in pattern recognition. Often used for image/signal processing, extracting local features.

### Transformer

Processes data in parallel using self-attention, effective at learning long-range dependencies. Well-suited for multimodal input (EEG, EMG, IMU).

### SVM

Classifies data by finding an optimal separating hyperplane. Effective for binary/multiclass classification. Often used in biomedical signals.

### Adaptive SVM (A-SVM)

Improves on SVM by updating the hyperplane dynamically with new data. Useful in non-stationary environments where signals change over time.

### DeepConvNet

Like a CNN but deeper, with more layers, enabling more complex feature extraction.

## Journal 2: Real-time Transformer with Movement Classification, Linked to the Robotic Arm (the 8<sup>th</sup> of April)

*Conducted by: Tobias Bendix Nielsen*

*Purpose: Real-time testing of a Transformer model on multimodal biosignal data—and integration with a robotic arm*

### *Before the experiment*

#### Initial ideas and hypotheses

(Which questions can be investigated, what relationships do you expect to see and why, and which experiment(s) can answer these questions?)

Key question:

- Can movements be predicted by a Transformer model trained on movement intention, based on EEG, EMG, and IMU data from a single test subject?

The expectation is that the model can predict and classify movements with high accuracy as **binary values**, because it is trained on a single individual and multiple movement recordings. Several arm movements are performed, and movement initiation is marked in the data, enabling identification of **Bereitschaftspotentials**.

Unlike Appendix 3, which uses a public dataset, this appendix describes real-time measurements on myself using self-developed equipment. The goal is to examine practical applicability and robustness of the model in real-world situations.

### *Method description*

(Describe how the experiment will be carried out; use drawings if possible. Argue for variable control. This section should allow you to make an Excel table with a column for the independent variable and a column for the dependent variable so you're ready to record results.)

First, I will build a working EEG/EMG/IMU measurement system and synchronize it so the signals are recorded simultaneously. I will ensure the instruments share the same sampling rate; otherwise, data will be downsampled. I will band-pass and notch-filter the raw signals to remove irrelevant bands and mains noise, ensuring the cleanest possible data. A wearable EEG cap will be built with electrodes on mastoid, ground, C3, C4, and Cz placed according to the international 10–20 system (a swim cap serves as the headset).

**EMG electrodes** will be placed on: M. biceps brachii, M. triceps brachii (lateral), M. triceps brachii (long head), and M. flexor digitorum superficialis, plus ground/reference.

**Three IMUs** will be mounted on the wrist, forearm, and upper arm to measure arm motion. Each movement is mapped to a **binary value** which is the Transformer’s output. Thus, the model predicts a specific movement by outputting its binary code. Table 11 shows the different movements types and their corresponding bit values:

Movement	No movement (baseline)	Flexion of underarm	Extension of underarm	Raising of arm	Lowering of arm	Supination of wrist	Pronation of wrist
Photo of Movement							
Binary value	0000	0001	0010	0011	0100	0101	0110

Table 11: The different movement types<sup>130</sup>

Data will be collected and saved to my PC as .txt or .csv files, then processed and analyzed to train the Transformer.

### *Materials / apparatus*

- EMG equipment
- 6 EMG surface electrodes for the muscles above, reference placed on bone (e.g., elbow), plus a ground electrode

<sup>130</sup> The author’s own work

- Muscle sensor, electrodes, and amplifier: <link provided>
- 3 IMUs to capture motion of forearm, upper arm, and wrist; LoggerPro
- Alcohol wipes and cotton for skin prep
- EEG & EMG software
- Comfortable chair and table
- A dark, quiet room → minimal stimuli and artifacts
- 3-4 cameras to record the experiment

### *Safety considerations*

The equipment is home-built and somewhat fragile, handle with care. Electrodes must be placed precisely to avoid incorrect data. The EEG cap should fit comfortably and firmly to minimize noise. Hair should be washed; EEG electrodes applied with gel; the arm cleaned with alcohol to improve signal quality. All devices must be powered and started simultaneously using a synchronization board. No movements should occur behind the subject, as IMUs may pick up unintended signals. Ensure all cables are secured.

### *After the experiment*

#### Procedure

I will first build and test the EEG and EMG setups and their code. Then I will fit the EEG cap, measure head landmarks according to the 10–20 system, and place electrodes at C3, C4, Cz, AFz, and FCz. I will wash my hair and apply electrode gel to reduce impedance, then secure the cap so electrodes don't shift. Next, I will set up the EMG gear. *Figures below show electrode placements and the completed EEG setup.*

I will clean my right arm and disinfect it. Electrodes are placed on M. biceps brachii, M. triceps brachii (lateral), M. triceps brachii (long head), and M. flexor digitorum superficialis, with the reference on a bony area. *Figure 53 shows the EMG setup on my arm.*

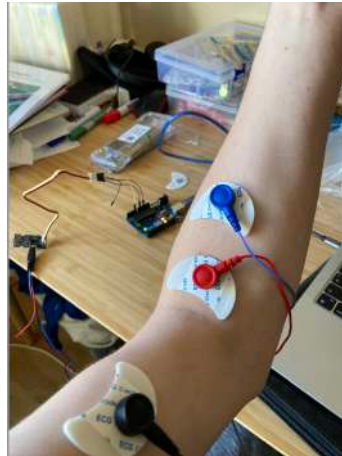


*Figure 53: The EMG-setup with electrodes placed on my arm<sup>131</sup>*

Both systems are then connected to power and to my computer to begin acquisition. I will sit in a comfortable chair in a quiet room with minimal stimuli. I will fixate on a black cross on the wall to focus on the movements and reduce artifacts.

IMUs are mounted on forearm, upper arm, and wrist of the right arm and switched on together with EEG and EMG. IMUs provide motion data to cross-correlate with EMG (which can be noisy) and indicate direction and type of movement (velocity, acceleration, angle changes, intensity). Figure 54 shows IMU placements.

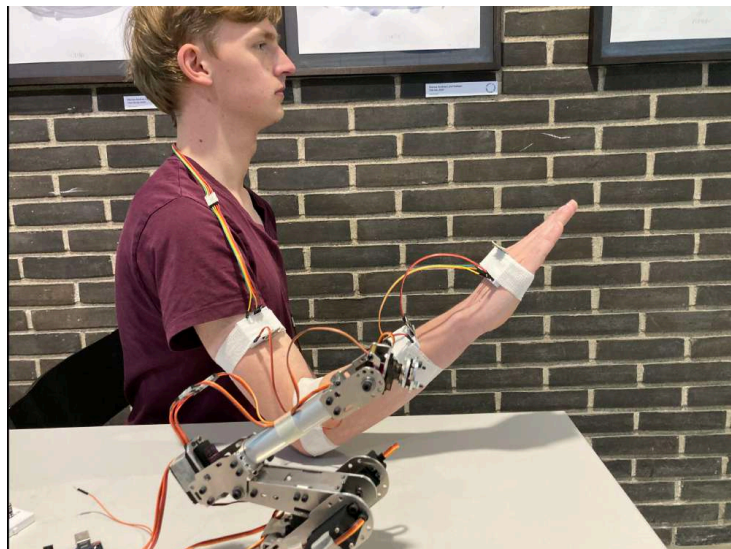


*Figure 54: Placement of IMU's on my arm<sup>132</sup>*

---

<sup>131</sup> The author's own work

<sup>132</sup> The author's own work

With my right arm, I will perform the movements listed earlier (e.g., flexion/extension, pronation/supination), but only **two opposing movements per recording** (e.g., flex vs. extend). This helps isolate the underlying Bereitschaftspotential. Each recording lasts **3 minutes**; I perform one movement every **20 seconds** for ~5 seconds. An LED turns on to mark movement onset and off to mark stop; this interval is embedded in both EEG and EMG.

After each recording, I rest for 5 minutes. New recordings follow with a different pair of movements. After all data are collected, I process them and train my Transformer model.

In future work, I will perform the same recordings with my father (who has Parkinson's). A separate Transformer (same code) will be trained on his data and evaluated for binary movement classification.

### *Observations / results / processing*

(Insert tables and graphs with trend lines; label axes with SI units. Include regression equations with correct symbols/units and percent deviation from reference values if applicable.)

Results will be added after data collection. Planned processing includes band-pass, notch, etc. Evaluation metrics: **F1-score, AUC, accuracy, confusion matrix, inference time**.

Based on expectations, the Transformer will achieve high classification accuracy and reliably identify a movement from the **intended** EEG signal when trained jointly with EMG/IMU. Thus, the model can effectively predict movements from thought.

### *Evidence*

(Which results/interpretations support your conclusions?)

Expected outcomes: high accuracy on both offline and real-time datasets; average  $F1 = X$ ,  $AUC = Y$ , and low inference time → real-time prediction. Confusion matrices should show clear separation of binary classes; ROC curves should confirm discriminative performance. The robotic arm is expected to respond correctly in real time to the model's binary outputs, demonstrating the pipeline **intention → Transformer → actuator** works in practice.



## Discussion

(Do your results align with prior research? Include uncertainties and error sources.)

Results are expected to align with previous work on movement prediction from EEG/EMG (Kueper et al., 2024; Silva-Acosta et al., 2021; Mahmoodi et al., 2021). A key strength is introducing a **third modality (IMU)**, which supports EMG in detecting movement and reduces misclassification risk. Prior research (e.g., Silva-Acosta et al., 2021) also shows that combining EEG/EMG with IMU can improve model performance.

Limitations and uncertainties:

- EEG is measured with home-built equipment, potentially reducing signal quality
- Electrode contact quality may vary—especially during movement
- Data currently from **one healthy subject** → limited generalizability
- Only **six movement types** tested → limited scalability to free movements

Even so, the experiment should indicate that the Transformer can generalize well-defined intentional movements under mild noise.

## Reflection

(What is the answer to the questions? What have you learned, experimentally and theoretically?)

The project is expected to show that **AI—specifically a Transformer architecture—can predict motor intentions** from EEG, EMG, and IMU. The system can convert intention into mechanical motion in real time, opening new possibilities for assistive technologies for movement disorders.

### Transformer code

Available at: [https://github.com/TobiasBN1005/From-thought-to-movement-/tree/main/Main\\_AI\\_model](https://github.com/TobiasBN1005/From-thought-to-movement-/tree/main/Main_AI_model)

### Arduino robotic-arm code

Available at: <https://github.com/TobiasBN1005/From-thought-to-movement-/tree/main/Robotarm>

## Robotic arm

This appendix documents the construction of a 6-axis robotic arm, its circuit design, and integration with three IMUs. The robotic arm was ordered and manually assembled. The control code for the robotic arm is developed in Arduino C.

The appendix is divided into two parts: a journal covering the integration of the robotic arm with the IMUs, and the construction of the robotic arm itself. The robotic arm serves as a proof-of-concept for the project, demonstrating how movement intentions can be translated into physical action via IMUs in real time.

The robotic arm was purchased from:

<https://arduinotech.dk/shop/6-axis-abb-industrial-robotic-arm/?srsltid=AfmBOoo-AZr3toKRdzCWPg3Jr5tGTd5CXOSLHlIB5t9q1ZwASUAPQr1Ln>

User manual:

<https://arduinotech.dk/wp-content/uploads/2021/04/Complete-6-Axis-ABB-Industrial-Robotic-Arm.pdf>

The robotic arm code can be found at:

<https://github.com/TobiasBN1005/From-thought-to-movement->

## Journal: Testing the Robotic Arm as a Proof-of-Concept (27<sup>th</sup> of February)

*Conducted by: Tobias Bendix Nielsen*

*Purpose: Move the robotic arm based on biosignals*

*Before the experiment*

*Initial ideas and hypotheses*

(Which questions can be investigated, what relationships are expected and why, and which experiments can answer them?)

Key question:

- Is it possible to control a robotic arm in real time via IMUs mounted on my arm?

I expected the robotic arm to closely mimic my movements because an IMU contains both an accelerometer and a gyroscope (measuring acceleration and angular velocity) and can therefore map the arm's pose; the Arduino code can then translate these signals in real time.

*Method description*

(Describe how the experiment will be carried out; include a drawing if possible. Argue for variable control. This section should enable an Excel table with independent/dependent variables.)

I began by assembling the robotic arm and writing the relevant Arduino IDE code. The arm was placed on a flat surface and connected to my PC, which provided signals derived from my IMUs. The arm then executed movements simultaneously with the test subject (me), so that the arm's motion matched my right arm. So far, I have two servos communicating with the Arduino code, allowing me to control the arm with a single IMU. In the future, I will add two more IMUs and have all five active servos communicating. The servo layout is shown on Figure 55:

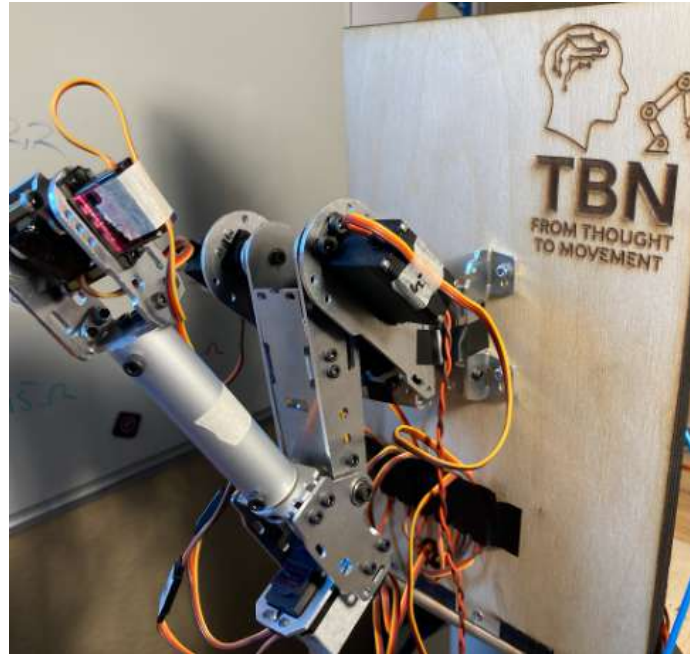


*Figure 55: The robotic arm used in this project<sup>133</sup>*

Servo 4 is not used, as it does not correspond to a physiologically meaningful human arm movement.

#### *Materials / apparatus*

- Arduino robotic arm
- Diagnostic LEDs
- Jumper wires
- Arduino IDE code for arm motion
- Breadboards
- PC
- Arduino UNO
- 6 V power supply
- Velcro for IMUs
- IMU(s)

---

<sup>133</sup> The author's own work

### *Safety considerations*

The robotic arm must not be over-extended, to avoid tipping over and damaging wires or the system. Movements should not be too abrupt, as wires may come loose from their pins. Current must be kept sufficiently low; likewise, resistance and voltage should remain low to prevent damage. Ground and power crocodile clips/leads must not touch (short-circuit risk). Servos require **6 V** and IMUs **5 V**.

### *After the experiment*

#### Procedure

I placed the arm on a flat surface and connected its six servos to the Arduino UNO on different input pins, which were connected to my PC and a 6 V power supply. (The circuit is shown at the end of this document.)

I then mounted three IMUs on the forearm, upper arm, and wrist using Velcro to measure arm pose as accurately as possible. *Figure 2 shows the placement of the IMUs on my arm.*

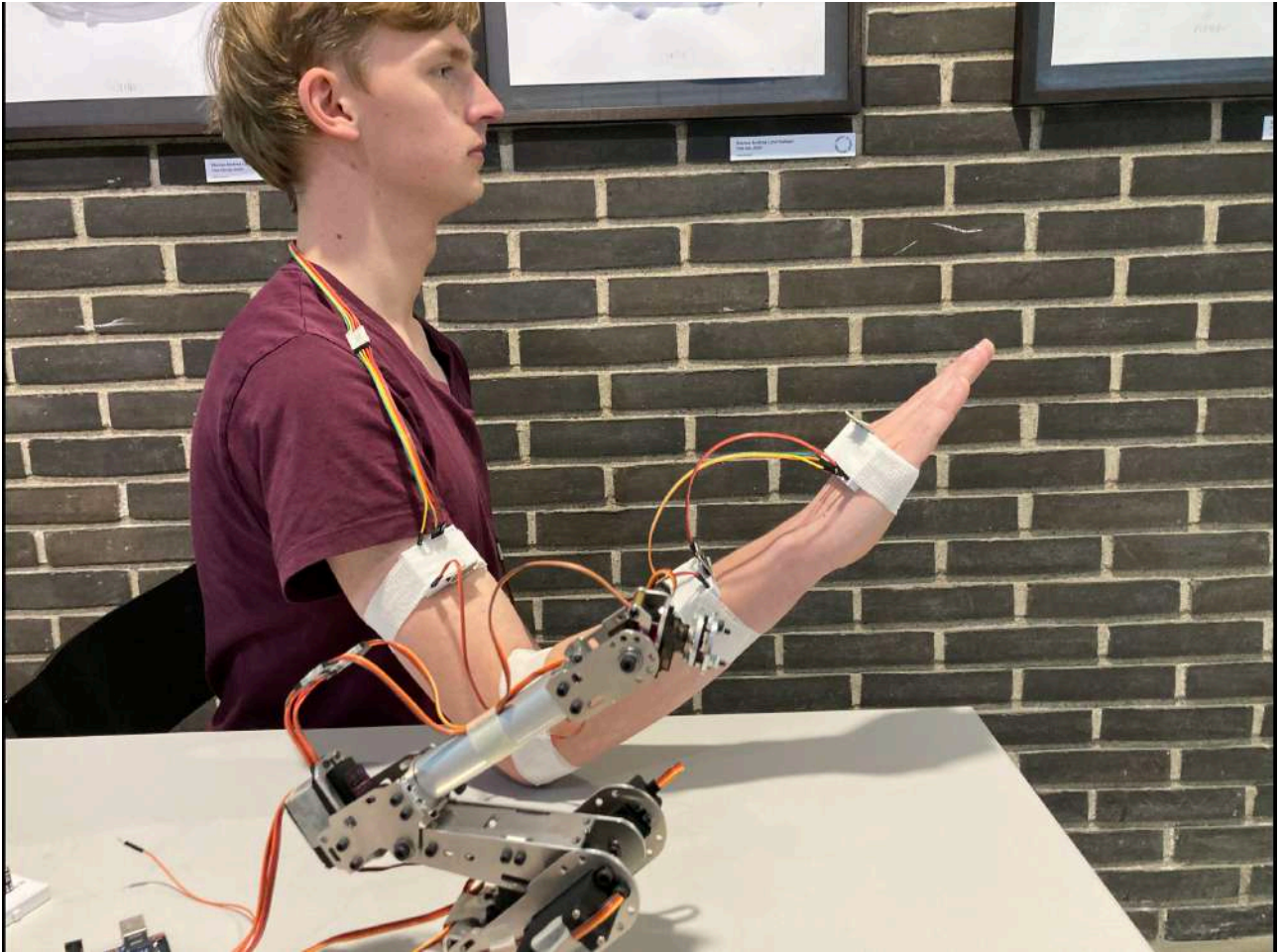


*Figure 56: Three IMUs are mounted on the right arm to track motion dynamics<sup>134</sup>*

Figure 57 shows the robotic arm setup:

---

<sup>134</sup> The author's own work

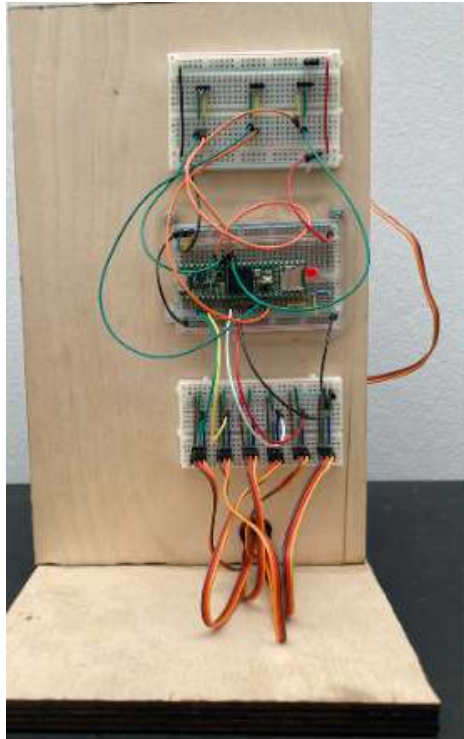


Figure 57: The circuit for the IMU, robotic arm Teensy 4.1 microcontroller<sup>135</sup>

I powered the system and moved my arm while wearing the IMUs.

### *Observations / results / processing*

The expectation is that the robotic arm can reproduce my arm's movements with high precision, since the IMUs measure the relevant kinematic data and their placement is chosen strategically.

### *Evidence*

Given high precision from the arm, we can conclude that it successfully serves as a proof-of-concept.

### *Discussion*

It is expected that the results will show the arm closely mirroring my arm's movement. This proof-of-concept demonstrates promising potential for AI-controlled systems to support movement in practice.

---

<sup>135</sup> The author's own work



## *Reflection*

It is expected that the Arduino code successfully translated my arm movements into control signals for the robotic arm, supporting the hypothesis.

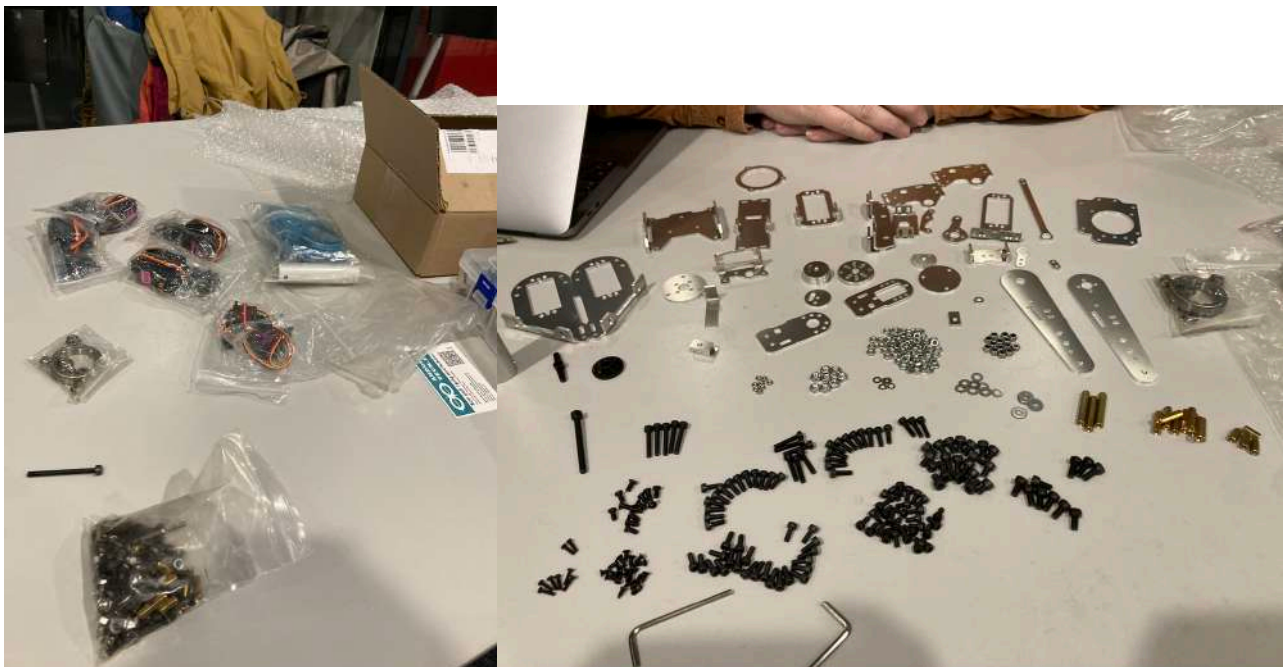
This proof-of-concept suggests potential for developing an actuator to assist individuals with motor impairments, such as Parkinson's patients. With further optimization, the system could be applied to rehabilitation after injury or integrated with neuroprostheses. Future iterations should expand data collection to more participants, implement more advanced models, and improve hardware components to increase precision and applicability.

## *Construction of the robotic arm*

This section documents the step-by-step build. All components were carefully sorted, assembled, and tested to ensure correct operation.

### *All components*

All parts used to build the robotic arm.



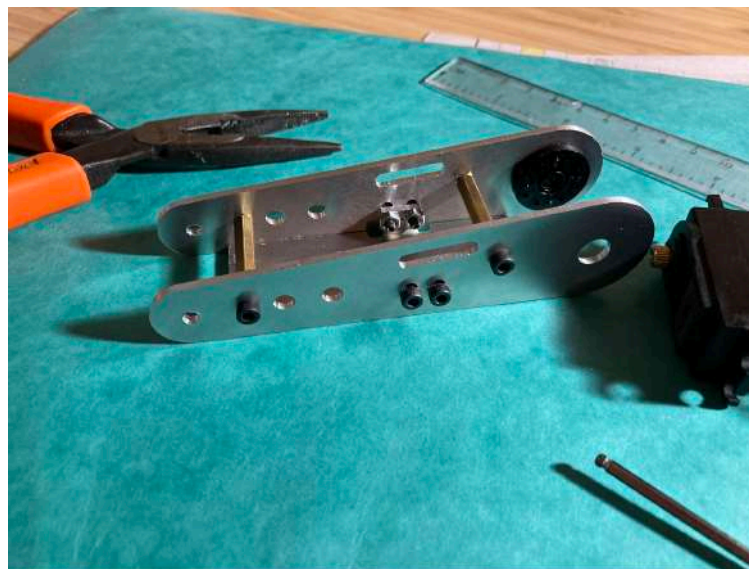
## Construction of the Robotic Arm

### **First part:**





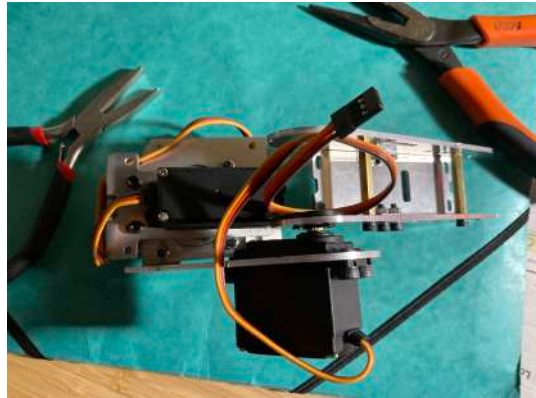
**Second part:**



**Third part:**



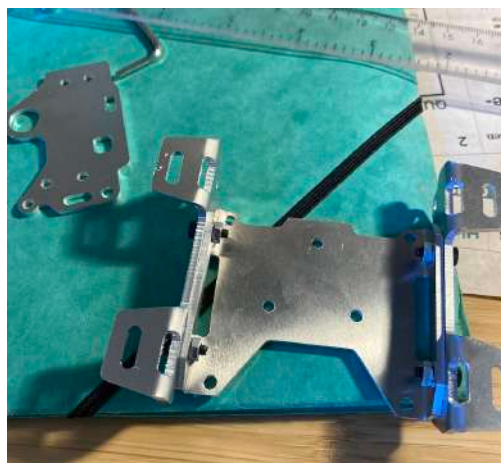
**Fourth part:**



**Fifth part:**



**Sixth part:**



**Seventh part:**



2.3) Finished robotic arm





## Photos of the robotic arm in action

Images of the completed robotic arm as used in the project.

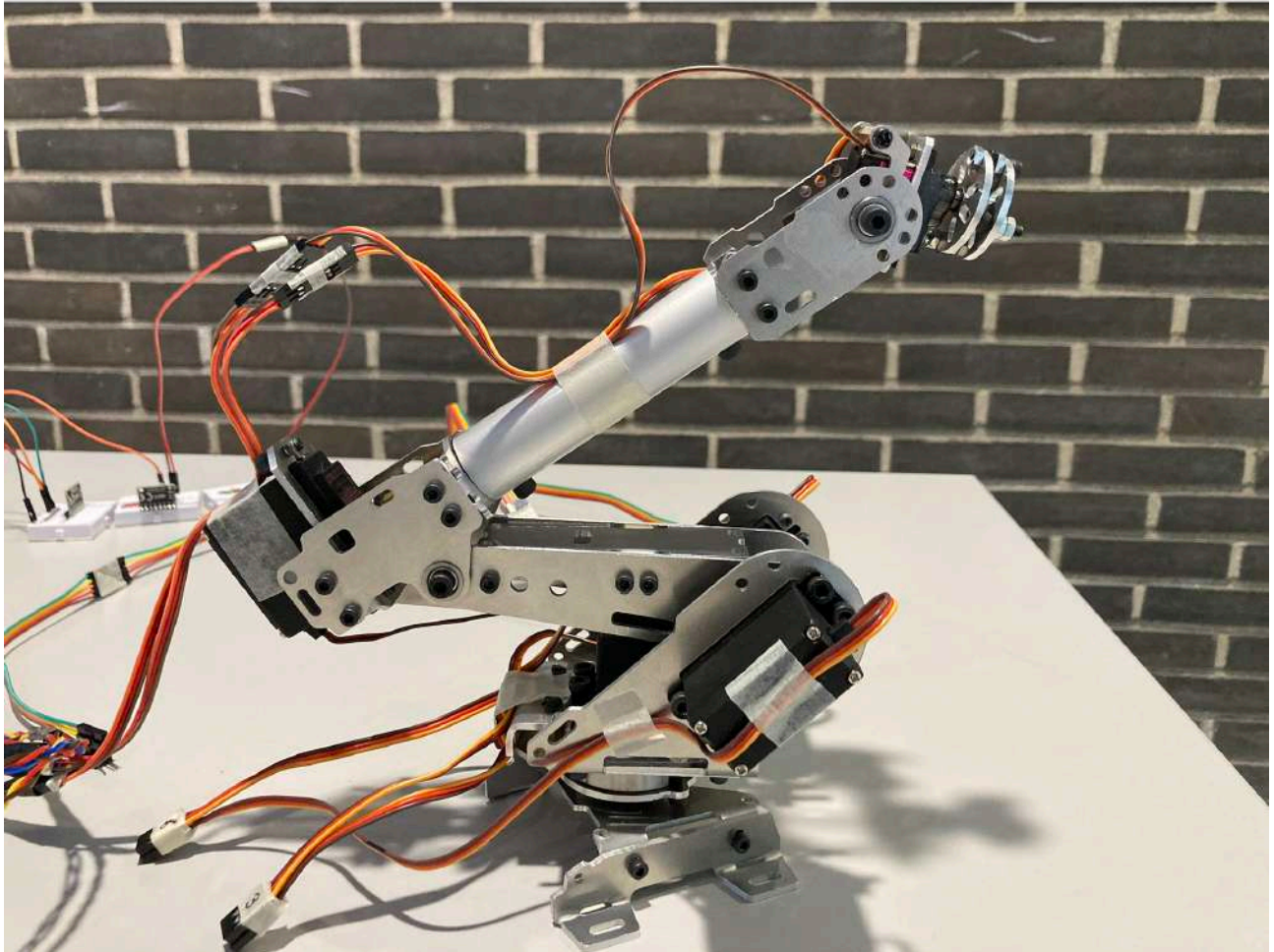


*Figure 58: Robotic arm connected to Arduino<sup>136</sup>*

---

<sup>136</sup> The author's own work

## Scientific Articles

- [1] R. Byrne, ‘Development of a Low Cost, Open-source, Electroencephalograph-Based Brain-Computer Interface’. Dublin Institute of Technology, May 28, 2018. Accessed: Jan. 10, 2025. [Online]. Available: <https://github.com/RonanB96/Low-Cost-EEG-Based-BCI/blob/master/Thesis/Development%20of%20a%20Low%20Cost%2C%20Open-source%2C%20Electroencephalograph-Based%20Brain-Computer%20Interface.pdf>
- [2] M. J. Antony *et al.*, ‘Classification of EEG Using Adaptive SVM Classifier with CSP and Online Recursive Independent Component Analysis’, *Sens. Basel*, vol. 22, no. 19, p. 7596, Oct. 2022, doi: 10.3390/s22197596.
- [3] A. Buerkle, W. Eaton, N. Lohse, T. Bamber, and P. Ferreira, ‘EEG based arm movement intention recognition towards enhanced safety in symbiotic Human-Robot Collaboration’, *Robot. Comput.-Integr. Manuf.*, vol. 70, p. 102137, Aug. 2021, doi: 10.1016/j.rcim.2021.102137.
- [4] D. Zhang, C. Hansen, F. D. Fréne, S. P. Kærgaard, and W. Qian, ‘Automated labeling and online evaluation for self-paced movement detection BCI’, *Knowl.-Based Syst.*, vol. 265, p. 110383, Feb. 2023, doi: 10.1016/j.knosys.2023.110383.
- [5] J. Aeles, F. Horst, S. Lapuschkin, L. Lacourpaille, and F. Hug, ‘Revealing the unique features of each individual’s muscle activation signatures’, *R. Soc. Publ. Interface*, vol. 18, no. 174, p. 20200770, Jan. 2021, doi: 10.1098/rsif.2020.0770.
- [6] V. del C. Silva-Acosta, I. Román-Godínez, S. Torres-Ramos, and R. A. Salido-Ruiz, ‘Automatic estimation of continuous elbow flexion–extension movement based on electromyographic and electroencephalographic signals’, *Biomed. Signal Process. Control*, vol. 70, p. 102950, Sept. 2021, doi: 10.1016/j.bspc.2021.102950.
- [7] M. Mahmoodi, Bahador Makkiabadi, M. Mahmoudi, and S. Sanei, ‘A new method for accurate detection of movement intention from single channel EEG for online BCI’, *Comput. Methods Programs Biomed. Update*, vol. 1, p. 100027, Aug. 2021, doi: 10.1016/j.cmpbup.2021.100027.
- [8] F. Karimi, J. Niu, K. Gouweleeuw, Q. Almeida, and N. Jiang, ‘Movement-related EEG signatures associated with freezing of gait in Parkinson’s disease: an integrative analysis’, *Brain Commun.*, vol. 3, no. 4, p. fcab277, Nov. 2021, doi: 10.1093/braincomms/fcab277.

- [9] H.-C. Wang, A. J. Lees, and P. Brown, ‘Impairment of EEG desynchronisation before and during movement and its relation to bradykinesia in Parkinson’s disease’, *J. Neurol. Neurosurg. Psychiatry*, vol. 66, no. 4, pp. 442–446, Apr. 1999, doi: 10.1136/jnnp.66.4.442.
- [10] A. Miladinović *et al.*, ‘EEG changes and motor deficits in Parkinson’s disease patients: Correlation of motor scales and EEG power bands’, *Procedia Comput. Sci.*, vol. 192, pp. 2616–2623, 2021, doi: 10.1016/j.procs.2021.09.031.
- [11] S. Farashi, A. Sarihi, M. Ramezani, S. Shahidi, and M. Mazdeh, ‘Parkinson’s disease tremor prediction using EEG data analysis-A preliminary and feasibility study’, *BMC Neurol.*, vol. 23, p. 420, Nov. 2023, doi: 10.1186/s12883-023-03468-0.
- [12] A. A. P. Suárez, S. B. Batista, I. P. Ibáñez, E. C. Fernández, M. F. Campos, and L. M. Chacón, ‘EEG-Derived Functional Connectivity Patterns Associated with Mild Cognitive Impairment in Parkinson’s Disease’, *Behav. Sci. Basel*, vol. 11, no. 3, p. 11030040, Mar. 2021, doi: 10.3390/bs11030040.
- [13] M. Conti *et al.*, ‘Brain Functional Connectivity in de novo Parkinson’s Disease Patients Based on Clinical EEG’, *Front. Neurol.*, vol. 13, p. 844745, Mar. 2022, doi: 10.3389/fneur.2022.844745.
- [14] K. Desai, ‘Parkinson’s Disease Detection via Resting-State Electroencephalography Using Signal Processing and Machine Learning Techniques’, *arxiv*, Mar. 2023, doi: 10.48550/arXiv.2304.01214.
- [15] R. A. Zanini, E. L. Colombin, and M. C. F. de Castro, ‘Parkinson’s disease EMG signal prediction using Neural Networks’, *2019 IEEE Int. Conf. Syst. Man Cybern. SMC*, pp. 2446–2453, Sept. 2019.
- [16] A. Saikia, A. Saikia, Amit Ranjan Barua, and S. Paul, ‘EEG-EMG Correlation for Parkinson’s disease’, *Int. J. Eng. Adv. Technol. IJEAT*, vol. 8, no. 6, Aug. 2019, doi: 10.35940/ijeat.F8360.088619.
- [17] B. M. Doucet, A. Lam, and L. Griffin, ‘Neuromuscular Electrical Stimulation for Skeletal Muscle Function’, *Yale J. Biol. Med.*, vol. 85, no. 2, pp. 201–215, June 2012.
- [18] M. Popovic, T. Thrasher, M. Adams, V. Takes, V. Zivanovic, and M. Tonack, ‘Functional electrical therapy: retraining grasping in spinal cord injury’, *Spinal Cord*, vol. 44, pp. 143–151, Mar. 2006, doi: 10.1038/sj.sc.3101822.

- [19] M. Sun *et al.*, ‘FES-UPP: A Flexible Functional Electrical Stimulation System to Support Upper Limb Functional Activity Practice’, *Front. Neurosci.*, vol. 12, no. 449, July 2018, doi: 10.3389/fnins.2018.00449.
- [20] A. Cuesta-Gómez, F. Molina-Rueda, M. Carratala-Tejada, E. Imatz-Ojanguren, D. Torricelli, and J. C. Miangolarra-Page, ‘The Use of Functional Electrical Stimulation on the Upper Limb and Interscapular Muscles of Patients with Stroke for the Improvement of Reaching Movements: A Feasibility Study’, *Front. Neurol.*, vol. 8, May 2017, doi: 10.3389/fneur.2017.00186.
- [21] A. Biasiucci *et al.*, ‘Brain-actuated functional electrical stimulation elicits lasting arm motor recovery after stroke’, *Nat. Commun.*, vol. 9, no. 2421, June 2018, doi: 10.1038/s41467-018-04673-z.
- [22] M. A. Khan *et al.*, ‘A systematic review on functional electrical stimulation based rehabilitation systems for upper limb post-stroke recovery’, *Front. Neurol.*, vol. 14, no. 1272992, Dec. 2023, doi: 10.3389/fneur.2023.1272992.
- [23] M. B. Kebaetse, A. E. Turner, and S. A. Binder-Macleod, ‘Effects of stimulation frequencies and patterns on performance of repetitive, nonisometric tasks’, *J. Appl. Physiol.*, vol. 92, no. 1, pp. 109–116, Jan. 2002, doi: 10.1152/jappl.2002.92.1.109.
- [24] L. Zhang *et al.*, ‘Activation of Piezo1 by ultrasonic stimulation and its effect on the permeability of human umbilical vein endothelial cells’, *Biomed. Pharmacother.*, vol. 131, p. 110796, Nov. 2020, doi: 10.1016/j.biopha.2020.110796.
- [25] D. Liao, F. Li, D. Lu, and P. Zhong, ‘Activation of Piezo1 Mechanosensitive Ion Channel In HEK293T Cells by 30 MHz Vertically Deployed Surface Acoustic Waves’, *Biochem. Biophys. Res. Commun.*, vol. 518, no. 3, pp. 541–547, Oct. 2019, doi: 10.1016/j.bbrc.2019.08.078.
- [26] F. Haddad, M. Sawalha, Y. Khawaja, A. Najjar, and R. Karaman, ‘Dopamine and Levodopa Prodrugs for the Treatment of Parkinson’s Disease’, *Molecules*, vol. 23, no. 1, p. 40, Dec. 2017, doi: 10.3390/molecules23010040.
- [27] P. Solla, F. Marrosu, and M. G. Marrosu, ‘Therapeutic interventions and adjustments in the management of Parkinson disease: Role of combined carbidopa/levodopa/entacapone (Stalevo)’, *Neuropsychiatr. Dis. Treat.*, vol. 6, no. 1, pp. 483–490, July 2010.
- [28] C. R. Oehrns *et al.*, ‘Chronic adaptive deep brain stimulation versus conventional stimulation in Parkinson’s disease: a blinded randomized feasibility trial’, *Nat. Med.*, vol. 30, pp. 3345–3356, Aug. 2019, doi: doi.org/10.1038/s41591-024-03196-z.

[29] N. Kueper *et al.*, ‘EEG and EMG dataset for the detection of errors introduced by an active orthosis device’, *Front. Hum. Neurosci.*, vol. 18, p. 1304311, Jan. 2024, doi: 10.3389/fnhum.2024.1304311.

## Bibliography

- geeksforgeeks. (2024, Juni 24). *What is LSTM – Long Short Term Memory?* Retrieved Januar 10, 2025, from geeksforgeeks.org: <https://www.geeksforgeeks.org/deep-learning-introduction-to-long-short-term-memory/>
- geeksforgeeks. (2023, Januar 10). *Long short-term memory (LSTM) RNN in Tensorflow*. Retrieved Januar 10, 2025, from geeksforgeeks.org: <https://www.geeksforgeeks.org/long-short-term-memory-lstm-rnn-in-tensorflow/>
- Hamad, R. (2023, December 3). *What is LSTM? Introduction to Long Short-Term Memory*. Retrieved Januar 10, 2025, from medium.com: <https://medium.com/@rebeen.jaff/what-is-lstm-introduction-to-long-short-term-memory-66bd3855b9ce>
- Wikipedia. (2025, Januar 7). *Recurrent Neural Network*. Retrieved Januar 10, 2025, from en.wikipedia.org: [https://en.wikipedia.org/wiki/Recurrent\\_neural\\_network](https://en.wikipedia.org/wiki/Recurrent_neural_network)
- Regalado, A. (2014, Juni 17). *The Thought Experiment*. Retrieved Januar 10, 2025, from technologyreview.com: <https://www.technologyreview.com/2014/06/17/172276/the-thought-experiment/>
- Wikipedia. (2024, December 30). *Electroencephalography*. Retrieved Januar 10, 2025, from en.wikipedia.org: <https://en.wikipedia.org/wiki/Electroencephalography>
- Chaddad, A., Wu, Y., Kateb, R., & Bouridane, A. (2023, Juli 13). Electroencephalography Signal Processing: A Comprehensive Review and Analysis of Methods and Techniques. *Sensors*.
- Parkinson.dk. (n.d.). *Hvad er parkinson?* Retrieved Januar 10, 2025, from parkinson-dk: <https://parkinson.dk/viden-forskning/om-parkinson/hvad-er-parkinson/>
- Paulson, O. B. (2024, Oktober 10). *Parkinsons sygdom*. Retrieved Januar 10, 2025, from lex.dk: [https://lex.dk/Parkinsons\\_sygdom?gad\\_source=1&gclid=CjwKCAiAp4O8BhAkEiwAqv2U](https://lex.dk/Parkinsons_sygdom?gad_source=1&gclid=CjwKCAiAp4O8BhAkEiwAqv2U)



qKvBVEG0S1tye5eNw\_jpHgKSi1qq63S0RQx12dwPH\_CZ9aiYgT-  
VuhoCVr0QAvD\_BwE

Keita, Z. (2023, November 14). *An Introduction to Convolutional Neural Networks (CNNs)*.

Retrieved Januar 10, 2025, from datacamp.com:

<https://www.datacamp.com/tutorial/introduction-to-convolutional-neural-networks-cnns>

Mishra, M. (2020, August 26). *Convolutional Neural Networks, Explained*. Retrieved Januar 14, 2025, from towardsdatascience.com: <https://towardsdatascience.com/convolutional-neural-networks-explained-9cc5188c4939>

Jorgecardete. (2024, Februar 7). *Convolutional Neural Networks: A Comprehensive Guide*.

Retrieved Januar 14, 2025, from medium.com:

<https://medium.com/thedeephub/convolutional-neural-networks-a-comprehensive-guide-5cc0b5eae175>

ibm. (n.d.). *What are convolutional neural networks?* Retrieved from ibm.com:

<https://www.ibm.com/think/topics/convolutional-neural-networks>

Gupta, A., Vardalakis, N., & Wagner, F. B. (2023, Januar 6). Neuroprosthetics: from sensorimotor to cognitive disorders. *Communications Biology*.

Nicolas-Alonso, L. F., & Gomez-Gil, J. (2012, Januar 31). Brain Computer Interfaces, a Review. *Sensors*.

Byrne, R. (2018). *Development of a Low Cost, Open-source, Electroencephalograph-Based Brain-Computer Interface*. Honours Degree in Electrical and Electronic Engineering (DT021A) of the Dublin Institute of Technology.

Kueper, N., Chari, K., Bütetür, J., Habenicht, J., Rossol, T., Kim, S. K., . . . Kirchner, E. A. (2024, Januar 22). EEG and EMG dataset for the detection of errors introduced by an active orthosis device . *Brain-Computer Interfaces*.

Wikipedia. (2024, November 28). *Motor cortex*. Retrieved Januar 22, 2025, from en.wikipedia.org: [https://en.wikipedia.org/wiki/Motor\\_cortex](https://en.wikipedia.org/wiki/Motor_cortex)

Knierum, J. (2020, Oktober 20). *Motor Systems*. Retrieved Januar 22, 2025, from nba.uth.tmc.edu: <https://nba.uth.tmc.edu/neuroscience/s3/chapter03.html>

Ackermann, S. (1992). *Major Structures and Functions of the Brain*. Retrieved from ncbi.nlm.nih.gov: <https://www.ncbi.nlm.nih.gov/books/NBK234157/>

wikipedia.org. (2024, December 26). *Savitzky-Golay filter*. Retrieved Januar 25, 2025, from en.wikipedia.org: [https://en.wikipedia.org/wiki/Savitzky%E2%80%93Golay\\_filter](https://en.wikipedia.org/wiki/Savitzky%E2%80%93Golay_filter)

Jensen, P. M., & Jensen, C. M. (2019, Oktober). *Sensorer - Anvendt el-lære*. Retrieved 2022, from sensorer.systime: <https://sensorer.systime.dk/?id=1>

Google colab. (n.d.). *Fourier Transform*. Retrieved from colab.research.google.com: <https://colab.research.google.com/github/jinglescode/python-signal-processing/blob/main/tutorials/Fourier%20Transform.ipynb>

Google colab. (n.d.). *Signal Filters*. Retrieved from colab.research.google.com: [https://colab.research.google.com/github/iotanalytics/IoTTutorial/blob/main/code/preprocessing\\_and\\_decomposition/Signal\\_Filters.ipynb](https://colab.research.google.com/github/iotanalytics/IoTTutorial/blob/main/code/preprocessing_and_decomposition/Signal_Filters.ipynb)

geeksforgeeks. (2022, Januar 19). *Plotting a Spectrogram using Python and Matplotlib*. Retrieved Januar 25, 2025, from geeksforgeeks.org: <https://geeksforgeeks.org/plotting-a-spectrogram-using-python-and-matplotlib/>

Wikipedia. (2024, November 1). *Bereitschaftspotential*. Retrieved Januar 26, 2025, from en.wikipedia.org: <https://en.wikipedia.org/wiki/Bereitschaftspotential>

Wikipedia. (2025, Januar 25). *Deep Brain Stimulation*. Retrieved Februar 7, 2025, from en.wikipedia.org: [https://en.wikipedia.org/wiki/Deep\\_brain\\_stimulation](https://en.wikipedia.org/wiki/Deep_brain_stimulation)

Johns Hopkins Medicine. (2025). *Deep Brain Stimulation*. Retrieved Februar 7, 2025, from hopkinsmedicine.org: <https://www.hopkinsmedicine.org/health/treatment-tests-and-therapies/deep-brain-stimulation>

Hospital, B. o. (Director). (2014). *Deep Brain Stimulation mod Parkinsons sygdom - hvordan foregår det, hvorfor virker det?* [Motion Picture].

Cleveland Clinic. (2022, Maj 23). *Deep Brain stimulation*. Retrieved Februar 7, 2025, from my.clevelandclinic.org: <https://my.clevelandclinic.org/health/treatments/21088-deep-brain-stimulation>

Wikipedia. (2025, Februar 5). *Brain-Computer-Interface*. Retrieved Februar 7, 2025, from en.wikipedia.org: [https://en.wikipedia.org/wiki/Brain%E2%80%93computer\\_interface](https://en.wikipedia.org/wiki/Brain%E2%80%93computer_interface)

Friedenberg, D. A., Schwemmer, M. A., Landgraf, A. J., Annetta, N. V., Bockbrader, M. A., Bouton, C. E., . . . Sharma, G. (2017, August 21). Neuroprosthetic-enabled control of graded arm muscle contraction in a paralyzed human. *Nature*.

Wikipedia. (2024, November 30). *Neuroprosthetics*. Retrieved Februar 7, 2025, from en.wikipedia.org: <https://en.wikipedia.org/wiki/Neuroprosthetics>

Parkinson.org. (2025). *Statistics*. Retrieved from parkinson.org: <https://www.parkinson.org/understanding-parkinsons/statistics>

- Zhang, D., Hansen, C., De Fréne, F., Kærgaard, S. P., Qian, W., & Chen, K. (2023, April 8). *Automated labeling and online evaluation for self-paced movement detection BCI*. Retrieved Februar 10, 2025, from sciencedirect.com:  
<https://www.sciencedirect.com/science/article/pii/S0950705123001338?via%3Dihub>
- Georgiev, D., Lange, F., Seer, C., Kopp, B., & Johanshahi, M. (2016, Juni 6). *Movement-related potentials in Parkinson's disease*. Retrieved from sciencedirect.com:  
<https://www.sciencedirect.com/science/article/abs/pii/S1388245716300219>
- Johns Hopkins Medicine. (n.d.). *Electromyography (EMG)*. Retrieved from hopkinsmedicine.org:  
<https://www.hopkinsmedicine.org/health/treatment-tests-and-therapies/electromyography-emg>
- wikipedia. (2025, Februar 7). *Electromyography*. Retrieved Januar 15, 2025, from en.wikipedia.org:  
<https://en.wikipedia.org/wiki/Electromyography>
- Cleveland Clinic. (2023, Oktober 2). *EMG (Electromyography)*. Retrieved Januar 17, 2025, from my.clevelandclinic.org: <https://my.clevelandclinic.org/health/diagnostics/4825-emg-electromyography>
- Antony, M. J., Sankaralingam, B. P., Mahendran, R. K., Gardezi, A. A., Shafiq, M., Choi, J.-G., & Hamam, H. (2022, Oktober 7). *Classification of EEG Using Adaptive SVM Classifier with CSP and Online Recursive Independent Component Analysis*. Retrieved Februar 13, 2025, from pmc.ncbi.nlm.nih.gov: <https://pmc.ncbi.nlm.nih.gov/articles/PMC9573537/>
- 3Blue1Brown. (2024, December 12). *Neural Networks*. Retrieved Februar 18, 2025, from youtube.com:  
[https://www.youtube.com/playlist?list=PLZHQObOWTQDNU6R1\\_67000Dx\\_ZCJB-3pi](https://www.youtube.com/playlist?list=PLZHQObOWTQDNU6R1_67000Dx_ZCJB-3pi)
- Wikipedia. (2025, Februar 18). *Transformer (Deep learning architecture)*. Retrieved Februar 18, 2025, from en.wikipedia.org:  
[https://en.wikipedia.org/wiki/Transformer\\_\(deep\\_learning\\_architecture\)#Full\\_transformer\\_architecture](https://en.wikipedia.org/wiki/Transformer_(deep_learning_architecture)#Full_transformer_architecture)
- Geeksforgeeks. (2024, December 6). *Transformers in Machine Learning*. Retrieved Februar 18, 2025, from geeksforgeeks.org: <https://www.geeksforgeeks.org/getting-started-with-transformers/>
- Sachinsoni. (2024, September 5). *Transformer Architecture Part-I*. Retrieved Februar 18, 2025, from pub.towards.ai.net: <https://pub.towardsai.net/transformer-architecture-part-1-d157b54315e6>

- Geeksforgeeks. (2025, Januar 27). *Support Vector Machine (SVM) algorithm*. Retrieved Februar 18, 2025, from [geeksforgeeks.org: https://www.geeksforgeeks.org/support-vector-machine-algorithm/](https://www.geeksforgeeks.org/support-vector-machine-algorithm/)
- Singh, R. (2024, Oktober 17). *Support Vector Machines (SVM)*. Retrieved Februar 18, 2025, from [medium.com: https://medium.com/@RobuRishabh/support-vector-machines-svm-27cd45b74fbb](https://medium.com/@RobuRishabh/support-vector-machines-svm-27cd45b74fbb)
- Wikipedia. (2025, Februar 17). *Support Vector Machine*. Retrieved Februar 18, 2025, from [en.wikipedia.org: https://en.wikipedia.org/wiki/Support\\_vector\\_machine](https://en.wikipedia.org/wiki/Support_vector_machine)
- IBM. (n.d.). *What is a Neural Network?* Retrieved Februar 19, 2025, from [ibm.com: https://www.ibm.com/think/topics/neural-networks](https://www.ibm.com/think/topics/neural-networks)
- Geeksforgeeks. (2024, December 6). *What is a Neural Network?* Retrieved Februar 19, 2025, from [geeksforgeeks.org: https://www.geeksforgeeks.org/neural-networks-a-beginners-guide/](https://www.geeksforgeeks.org/neural-networks-a-beginners-guide/)
- Hansen, S. (2002). *Fra neuron til neurose*. Gads Forlag.
- Wikipedia. (2024, November 21). *Huber loss*. Retrieved Februar 19, 2025, from [en.wikipedia.org: https://en.wikipedia.org/wiki/Huber\\_loss](https://en.wikipedia.org/wiki/Huber_loss)
- Wikipedia. (2025, Februar 16). *Mean absolute error*. Retrieved Februar 19, 2025, from [en.wikipedia.org: https://en.wikipedia.org/wiki/Mean\\_absolute\\_error](https://en.wikipedia.org/wiki/Mean_absolute_error)
- IBM. (2024, Juli 12). *What is a loss function?* Retrieved Februar 19, 2025, from [ibm.com: https://www.ibm.com/think/topics/loss-function](https://www.ibm.com/think/topics/loss-function)
- Magnetoencephalography*. (2024, November 22). Retrieved Marts 23, 2025, from [en.wikipedia.org: https://en.wikipedia.org/wiki/Magnetoencephalography](https://en.wikipedia.org/wiki/Magnetoencephalography)
- Cleveland Clinic. (2025). *Magnetoencephalography (MEG)*. Retrieved Marts 23, 2025, from [my.clevelandclinic.org: https://my.clevelandclinic.org/health/diagnostics/17218-magnetoencephalography-meg](https://my.clevelandclinic.org/health/diagnostics/17218-magnetoencephalography-meg)
- Tierney, T. M., & et al., I. (2019, Oktober 1). *Optically pumped magnetometers: From quantum origins to multi-channel magnetoencephalography*. Retrieved Marts 23, 2025, from [pmc.ncbi.nlm.nih.gov: https://pmc.ncbi.nlm.nih.gov/articles/PMC6988110/](https://pmc.ncbi.nlm.nih.gov/articles/PMC6988110/)
- Virginia Tech. (2021, Maj 12). *Virginia Tech launches 'next generation' human brain imaging lab*. Retrieved Marts 23, 2025, from [news.vt.edu: https://news.vt.edu/articles/2021/05/virginia-tech-launches--next-generation--human-brain-imaging-lab.html](https://news.vt.edu/articles/2021/05/virginia-tech-launches--next-generation--human-brain-imaging-lab.html)
- Miladinovic, A., & et al., I. (2021). *EEG changes and motor deficits in Parkinson's disease patients: Correlation of motor scales and EEG power bands* [Author links open overlay](#)

- panel. Retrieved Marts 23, 2025, from sciencedirect.com:  
<https://www.sciencedirect.com/science/article/pii/S1877050921017683>
- Conti, M., & et al., I. (2022, Marts 15). *Brain Functional Connectivity in de novo Parkinson's Disease Patients Based on Clinical EEG*. Retrieved Marts 23, 2025, from frontiersin.org:  
<https://www.frontiersin.org/journals/neurology/articles/10.3389/fneur.2022.844745/full>
- Peláez Suárez, A. A., & et al., I. (2021, Marts 23). *EEG-Derived Functional Connectivity Patterns Associated with Mild Cognitive Impairment in Parkinson's Disease*. Retrieved Marts 23, 2025, from pmc.ncbi.nlm.nih.gov: <https://pmc.ncbi.nlm.nih.gov/articles/PMC8005012/>
- Desai, K. (2023, Marts 29). *Parkinsons Disease Detection via Resting-State Electroencephalography Using Signal Processing and Machine Learning Techniques*. Retrieved Marts 23, 2025, from arxiv.org: <https://arxiv.org/abs/2304.01214>
- Wang, H.-C., & et al., I. (1999). *Impairment of EEG desynchronisation before and during movement and its relation to bradykinesia in Parkinson's disease*. Retrieved Marts 23, 2025, from pmc.ncbi.nlm.nih.gov: <https://pmc.ncbi.nlm.nih.gov/articles/PMC1736289/>
- Farashi, S., & et al., I. (2023). *Parkinson's disease tremor prediction using EEG data analysis-A preliminary and feasibility study*. Retrieved Marts 13, 2025, from link.springer.com:  
<https://link.springer.com/article/10.1186/s12883-023-03468-0>
- Zanini, R., & et al., I. (2019, September). *Parkinson's disease EMG signal prediction using Neural Networks*. Retrieved Marts 13, 2025, from researchgate.net:  
[https://www.researchgate.net/publication/336890507\\_Parkinson's\\_disease\\_EMG\\_signal\\_prediction\\_using\\_Neural\\_Networks](https://www.researchgate.net/publication/336890507_Parkinson's_disease_EMG_signal_prediction_using_Neural_Networks)
- Saikia, A., & et al., I. (2019, September). *EEG-EMG Correlation for Parkinson's disease*. Retrieved Marts 13, 2025, from researchgate.net:  
[https://www.researchgate.net/publication/335620895\\_EEG-EMG\\_Correlation\\_for\\_Parkinson's\\_disease](https://www.researchgate.net/publication/335620895_EEG-EMG_Correlation_for_Parkinson's_disease)
- Oehr, C. R., & et al., I. (2024). *Chronic adaptive deep brain stimulation versus conventional stimulation in Parkinson's disease: a blinded randomized feasibility trial*. Retrieved Marts 13, 2025, from nature.com: <https://www.nature.com/articles/s41591-024-03196-z#Ack1>
- Andrusca, A. (2023, Oktober 30). *Basal ganglia pathways*. Retrieved Marts 25, 2025, from kenhub.com: <https://www.kenhub.com/en/library/anatomy/direct-and-indirect-pathways-of-the-basal-ganglia>

- Hunt, W., & Sugano, Y. (2020, Juni 30). *The Basal Ganglia*. Retrieved Marts 25, 2025, from teachmeanatomy.info: <https://teachmeanatomy.info/neuroanatomy/structures/basal-ganglia/>
- Buerkle, A., & et al. (2021, August). *EEG based arm movement intention recognition towards enhanced safety in symbiotic Human-Robot Collaboration*. Retrieved Februar 14, 2025, from sciencedirect.com: <https://www.sciencedirect.com/science/article/pii/S0736584521000223>
- Karimi, F., & et al. (2021, November 24). *Movement-related EEG signatures associated with freezing of gait in Parkinson's disease: an integrative analysis*. Retrieved Februar 13, 2025, from academic.oup.com: [https://academic.oup.com/braincomms/article/3/4/fcab277/6437995?utm\\_source=chatgpt.com&login=false](https://academic.oup.com/braincomms/article/3/4/fcab277/6437995?utm_source=chatgpt.com&login=false)
- S., F., & R., E. (1987). *Parkinson's Disease Research, Education and Clinical Centers*. Retrieved Marts 26, 2025, from parkinsons.va.gov: <https://www.parkinsons.va.gov/resources/UPDRS.asp>
- Geeksforgeeks. (2025, Januar 8). *Functional vs. Non Functional Requirements*. Retrieved Marts 27, 2025, from geeksforgeeks.org: <https://www.geeksforgeeks.org/functional-vs-non-functional-requirements/>
- Silva-Acosta, V. D., & et al. (2021, September). *Automatic estimation of continuous elbow flexion–extension movement based on electromyographic and electroencephalographic signals*. Retrieved Februar 13, 2025, from sciencedirect.com: <https://www.sciencedirect.com/science/article/pii/S1746809421005474>
- Mahmoodi, M., & et al., I. (2021, August 18). *A new method for accurate detection of movement intention from single channel EEG for online BCI*. Retrieved from sciencedirect.com: <https://www.sciencedirect.com/science/article/pii/S2666990021000264>
- wikipedia. (2025, Februar 11). *PIEZO1*. Retrieved Marts 31, 2025, from en.wikipedia.org: <https://en.wikipedia.org/wiki/PIEZO1>
- Evident. (n.d.). *What Is a Phased Array Transducer?* Retrieved Marts 31, 2025, from ims.evidentscientific.com: <https://ims.evidentscientific.com/en/learn/ndt-tutorials/transducers/phased-array-transducer>
- Wikipedia. (2024, Oktober 29). *Phased array ultrasonics*. Retrieved Marts 31, 2025, from en.wikipedia.org: [https://en.wikipedia.org/wiki/Phased\\_array\\_ultrasonics](https://en.wikipedia.org/wiki/Phased_array_ultrasonics)

- Demi, L. (2018, August 31). *Practical Guide to Ultrasound Beam Forming: Beam Pattern and Image Reconstruction Analysis*. Retrieved Marts 31, 2025, from mdpi.com:  
<https://www.mdpi.com/2076-3417/8/9/1544>
- University of Calgary. (2025). *What is a Brain Computer Interface?* Retrieved April 4, 2025, from cumming.ucalgary.ca: <https://cumming.ucalgary.ca/research/pediatric-bci/bci-program/what-bci>
- Brodal, P. (1995). *Sentral Nerve Systemet* (2 ed.). Oslo: Tano.
- Wikipedia. (2025, Marts 25). *Event-related potential*. Retrieved April 5, 2025, from en.wikipedia.org: [https://en.wikipedia.org/wiki/Event-related\\_potential](https://en.wikipedia.org/wiki/Event-related_potential)
- Aeles, J., & et al. (2021, Januar 13). Revealing the unique features of each individual's muscle activation signatures. *Journal of the Royal Society Interface*, 18(174). Retrieved Februar 13, 2025, from pmc.ncbi.nlm.nih.gov: <https://pmc.ncbi.nlm.nih.gov/articles/PMC7879771/>
- Silva-Acosta, V. D., & et al. (2021, September). *Automatic estimation of continuous elbow flexion–extension movement based on electromyographic and electroencephalographic signals*. Retrieved Februar 13, 2025, from sciencedirect.com:  
<https://www.sciencedirect.com/science/article/pii/S1746809421005474>
- Mahmoodi, M., & et al., I. (2021, August 18). *A new method for accurate detection of movement intention from single channel EEG for online BCI*. Retrieved from sciencedirect.com:  
<https://www.sciencedirect.com/science/article/pii/S2666990021000264>

## Interviews & Input

Per Borghammer (Clinical Professor, Ph.D., Dr. Med., Department of Clinical Medicine, Nuclear Medicine and PET, AUH) and Casper Skjærbæk (Ph.D. candidate, Department of Clinical Medicine - Nuclear Medicine and PET, AUH), who answered my questions about Parkinson's disease and provided constructive feedback on the project.

Dan Bang (Associate Professor, PhD, Department of Clinical Medicine, Center for Functional Integrative Neuroscience (CFIN), AU) and Andreas Nørgaard Glud (Clinical Associate Professor, MD, PhD, Department of Clinical Medicine, Neurosurgery, AU), who answered my questions about the brain and Parkinson's disease, and for inviting me to their research group to gain valuable insights and feedback.

Thomas Nielsen (Associate Professor, Department of Electrical and Computer Engineering, Biomedical Engineering, AU) and Preben Kidmose (Professor, Department of Electrical and Computer Engineering - Biomedical Engineering, AU) for discussing my ideas and helped finishing off the self-assembled EEG-circuit. Also, for loaning me their equipment.

My mentor and previous physics teacher Pia Møller Jensen must also get a colossal, enormous thanks, for her unvaluable help and guidance. Without her, wouldn't the project ever had been possible! I owe all my success to her!

In total, all the experts and mentor gave me a deep insight to neurology, engineering and AI-modelling. With constructive critique they made the project blossom throughout its development.



## Photos

Here are some photos from my very early sketches of project idea back from December:

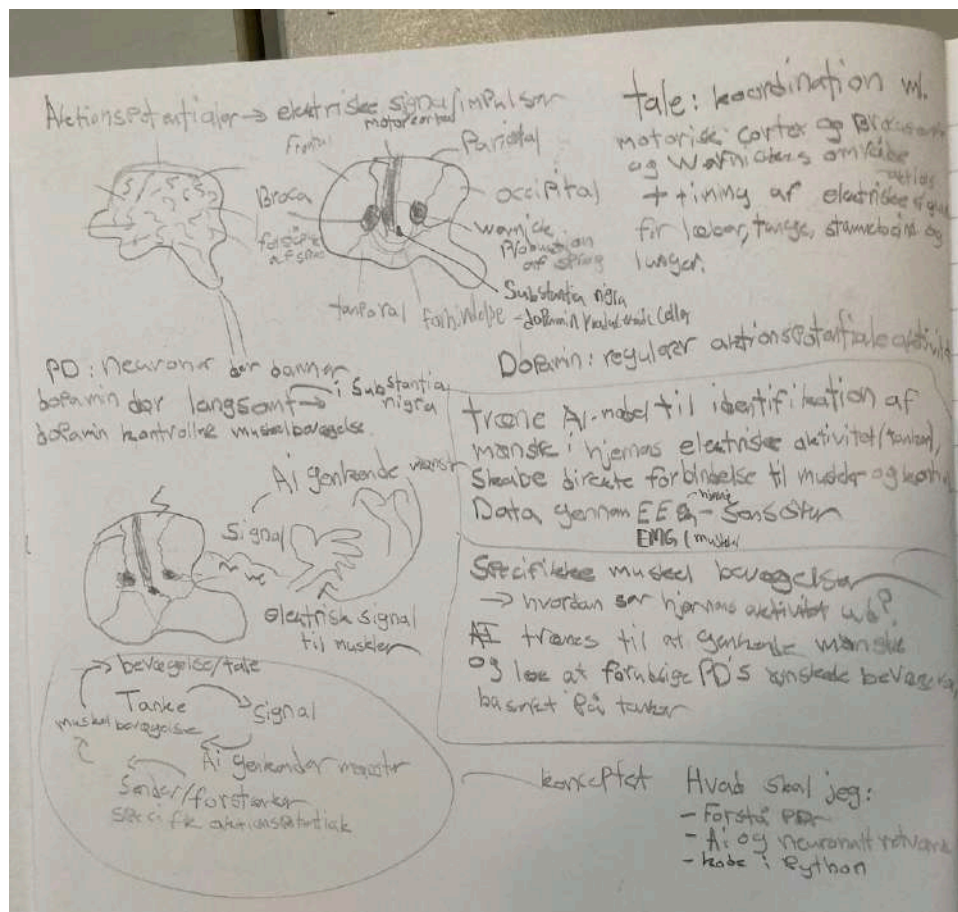


Figure 59: The first sketch of idea: from brain activity, through AI-model to execution of movement<sup>137</sup>

<sup>137</sup> The author's own work

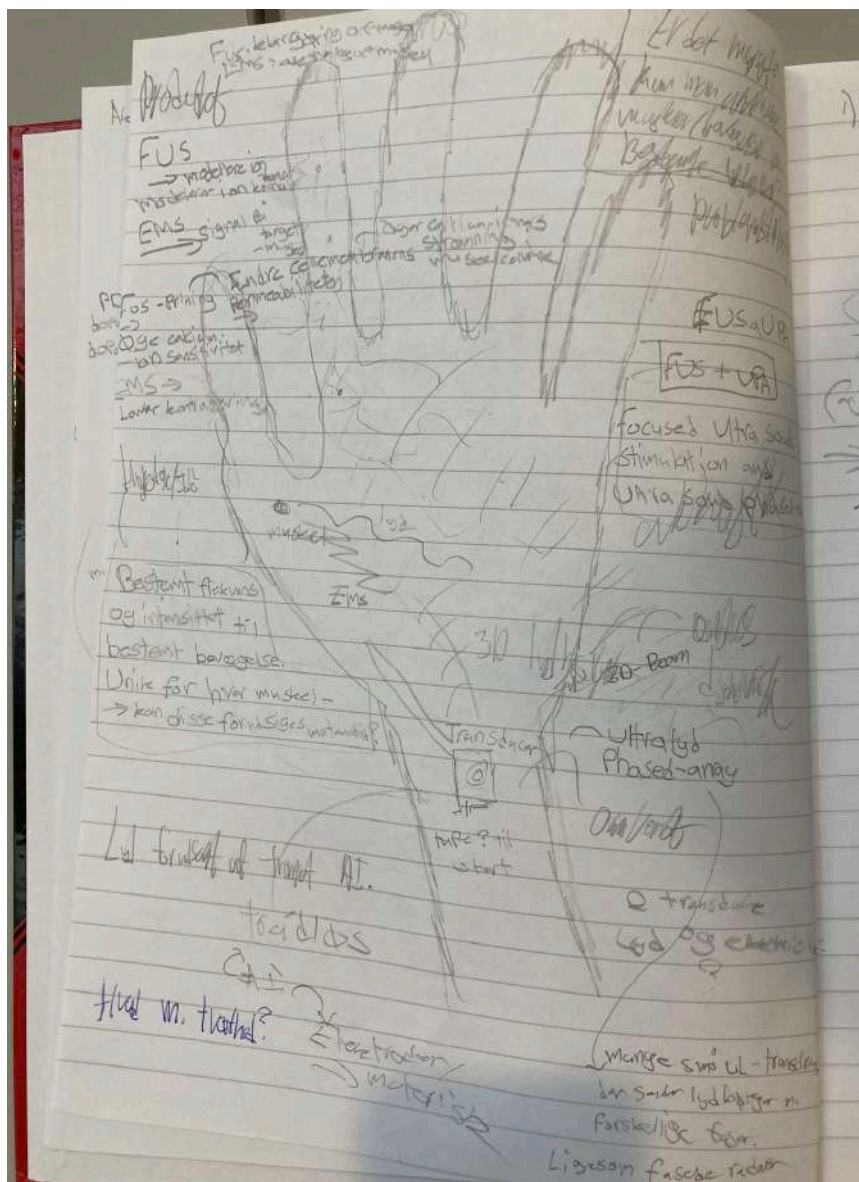


Figure 60: My sketch of a BPI solution. I put my hand on a piece of paper and thereafter I started to draw the solution<sup>138</sup>

<sup>138</sup> The author's own work

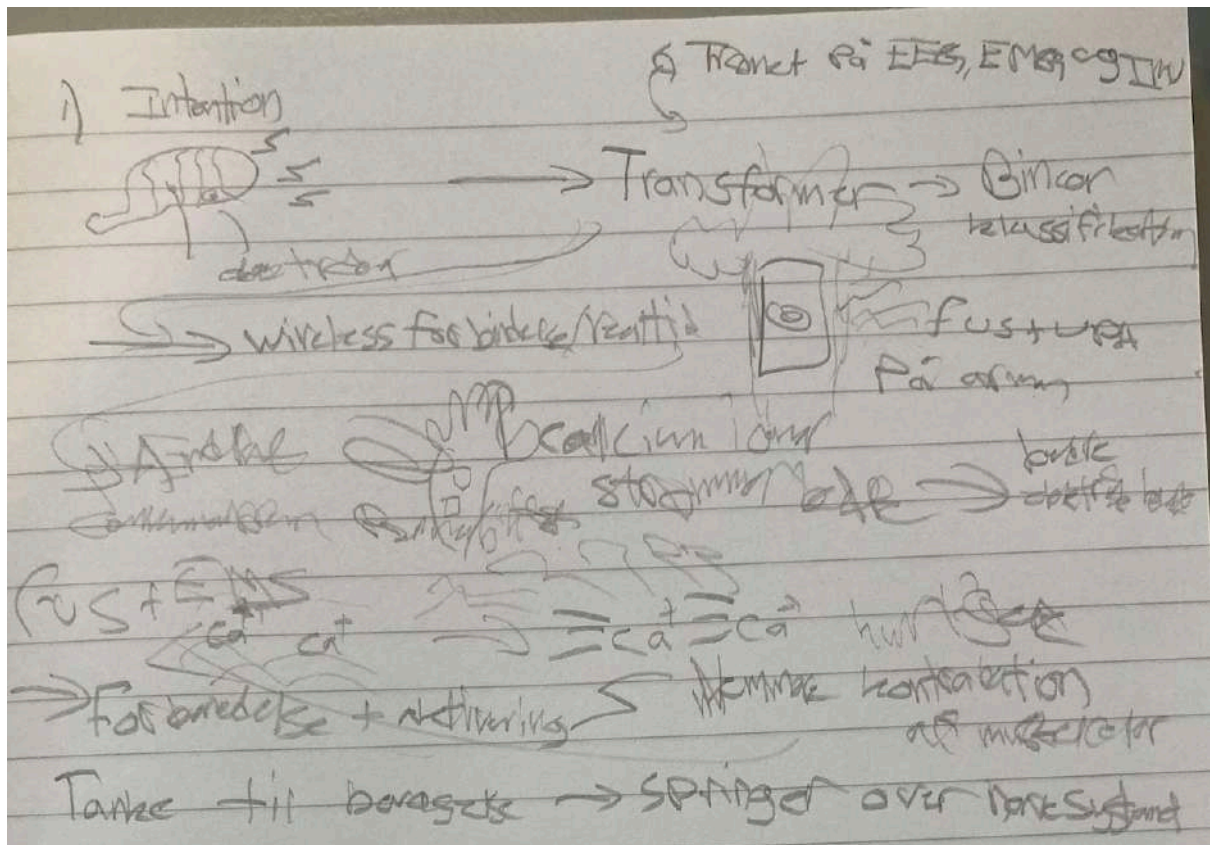


Figure 61: From intention to the reactivation of the muscles through a BPI<sup>139</sup>

<sup>139</sup> The author's own work